Online ISSN : 2249-4596
Print ISSN : 0975-5861
DOI : 10.17406/GJRE

Global Journal

of Researches in Engineering: C

Chemical Engineering

Highlights

Polymers in the Particle

Seawater Fouling Potential

Scenarios Involving Hydrogen

Effect of Chemical Pretreatment

Discovering Thoughts, Inventing Future

VOLUME 17 ISSUE 3 VERSION 1.0

Global Journal of Researches in Engineering: C
Chemical Engineering

Global Journal of Researches in Engineering: C
Chemical Engineering
Volume 17 Issue 3 (Ver. 1.0)

Open Association of Research Society

Incorporation No.: 0423089
License No.: 42125/022010/1186
Registration No.: 430374
Import-Export Code: 1109007027
Employer Identification Number (EIN):
USA Tax ID: 98-0673427

Global Journals Inc.

*(A Delaware USA Incorporation with "Good Standing"; **Reg. Number: 0423089**)*

Sponsors: Open Association of Research Society
Open Scientific Standards

Publisher's Headquarters office

Global Journals® Headquarters
945th Concord Streets,
Framingham Massachusetts Pin: 01701,
United States of America
USA Toll Free: +001-888-839-7392
USA Toll Free Fax: +001-888-839-7392

Offset Typesetting

Global Journals Incorporated
2nd, Lansdowne, Lansdowne Rd., Croydon-Surrey,
Pin: CR9 2ER, United Kingdom

Packaging & Continental Dispatching

Global Journals
E-3130 Sudama Nagar, Near Gopur Square,
Indore, M.P., Pin:452009, India

Find a correspondence nodal officer near you

To find nodal officer of your country, please email us at *local@globaljournals.org*

eContacts

Press Inquiries: *press@globaljournals.org*
Investor Inquiries: *investors@globaljournals.org*
Technical Support: *technology@globaljournals.org*
Media & Releases: *media@globaljournals.org*

Pricing (Including by Air Parcel Charges):

For Authors:
22 USD (B/W) & 50 USD (Color)
Yearly Subscription (Personal & Institutional):
200 USD (B/W) & 250 USD (Color)

Editorial Board

Global Journal of Research in Engineering

Dr. Joaquim Carneiro

Ph.D. in Mechanical Engineering,
Faculty of Engineering,
University of Porto(FEUP),
University of Minho,
Department of Physics, Portugal

Dr. Hai-Wen Li

Ph.D., Materials Engineering
Kyushu University
Fukuoka
Guest Professor at Aarhus University, Japan

Dr. Wei-Hsin Chen

Ph.D., National Cheng Kung University
Department of Aeronautics
and Astronautics, Taiwan

Dr. Saeed Chehreh Chelgani

Ph.D. in Mineral Processing
University of Western Ontario,
Adjunct professor,
Mining engineering and Mineral processing
University of Michigan

Belen Riveiro

Ph.D.,
School of Industrial Engineering
University of Vigo, Spain

Dr. Bin Chen

B.Sc., M.Sc., Ph.D., Xi'an Jiaotong University, China.
State Key Laboratory of Multiphase Flow in Power Engineering
Xi'an Jiaotong University, China

Dr. Maurizio Palesi

Ph.D. in Computer Engineering,
University of Catania
Faculty of Engineering and Architecture
Italy

Dr. Cesar M. A. Vasques

Ph.D., Mechanical Engineering
Department of Mechanical Engineering
School of Engineering, Polytechnic of Porto
Porto, Portugal

Dr. Stefano Invernizzi

Ph.D. in Structural Engineering
Technical University of Turin,
Department of Structural,
Geotechnical and Building Engineering, Italy

Dr. T.S. Jang

Ph.D. Naval Architecture and Ocean Engineering
Seoul National University, Korea
Director, Arctic Engineering Research Center,
The Korea Ship and Offshore Research Institute,
Pusan National University, South Korea

Dr. Jun Wang

Ph.D. in Architecture, University of Hong Kong, China
Urban Studies
City University of Hong Kong, China

Dr. Salvatore Brischetto

Ph.D. in Aerospace Engineering, Polytechnic University of Turin and
in Mechanics, Paris West University Nanterre La Défense
Department of Mechanical and Aerospace Engineering,
Polytechnic University of Turin, Italy

Dr. Francesco Tornabene

Ph.D. in Structural Mechanics, University of Bologna
Professor Department of Civil, Chemical, Environmental and Materials Engineering
University of Bologna, Italy

Dr. Wesam S. Alaloul

B.Sc., M.Sc.,
Ph.D. in Civil and Environmental Engineering,
University Technology Petronas, Malaysia

Dr. Togay Ozbakkaloglu

B.Sc. in Civil Engineering
Ph.D. in Structural Engineering, University of Ottawa, Canada
Senior Lecturer University of Adelaide, Australia

Dr. Sofoklis S. Makridis

B.Sc(Hons), M.Eng, Ph.D.
Professor Department of Mechanical Engineering
University of Western Macedonia, Greece

Dr. Paolo Veronesi

Ph.D., Materials Engineering
Institute of Electronics, Italy
President of the master Degree in Materials Engineering
Dept. of Engineering, Italy

Dr. Ananda Kumar Palaniappan

B.Sc., MBA, MED, Ph.D. in Civil and Environmental Engineering,
Ph.D. University of Malaya, Malaysia
University of Malaya, Malaysia

Dr. Maria Daniela

Ph.D. in Aerospace Science and Technologies
Second University of Naples
Research Fellow University of Naples "Federico II", Italy

Dr. Zhen Yuan

B.E., Ph.D. in Mechanical Engineering
University of Sciences and Technology of China, China
Professor, Faculty of Health Sciences, University of Macau, China

Dr. Charles-Darwin Annan

Ph.D.,
Professor Civil and Water Engineering University Laval, Canada

Dr. Hugo Silva

Associate Professor
University of Minho
Department of Civil Engineering
Ph.D., Civil Engineering
University of Minho, Portugal

Dr. Stefano Mariani

Associate Professor
Structural Mechanics
Department of Civil
and Environmental Engineering,
Ph.D., in Structural Engineering
Polytechnic University of Milan, Italy

Dr. Jui-Sheng Chou

Ph.D. University of Texas at Austin, U.S.A.
Department of Civil and Construction Engineering
National Taiwan University of Science and Technology (Taiwan Tech)

Dr. Shaoping Xiao

BS, MS
Ph.D. Mechanical Engineering, Northwestern University
The University of Iowa
Department of Mechanical and Industrial Engineering
Center for Computer-Aided Design

Dr. Fausto Gallucci

Associate Professor
Chemical Process Intensification (SPI)
Faculty of Chemical
Engineering and Chemistry
Assistant Editor
International J. Hydrogen Energy, Netherlands

Dr. Vladimir Gurao

Associate Professor
Ph.D. in Mechanical /
Aerospace Engineering
University of Miami
Engineering Technology

Prof. (LU) Prof. (UoS) Dr. Miklas Scholz

Cand Ing, BEng (equiv), PgC, MSc, Ph.D., CWEM, CEnv, CSci, CEng,
FHEA, FIEMA, FCIWEM, FICE, Fellow of IWA,
VINNOVA Fellow, Marie Curie Senior Fellow,
Chair in Civil Engineering (UoS)
Wetland systems, sustainable drainage, and water quality

Dr. Adel Al Jumaily

Ph.D. Electrical Engineering (AI)
Faculty of Engineering and IT
University of Technology, Sydney

Dr. Houfa Shen

Ph.D. Manufacturing Engineering, Mechanical Engineering, Structural Engineering
Department of Mechanical Engineering
Tsinghua University, China

Dr. A. Stegou-Sagia

Ph.D. Mechanical Engineering, Environmental
Engineering School of Mechanical Engineering
National Technical University of Athens

Dr. Kitipong Jaojaruek

B. Eng, M. Eng
D. Eng (Energy Technology, Asian Institute of Technology).
Kasetsart University Kamphaeng Saen (KPS) Campus
Energy Research Laboratory of Mechanical Engineering

Dr. Jalal Kafashan

Mechanical Engineering
Division of Mechatronics
KU Leuven, BELGIUM

Dr. Haijian Shi

Ph.D. Civil Engineering
Structural Engineering
Oakland, CA, United States

Dr. Zhibin Lin

Center for Infrastructure Engineering Studies
Missouri University of Science and Technology
ERL, 500 W. 16th St. Rolla,
Missouri 65409, US

Dr. Chao Wang

Ph.D. in Computational Mechanics
Rosharon, TX,
US

Dr. Shun-Chung Lee

Department of Resources Engineering,
National Cheng Kung University, Taiwan

Hiroshi Sekimoto

Professor Emeritus
Tokyo Institute of Technology, Japan
Ph.D., University of California, Berkeley

Dr. Philip T Moore

Ph.D., Graduate
Master Supervisor
School of Information
Science and engineering
Lanzhou University, China

Dr. Steffen Lehmann

Faculty of Creative and
Cultural Industries
PhD, AA Dip
University of Portsmouth, UK

Dr. Gordana Colovic

B.Sc Textile Technology, M.Sc. Technical Science
Ph.D. in Industrial management.
The College of Textile – Design, Technology and Management, Belgrade, Serbia

Dr. Yudong Zhang

B.S., M.S., Ph.D. Signal and Information Processing,
Southeast University
Professor School of Information Science and Technology at Nanjing Normal University, China

Dr. Xianbo Zhao

Ph.D. Department of Building,
National University of Singapore, Singapore,
Senior Lecturer, Central Queensland University, Australia

Dr. Philip G. Moscoso

Technology and Operations Management
IESE Business School, University of Navarra
Ph.D in Industrial Engineering and Management, ETH Zurich
M.Sc. in Chemical Engineering, ETH Zurich
Link: Philip G. Moscoso personal webpage

Contents of the Issue

Global Journal of Researches in Engineering: C
Chemical Engineering
Volume 17 Issue 3 Version 1.0 Year 2017
Type: Double Blind Peer Reviewed International Research Journal
Publisher: Global Journals Inc. (USA)
Online ISSN: 2249-4596 & Print ISSN: 0975-5861

A Laboratory Scale Prodution Method of Raw Manganese (II) Sulphate from Waste used Alkaline Batteries

By M. Sathiyamoorthy, Ayesha Jasim Alhammadi
& Somaya Ibrahim Alhamadi

Abstract- This experimental project deals with the laboratory scale production method of raw manganese (II) sulphate from waste used alkaline batteries. The Batteries have wide range of applications which includes automobile, household, industrial, electronics, mobile gadgets etc. There are many types of Batteries like alkaline battery, zinc carbon battery, lead acid battery, nickel cadmium battery, lithium battery etc. In UAE, millions of products using the lead acid batteries and alkaline batteries. The batteries are exhausted, after many recharge cycles. These waste used batteries are disposed to atmosphere and makes many environmental pollutions. This experimental research project explains how to synthesis Manganese (II) sulphate from these waste batteries by simple method in lab scale with step by step. Because, MnSO4 has lots of uses and can be produced from these waste batteries. It is one of the great business idea for Chemical Engineers in the present and future UAE industrial sectors.

Keywords: *batteries, manganese sulphate, manganese dioxide, used batteries, alkaline battereies, lead acid batteries.*

GJRE-C Classification: *FOR Code: 090499*

Strictly as per the compliance and regulations of:

A Laboratory Scale Prodution Method of Raw Manganese (II) Sulphate from Waste used Alkaline Batteries

M. Sathiyamoorthy [α], Ayesha Jasim Alhammadi [σ] & Somaya Ibrahim Alhamadi [ρ]

Abstract- This experimental project deals with the laboratory scale production method of raw manganese (II) sulphate from waste used alkaline batteries. The Batteries have wide range of applications which includes automobile, household, industrial, electronics, mobile gadgets etc. There are many types of Batteries like alkaline battery, zinc carbon battery, lead acid battery, nickel cadmium battery, lithium battery etc. In UAE, millions of products using the lead acid batteries and alkaline batteries. The batteries are exhausted, after many recharge cycles. These waste used batteries are disposed to atmosphere and makes many environmental pollutions. This experimental research project explains how to synthesis Manganese (II) sulphate from these waste batteries by simple method in lab scale with step by step. Because, $MnSO_4$ has lots of uses and can be produced from these waste batteries. It is one of the great business idea for Chemical Engineers in the present and future UAE industrial sectors.

Keywords: batteries, manganese sulphate, manganese dioxide, used batteries, alkaline battereies, lead acid batteries.

I. Introduction

Battery is a device consisting of one or more electrochemical cells with external connections provided to power electrical device such as flash light, smart phones and electric cars. When a battery is supplying electric power, its positive terminal is the cathode, and its negative terminal is the anode. The present method is to prepare manganese (II) sulfate from manganese dioxide which is extracted from the waste used batteries. Mainly alkaline batteries are used for this purposes. The product produced is the raw and impure. It has to be further purified.

a) *Types of batteries*

Primary (single-use or "disposable") batteries are used once and discarded; the electrode materials are irreversibly changed during discharge. Common examples are the alkaline battery used for flashlights and a multitude of portable electronic devices. Secondary batteries can be discharged and recharged multiple times using an applied electric current;

Secondary (rechargeable) batteries can be discharged and recharged multiple times using an applied electric current; the original composition of the electrodes can be restored by reverse current. Examples include the lead-acid batteries used in vehicles and lithium-ion batteries used for portable electronics such as laptops.

Batteries come in many shapes and sizes, from miniature cells used to power hearing aids and wristwatches to small, thin cells used in smart phones, to large lead acid batteries used in cars and trucks, and at the largest extreme, huge battery banks the size of rooms that provide standby or emergency power for telephone exchanges and computer data centers.

Reuse of the recovered materials from solid wastes is the other principal mode of energy conservations. Therefore attention has been focused in the utilization of industrial wastes and low grade ores for the recovery of metals due to increased mining costs and depletion of mineral wealth. During the last decade a great increase in environmental awareness took place and legislation on wastes developed. It is estimated that in India alone, about 115 million of urban population produces nearly 15 million tons of solid waste causing chronic pollution of land and water.

Recent developments have allowed successful commercial introduction of rechargeable zinc alkaline and manganese dioxide batteries. But dry Lechlanche cell once discharged cannot be recharged again. Household batteries contribute many potentially hazardous compounds to the municipal solid waste stream, including zinc, lead, nickel, alkaline, manganese, carbon-zinc, mercuric oxide, zinc-air, silver oxide, and other types of button batteries.

Higher levels of manganese are toxic and cause brain damage. Very little or no information appeared in the literature on estimation of manganese and its utilization for different analytical applications.

i. *Primary cell*

Primary batteries, or primary cells, can produce current immediately on assembly. These are most commonly used in portable devices that have low current drain, are used only intermittently, or are used well away from an alternative power source, such as in alarm and communication circuits where other electric

Author α: Faculty, Department of Chemical Engineering, Higher Colleges of Technology, Al Ruwais, United Arab Emirates.
e-mail: sathyachemical@gmail.com
Author σ: Final year student, Department of Chemical Engineering, Higher Colleges of Technology, Al Ruwais, United Arab Emirates.

power is only intermittently available. Disposable primary cells cannot be reliably recharged, since the chemical reactions are not easily reversible and active materials may not return to their original forms. Battery manufacturers recommend against attempting to recharge primary cells. In general, these have higher energy densities than rechargeable batteries, but disposable batteries do not fare well under high-drain applications with loads under 75 ohms (75 Ω). Common types of disposable batteries include zinc–carbon batteries and alkaline batteries.

ii. *Secondary battery*

Secondary batteries, also known as secondary cells, or rechargeable batteries, must be charged before first use; they are usually assembled with active materials in the discharged state. Rechargeable batteries are (re)charged by applying electric current, which reverses the chemical reactions that occur during discharge/use. Devices to supply the appropriate current are called chargers.

The oldest form of rechargeable battery is the lead–acid battery, which are widely used in automotive and boating applications. This technology contains liquid electrolyte in an unsealed container, requiring that the battery be kept upright and the area be well ventilated to ensure safe dispersal of the hydrogen gas it produces during overcharging. The lead–acid battery is relatively heavy for the amount of electrical energy it can supply. Its low manufacturing cost and its high surge current levels make it common where its capacity (over approximately 10 Ah) is more important than weight and handling issues. A common application is the modern car battery, which can, in general, deliver a peak current of 450 amperes.

iii. *Life time*

Battery life (and its synonym battery lifetime) has two meanings for rechargeable batteries but only one for non-chargeable. For rechargeable, it can mean either the length of time a device can run on a fully charged battery or the number of charge/discharge cycles possible before the cells fail to operate satisfactorily. For a non-rechargeable these two lives are equal since the cells last for only one cycle by definition. (The term shelf life is used to describe how long a battery will retain its performance between manufacture and use.) Available capacity of all batteries drops with decreasing temperature. In contrast to most of today's batteries, the Zamboni pile, invented in 1812, offers a very long service life without refurbishment or recharge, although it supplies current only in the nano amp range. The Oxford Electric Bell has been ringing almost continuously since 1840 on its original pair of batteries, thought to be Zamboni piles.

Today, batteries are all around us.

The power our wristwatches for months at a time. They keep our alarm clocks and telephones working, even if the electricity goes out. They run our smoke detectors, electric razors, power drills, mp3 players, thermostats and the list goes on. If you're reading this article on your laptop or smartphone, you may even be using batteries right now! However, because these portable power packs are so prevalent, it's very easy to take them for granted. This article will give you a greater appreciation for batteries by exploring their history, as well as the basic parts, reactions and processes that make them work. So cut that cord and click through our informative guide to charge up your knowledge of batteries.

iv. *Waste batteries*

Waste batteries that are classified as hazardous waste can be collected under the streamlined collection standards for universal waste. These universal waste standards were created in an attempt to make it easier to collect the waste batteries and send them for recycling (or proper treatment and disposal). The requirements specific to batteries are described below.

Batteries and accumulators play an essential role to ensure that many daily-used products, appliances and services work properly, constituting an indispensable energy source in our society. Every year, approximately 800.000 tons of automotive batteries, 190.000 tons of industrial batteries, and 160.000 tons of consumer batteries enter the GCC.

Not all these batteries are properly collected and recycled at the end of their life, which increases the risk of releasing hazardous substances and constitutes a waste of resources. Many of the components of these batteries and accumulators could be recycled, avoiding the release of hazardous substances to the environment and, in addition, providing valuable materials to important products and production processes in gulf region.

To achieve these objectives, the Directive prohibits the marketing of batteries containing some hazardous substances, defines measures to establish schemes aiming at high level of collection and recycling, and fixes targets for collection and recycling activities. The Directive also sets out provisions on labelling of batteries and their removability from equipment.

It also aims to improve the environmental performance of all operators involved in the life cycle of batteries and accumulators, e.g. producers, distributors and end-users and, in particular, those operators directly involved in the treatment and recycling of waste batteries and accumulators. Producers of batteries and accumulators and producers of other products incorporating a battery or accumulator are given responsibility for the waste management of batteries and accumulators that they place on the market

v. *Battery recycling*

Battery recycling is a recycling activity that aims to reduce the number of batteries being disposed as municipal solid waste. Batteries contain a number of heavy metals and toxic chemicals and disposing them by the same process as regular trash has raised concerns over soil contamination and water pollution.

Most types of batteries can be recycled. However, some batteries are recycled more readily than others, such as lead–acid automotive batteries (nearly 90% are recycled) and button cells (because of the value and toxicity of their chemicals).Other types, such as alkaline and rechargeable, e.g., nickel–cadmium (Ni-Cd), nickel metal hydride (Ni-MH), lithium-ion (Li-ion) and nickel–zinc (Ni-Zn), can also be recycled.

vi. *Alkaline batteries*

Alkaline batteries are a type of primary battery dependent upon the reaction between zinc and manganese dioxide (Zn/MnO_2). Another type of alkaline batteries are secondary rechargeable alkaline battery, which allows reuse of specially designed cells. Compared with zinc-carbon batteries of the Leclanché or zinc chloride types, alkaline batteries have a higher energy density and longer shelf-life, with the same voltage.

The alkaline battery gets its name because it has an alkaline electrolyte of potassium hydroxide, instead of the acidic ammonium chloride or zinc chloride electrolyte of the zinc-carbon batteries. Other battery systems also use alkaline electrolytes, but they use different active materials for the electrodes. Alkaline batteries account for 80% of manufactured batteries in the Asia and over 10 billion individual units produced worldwide. In Japan alkaline batteries account for 46% of all primary battery sales. In Switzerland alkaline batteries account for 68%, in the UK 60% and in the EU 47% of all battery sales including secondary types. Alkaline batteries are used in many household items such as MP3 players, CD players, digital cameras, pagers, toys, lights, and radios.

The alkaline battery is an advanced form of zinc-manganese dioxide batteries and thus of the Leclanché element. It shows a better performance due to three times higher capacity compared to conventional batteries. The active material of the negative electrode is zinc in powder form to reach a high specific surface. The powder is hold by a synthetic gel. The positive electrode consists of manganese dioxide as active material and graphite as conducting additive, both also in powder form. A solution of potassium hydroxide with a mass fraction of 30 % to 45% is used as electrolyte and not used in reaction.

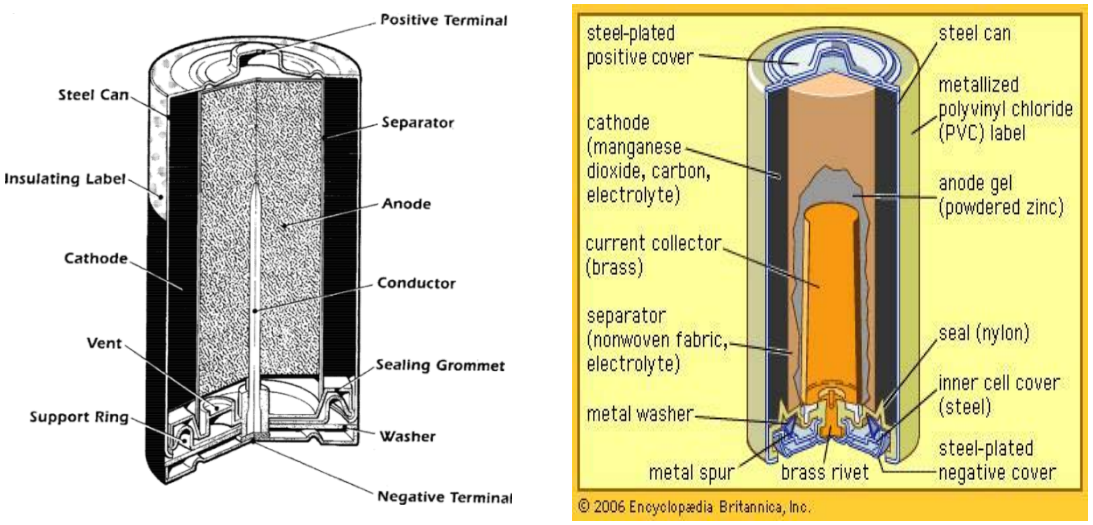

Figure 1: Alkaline battery components

The positive and the negative electrodes are separated by a material, which has to be permeable for hydroxide ions, since equal amounts of them are consumed and produced in both half cells.

b) Manganese sulphate

Manganese (II) sulfate usually refers to the inorganic compound with the formula $MnSO_4 \cdot H_2O$. This pale pink deliquescent solid is a commercially significant manganese (II) salt. Approximately 460 thousand tonnes of manganese (II) sulfate were produced worldwide in 2015. It is the precursor to manganese metal and many other chemical compounds. Mn-deficient soil is remediated with this salt.

Like many metal sulfates, manganese sulfate forms a variety of hydrates: monohydrate, tetra hydrate, pentahydrate, and heptahydrate. The monohydrate is most common. All of these salts dissolve to give faintly pink solutions of the aquo complex $[Mn(H_2O)_6]2+$. The pale pink color of Mn (II) salts is highly characteristic.

Typically, manganese ores are purified by their conversion to manganese (II) sulfate. Treatment of aqueous solutions of the sulfate with sodium carbonate leads to precipitation of manganese carbonate, which can be calcined to give the oxides MnOx. In the laboratory, manganese sulfate can be made by treating manganese dioxide with sulfur dioxide.

$$MnO_2 + SO_2 \rightarrow MnSO_4$$

It can also be made by mixing potassium permanganate with sodium hydrogen sulfate and hydrogen peroxide. Manganese sulfate is a by-product of various industrially significant oxidations that use manganese dioxide, including the manufacture of hydroquinone and anisaldehyde. Electrolysis of manganese sulfate yields manganese dioxide, which is called EMD for electrolytic manganese dioxide. Alternatively oxidation of manganese sulfate with potassium permanganate yields the so-called chemical manganese dioxide (CMD). These materials, especially EMD, are used in dry-cell batteries.

Plants use manganese (Mn) for enzyme activity involved in carbohydrate metabolism. They also use it for making fatty acids in every transfers during photosynthesis. Manganese Sulphate supplies manganese, which is used to alleviate manganese deficiencies. These are most common in peat mixes. A manganese sulphate solution is used to correct and prevent manganese deficiency in a wide range of agricultural and horticultural crops.

Manganese sulphate is also applied to mixes or as a foliar application for crop production where a history of Mn deficiency exists. If applied as a foliar, ensure Manganese Sulphate Soluble is requested. Foliar sprays are the most effective way of applying manganese sulfate solution. If applied directly to the soil the manganese can become “locked up” especially in calcareous high pH soils.

Manganese deficiency occurs mainly in high pH conditions, sandy soils that are low in organic matter, organic miss (peats) and in over-limed soils. Uptake of manganese decreases with increased soil pH and is adversely affected by high levels of available iron (Fe). Cereal crops, potatoes, vines and fruit crops grown on high pH conditions are particularly sensitive to manganese deficiency.

i. *Properties*

Compound Chemical Formula	: $MnSO_4$
Molecular Weight	: 169.02
Melting Point	: 700^0C; 1292^0F
Boiling Point	: 850^0C; 1562^0F
State at Room Temperature	: Grey/Pink Crystalline Powder
Ionic Compound	
Molecular Geometry	: Octahedral

Uses of $MnSO_4$: Manganese Sulfate is used in fertilizers, feed additives, paints, varnishes, ceramic, textile dyes, medicines, and fungicides.

Manganese sulfate is used in dying, for glazes on porcelain, boiling oils for varnishes, in feeds, and in fertilizers. Crops with high manganese requirements include beans, oat, soybean, sorghum and wheat. Those with medium relative manganese needs are barley, beet, cabbage, potato and tomato.

Manganese sulfate can also produced from manganese dioxide, performing a direct chemical reaction between gaseous sulfur dioxide and solid MnO_2 Another process relates to the use of ferromanganese for the production of $MnSO_4$-solution for the electrolytic or chemical precipitation of manganese dioxides. In an alternative technology, MnO_2 ore powder (80-100 mesh size) is mixed with water (30%w),then the slurry is fed counter-currently to an absorption column to sulfur-containing fumes at a temperature of 60^0C. The sulfurous acid formed (H_2SO_3) will react with MnO_2 to form final product.

Any other useful information: Health Hazards for Manganese Sulfate if swallowed, it may cause gastro intestinal irritation with nausea, vomiting, and diarrhea. If contact with eyes, it may cause a mild eye irritation. If contact with the skin, it may cause skin irritation. If inhaled it may cause a respiratory tract irritation Manufacturing of manganese sulfate (fertilizer grade) and Manganese dioxide (battery grade) were frequently the objectives of the many project. Preliminary techno-economic feasibility studies together with profitability analysis were the basis of products assessment. The project strategy will fulfill the establishment of native Mn-chemical industries and diminish export potentials, and partially cover local market demands.

II. Materials and Methods

Batteries contain cadmium, mercury, copper, zinc, lead, manganese, nickel and lithium, which may create a hazard when disposed incorrectly. The most important non metallurgical use of manganese is in the form of manganese dioxide, which is used as a depolarizer in dry cell batteries. Simply the black powder in the alkaline battery is the raw manganese dioxide powder. Our first objective is to separate this manganese dioxide powder from the battery then it is used to produce manganese (ii) sulphate.

a) Materials required

- U se d alkaline batteries
- Mechanical tools
- Personal protective equipment
- Glass wares
- Sulphuric acid 98%
- Oxalic acid

i. *Battery dismantling & pretreatments*

House hold disposed dry batteries from different suppliers and places were collected. These batteries were manually dismantled. The steps were shown in the below figures one by one.

Figure 2: Battery dismantling

The outer shell of the battery is removed first. Then the zinc thin cover is also removed. The metallic scraps and plastic/paper films were removed if any. There is a mixture of cathodic (Manganese dioxide and graphite) and anodic (zinc and electrolytic solution) materials. That paste has 55% of the total battery weight. The graphite electrode in the center of the battery is pulled out from the cell.

Figure 3: Battery outer cover removal

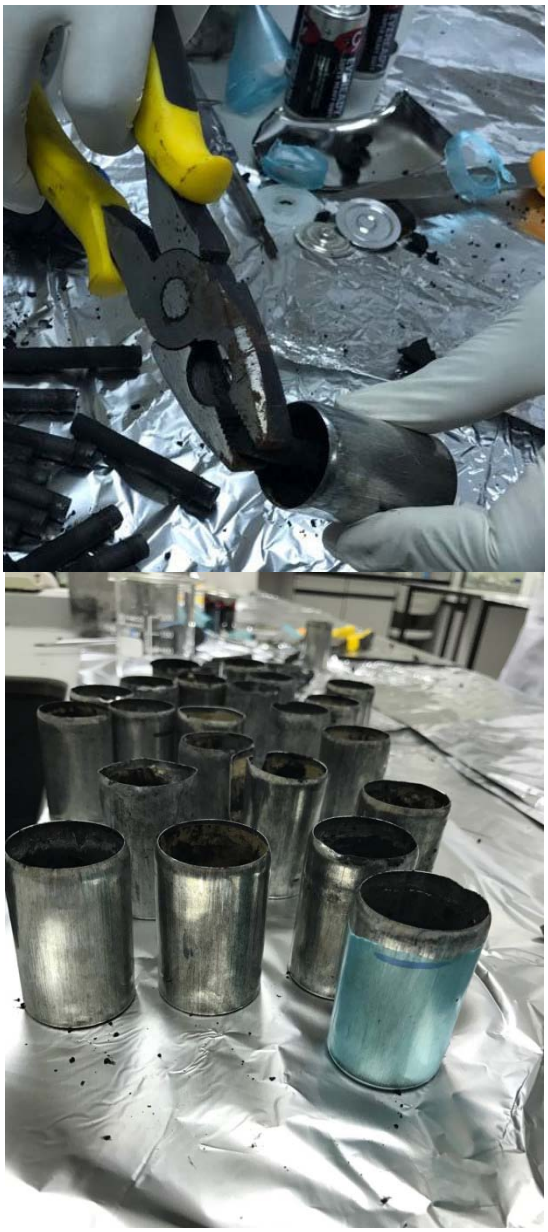

Figure 4: Battery graphite cathode removal

III. Experimental Setup & Procedure

The manganese sulphate is produced from the reaction between manganese dioxide and sulphuric acid in the presence if oxalic acid. The reaction of MnO_2 in the low manganese ore with oxalic acid could occur as follows:

$$C_2H_2O_4 + MnO_2 + 2H \text{ --------- } 2CO_2 + Mn + 2H_2$$

The leaching experiments should be carried out carried out in a 1000 mL three-neck flask (reactor). A magnetic heater stirrer was used to heat and agitate the reaction mixture. The reactor should have two entrances used for feeding of reactants and temperature measurement. A reflux condenser may be erected on the 3rd neck to capture any escaped vapors. So that it has very good control of the process which may yield the pure product.

But this project was carried out manually in the laboratory with different samples. In the leaching experiment the solution were prepared using distilled water, sulphuric acid and oxalic acid. The temperature of the reaction mixture were manually measure using thermometer.

When Manganese dioxide is reacting with 98% concentrated sulphuric acid in the presence of oxalic acid and yields manganese (II) sulphate. During the reaction carbon dioxide gas is evolved. The different reactions takes place during the process are

$$MnO_2 + H_2SO_4 + C_2O_4H_2 \longrightarrow MnSO_4 + 2H_2O + 2CO_2$$

$$Mn_2O_3 + H_2SO_4 \longrightarrow MnO_2 + MnSO_4 + H_2O$$

$$Mn_3O_4 + 2H_2SO_4 \longrightarrow MnO_2 + 2MnSO_4 + 2H_2O$$

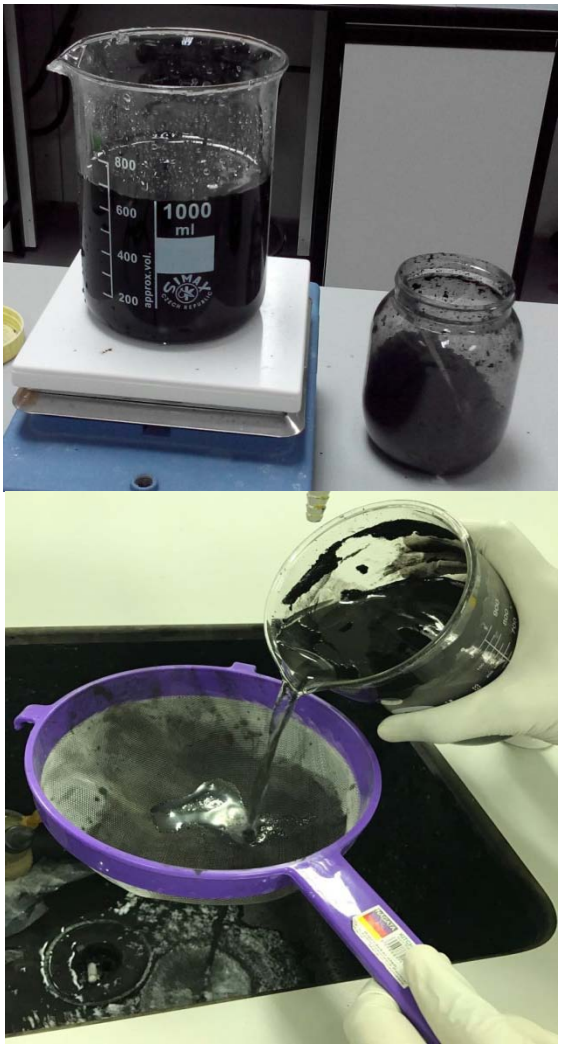

Figure 5: Manganese oxide washing

The step by step production methods are given in the below figures one by one. The battery paste (Manganese dioxide & manganese oxide) which is

collected from the batteries are washes with distilled water for many times and then filtered.

Normally the battery paste contain many impurities like the outer paper cover and other light materials. That's why it is washed so many time in order to remove those impurities. During washing with water the glass rod is continuously stirred in the battery paste so that it will be evenly distributed.

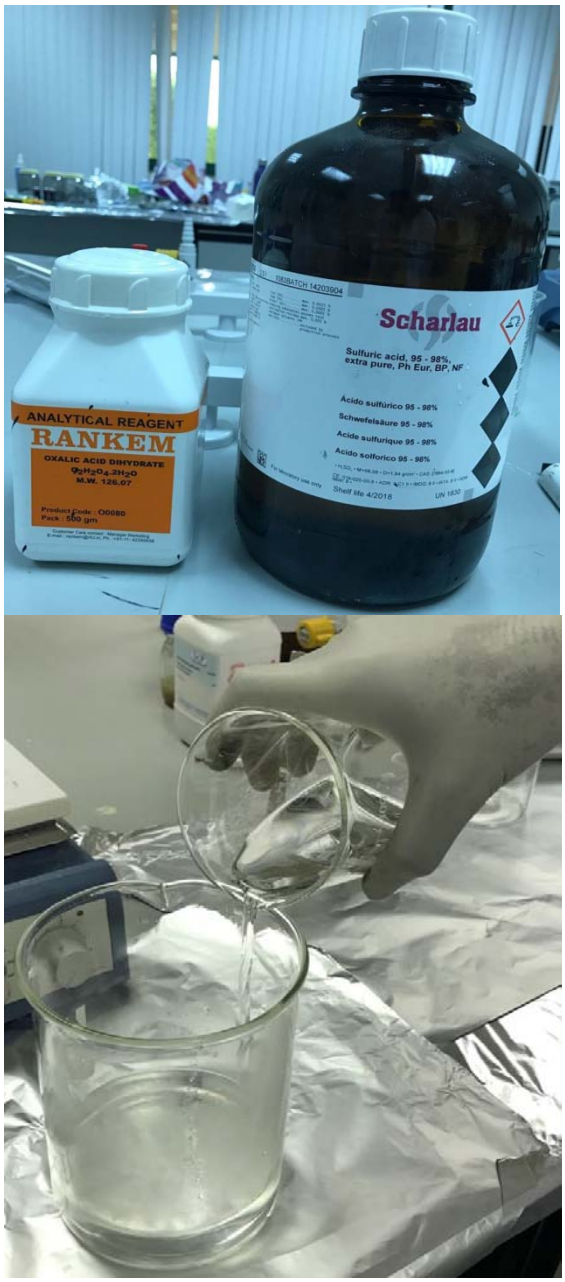

Figure 6: Sulphuric acid & Oxalic acid

The 98% sulphuric acid and oxalic acid salt were taken in different beakers. First the oxalic acid salt is dissolved in suitable amount of water. Then it is mixed with 98% concentrated sulphuric acid gently.

Now the battery paste (manganese dioxide) is kept on the magnetic stirrer hot plate and it is gently heated.

Figure 7: Manganese dioxide paste heated

The mixture of sulphuric acid and oxalic acid solutions are slowly added to the manganese dioxide paste. The reaction is carried out with evolution of carbon dioxide. The solution should be added very very slowly so that there should not be more fumes.

After adding the solution keep the mixture 30 minutes in order to complete the reaction. Then keep the solution at room temperature for 2-3 hours for cooling. The clear supernatant liquid is the manganese sulphate solution and the bottom precipitate is the reacted and unreacted manganese oxides with water.

Figure 8: Reaction

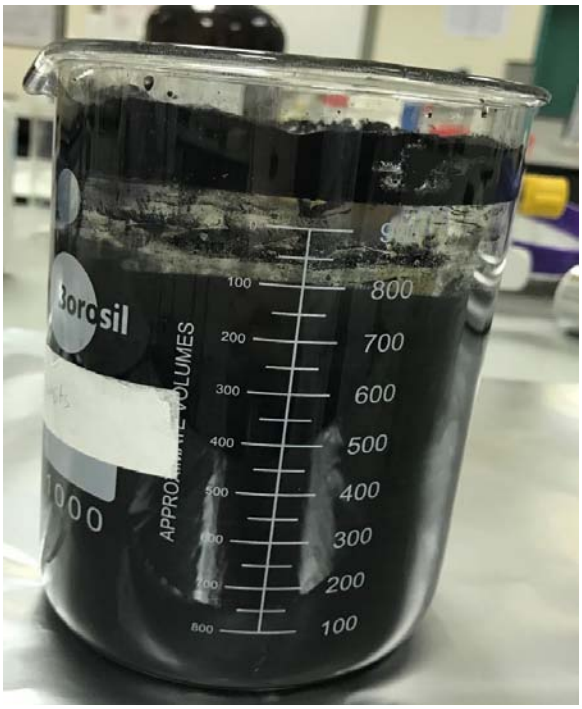

Figure 9: Reaction mixture

Then the supernatant liquid is filtered in the Whatmann filter paper in order to get the manganese sulphate solution. The solution is light pink in color and the black paste can be discarded.

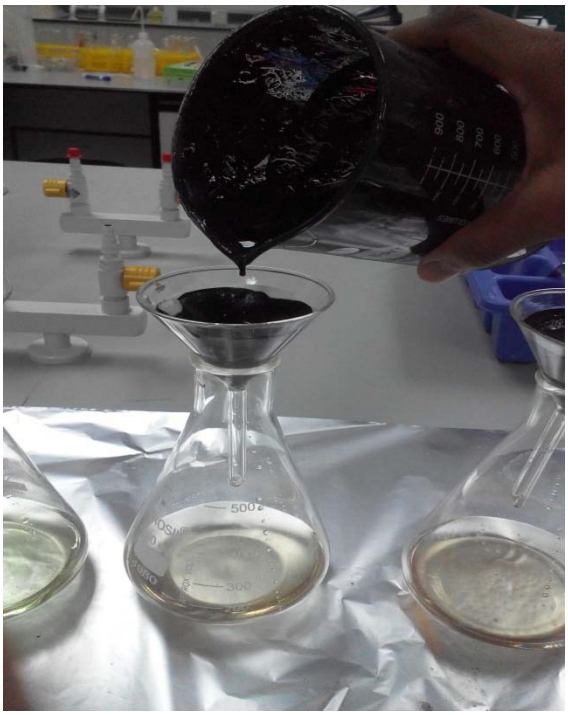

Figure 10: Manganese sulphate solution filtered

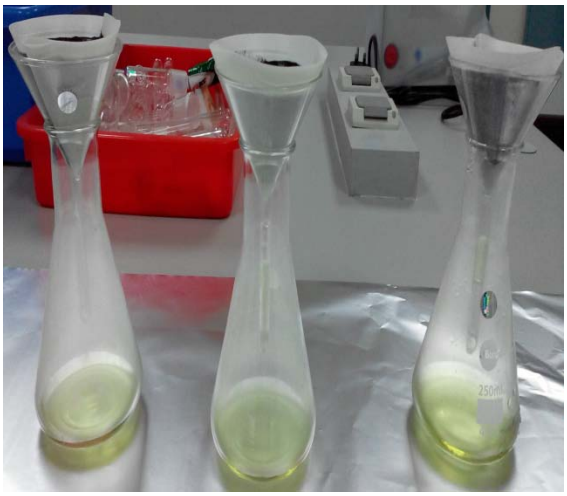

Figure 11: Manganese sulphate solution

The above manganese sulphate solutions are heated to evaporate the water and then it is crystalized by vacuum in order to get the manganese sulphate crystals.

The crystals which is formed from the solution is dried in the oven at 600C to get the dry manganese sulphate powder. This Manganese sulphate is analyzed in spectrophotometer to find the percentage is Manganese in the salt. This percentage determines its market value cost.

Figure 12: Manganese sulphate crystals

Figure 13: Manganese sulphate final product

Figure 14

IV. Conclusion

This experiment was carried out to produce manganese (II) sulphate from manganese dioxide which is extracted from waste used alkaline batteries. In UAE, the uses of alkaline batteries are vast. These batteries are simply makes the lots if environmental pollution after it is disposed to environment. Firstly this project eliminates this type of pollution. And secondly the production of Manganese (II) sulphate. Because of lots of uses of manganese sulphate, which is imported in larger quantities every year. It is one of the great business idea for chemical engineers in the present and future UAE industrial sectors. The product produced needs some more purification in order to improve the manganese content in the salt. The future studies are proposed for the quality improvement and also extracting manganese metal from the waste used batteries.

Acknowledgement

The authors are gratefully thanked to the management of Higher Colleges of Technology, Al Ruwais, United Arab Emirates, for providing facilities to carry out the project work.

References Références Referencias

1. Boyanov, V. V. Konareva, and N. K. Kolev, "Purification of zinc sulfate solutions from cobalt and nickel through activated cementation," Hydrometallurgy, vol. 73, no. 1-2, pp. 163–168, 2004.
2. C. C. B. M De Souza, D. C. De Oliveira, and J. A. S. Tenório, "Characterization of used alkaline batteries powder and analysis of zinc recovery by acid leaching," Journal of Power Sources, vol. 103, no. 1, pp. 120–126, 2001.
3. Dell RM, D.A.J.R and, "Understanding batteries" Chapter 5.2: Alkaline Manganese cell, pp: 59-64, the royal society of chemistry, 2001.
4. Devi, K. C. Nathsarma, and V. Chakravortty, "Extraction and separation of Mn(II) and Zn(II) from sulphate solutions by sodium salt of Cyanex 272," Hydrometallurgy, vol. 45, no. 1-2, pp. 169–179, 1997.
5. Fahim MS, El-Faramawy H., Ahmed AM, Ghali SN, Kandil AT. J of Minerals and Materials Characterization and Engineering 2013; 1: 68-74.

6. Ferella, G. Furlani, M. Navarra et al., "Hydrometallurgical plant to recycle alkaline and Zn-C spent batteries: process and economic analysis," in Proceedings of the 2nd International Conference on Engineering for Waste Valorization, Patras, Greece, 2008.
7. Gajbhiye, U. Bhattacharya, and V. S. Darshane, "Thermal decomposition of zinc-iron citrate precursor," Thermochimica Acta, vol. 264, pp. 219–230, 1995.
8. Himmelblau, Process Analysis by Statistical Methods, John Wiley & Sons, New York, NY, USA, 3rd edition, 1978.
9. Jantscher W, Binder L, Fiedler D A, Andreaus R, Kordesch K. Synthesis, characterization and application of doped electrolytic manganese dioxides. *Journal of Power Sources*, 1999, 79(1): 9-18.
10. Kim H S, Kim H J, Cho W, Cho B W, Ju J B. Discharge characteristics of chemically prepared MnO_2 and electrolytic MnO_2 in non-aqueous electrolytes. *Journal of Power Sources*, 2002, 112(4): 660-664.
11. Malloy A P, Donne S W. Surface characterization of chemically reduced electrolytic manganese dioxide. *Journal of Colloid and Interface Science*, 2008, 320(1): 210-218.
12. Maphanga R R, Parker S C, Ngoepe P E. Atomistic simulation of the surface structure of electrolytic manganese dioxide. *Surface Science*, 2009, 603(21): 3184-3190.
13. Morita M, Iwakura C, Tamura H. The anodic characteristics of manganese dioxide electrodes prepared by thermal decomposition of manganese nitrate. *Electro-chimica Acta*, 1977, 22(4): 325-328.
14. Nan, D. Han, M. Cui, M. Yang, and L. Pan, "Recycling spent zinc manganese dioxide batteries through synthesizing Zn-Mn ferrite magnetic materials," Journal of Hazardous Materials, vol. 133, no. 1-3, pp. 257–261, 2006.
15. Pagnanelli F, Sambenedetto C, Furlani G, Veglio F, ToroL. Preparation and characterization of chemical manganese dioxide: effect of the operating conditions. *Journal of Power Sources*, 2007, 166(2): 567-577.
16. Pagnanelli, F., C. Sambenedetto and L. Toro, 2007. Preparation and Characterization of Chemical Manganese Dioxide: Effect of the Operation Conditions. *Journal of Power Sources*, 166 (2): 567-577.
17. Salgado, A. M. O. Veloso, D. D. Pereira, G. S. Gontijo, A. Salum, and M. B. Mansur, "Recovery of zinc and manganese from spent alkaline batteries by liquid-liquid extraction with Cyanex 272," Journal of Power Sources, vol. 115, no. 2, pp. 367–373, 2003.
18. Sayilgan, T. Kukrer, F. Ferella, A. Akcil, F. Veglio, and M. Kitis, "Reductive leaching of manganese and zinc from spent alkaline and zinc-carbon batteries in acidic media," Hydrometallurgy, vol. 97, no. 1-2, pp. 73–79, 2009.
19. Sayilgan, T. Kukrer, G. Civelekoglu et al., "A review of technologies for the recovery of metals from spent alkaline and zinc-carbon batteries," Hydrometallurgy, vol. 97, no. 3-4, pp. 158–166, 2009.
20. Sunavala PD, Recycling of Municipal Agricultural and Industrial Wastes to regenerate renewable sources of Energy. *J. Sci. Ind. Res.* 1981, 547, 40.
21. Vatistas, M. Bartolozzi, and S. Arras, "The dismantling of the spent alkaline zinc manganese dioxide batteries and the recovery of the zinc from the anodic material," Journal of Power Sources, vol. 101, no. 2, pp. 182–187, 2001.
22. Wang S M, Zheng X W, Fan X M, Wang J F. Progress in the preparing methods of chemical manganese dioxide. *Journal of Shangluo University*, 2008, 22(2): 35-40.
23. Xará, J. N. Delgado, M. F. Almeida, and C. A. Costa, "Laboratory study on the leaching potential of spent alkaline batteries," Waste Management, vol. 29, no. 7, pp. 2121–2131, 2009.
24. Xi, Y. Li, and Y. Liu, "Study on preparation of manganese-zinc ferrites using spent Zn-Mn batteries," Materials Letters, vol. 58, no. 7-8, pp. 1164–1167, 2004.
25. http://data.energizer.com/pdfs/alkaline_appman.pdf
26. http://ec.europa.eu/environment/waste/batteries/
27. http://electronics.howstuffworks.com/everydaytech/battery.htm
28. http://makezine.com/projects/harvesting-chemicals-from-a-battery/
29. http://www.google.com/patents/US8440153
30. http://www.uobabylon.edu.iq/eprints/paper_4_22738_736.pdf
31. http://www.webmd.com/vitaminssupplements/ingredientmono-182manganese.aspx?Activeingredientid=182&
32. https://archive.epa.gov/epawaste/hazard/web/html/batteries.html
33. https://en.wikipedia.org/wiki/Alkaline_battery
34. https://en.wikipedia.org/wiki/Battery_(electricity)
35. https://en.wikipedia.org/wiki/Battery_recycling
36. https://en.wikipedia.org/wiki/Manganese(II)_sulfate
37. https://growguru.co.za/uses-for-manganese-sulphate-in-horticulture/
38. https://www.britannica.com/technology/batteryelectronics#ref71263

Global Journal of Researches in Engineering: C
Chemical Engineering
Volume 17 Issue 3 Version 1.0 Year 2017
Type: Double Blind Peer Reviewed International Research Journal
Publisher: Global Journals Inc. (USA)
Online ISSN: 2249-4596 & Print ISSN: 0975-5861

Assessing the Impacts of Viscosity and Radiative Transfer in Internal Detonation Scenarios Involving Hydrogen-Air Mixtures

By Lucky Nteke Mulenga & Gautham Krishnamoorthy
University of North Dakota

Abstract- Predictions from a hydro code are compared against those obtained from a computational fluid dynamics (CFD) framework to numericall yassess the effects of: viscous and radiative losses associated with a propagating pressure wave, the point source ignition approximation, and their subsequent impact on the over-pressure characteristics during internal detonation scenarios involving hydrogen-air mixtures. The hydro code employed: TNT equivalencies to represent the heat of hydrogen combustion and solved the inviscid (Euler) equations in conjunction with the JWL equation of state for momentum transport. The CFD simulations resolved the detonation wave employing: the SRK equation of state, Large Eddy Simulations and employed spectrally-averaged mean absorption coefficients for the radiative properties. Detonation wave propagation in air (non-reacting) as well as in premixed hydrogen-air mixtures(reacting) were studied employing a 21-step detailed chemistry mechanism.

Keywords: *hydrogen detonation; hydro code; detailed chemistry; radiative heat transfer; CFD.*

GJRE-C Classification: *FOR Code: 290699*

Strictly as per the compliance and regulations of:

Assessing the Impacts of Viscosity and Radiative Transfer in Internal Detonation Scenarios Involving Hydrogen-Air Mixtures

Lucky Nteke Mulenga [α] & Gautham Krishnamoorthy [σ]

Abstract- Predictions from a hydro code are compared against those obtained from a computational fluid dynamics (CFD) framework to numericall yassess the effects of: viscous and radiative losses associated with a propagating pressure wave, the point source ignition approximation, and their subsequent impact on the over-pressure characteristics during internal detonation scenarios involving hydrogen-air mixtures. The hydro code employed: TNT equivalencies to represent the heat of hydrogen combustion and solved the inviscid (Euler) equations in conjunction with the JWL equation of state for momentum transport. The CFD simulations resolved the detonation wave employing: the SRK equation of state, Large Eddy Simulations and employed spectrally-averaged mean absorption coefficients for the radiative properties. Detonation wave propagation in air (non-reacting) as well as in premixed hydrogen-air mixtures(reacting) were studied employing a 21-step detailed chemistry mechanism.

The adequacy of our modeling procedure was first established by obtaining reasonable greement between our predictions from the two modeling frameworks wither ported measurements from a small-scale explosion study. The same CFD modeling methodology was subsequently extended to larger scales. The heats of reaction resulted in acceleration and strengthening of the wave front in both lean and rich hydrogen-air mixtures investigated in this study, with trends agreeing with predictions from flame speed theory. However, viscous losses resulted in a noticeable weakening of the detonation wave during its propagation. Including the effects of radiative transfer had no impact on the wave propagation due to the relative magnitudes of the radiative source and chemical heat release terms.

Keywords: hydrogen detonation; hydro code; detailed chemistry; radiative heat transfer; CFD.

NOMENCLATURE

E	Energy released during detonation (J)
K	Absorption coefficient (m^{-1})
L	Path length (m)
T	Temperature (K)
P	Pressure (atm)
q	Radiative heat flux (W/m^2)
R	Distance from the center of the explosion
C	JWL constant
r	JWL constant

Greek symbols

ω	Specific heat (J/kg-K)
ϑ	Specific volume (m^3/kg)
γ	Specific heat ratio
ρ	density (kg/m^3)
ε	Internal energy (J/kg)
σ	Stefan-Boltzmann constant(5.67e-08 W/m^2-K^4)

Subscripts

∞	surrounding conditions
g	gas

Author α σ: Department of Chemical Engineering, PO Box 7101, Harrington Hall Room 323, 241 Centennial Drive, University of North Dakota, Grand Forks, ND 58202-7101, USA.
e-mails: lucky.mulenga@ndus.edu, gautham.krishnamoorthy@engr.und.edu

I. Introduction

The response of structures to dynamic pressure loading during an accidental detonation scenario is a critical component of industrial hazard assessment. In order to carry out this assessment accurately, fidelities in: the magnitude and duration of the overpressures, as well as the positive and negative impulses resulting from the detonation wave are desired. During the accidental detonation of an explosive mixture in a realistic scenario, the nature of interactions between the blast waves and structures in an irregular geometry is quite complex. This makes it difficult to use or extend analytical expressions for pressure profiles that have been established for simple enclosures to other geometric configurations [1].

Further, compositional non-homogeneities resulting from the convective and diffusive forces within the enclosure and after-burn effects can further strengthen a propagating detonation wave due to chemical heat release. This can reduce the applicability of established analytical expressions and scaling laws even further. Therefore, computational fluid dynamics (CFD) codes that can resolve these complex geometric and multi-physics characteristics adequately are often utilized to simulate such scenarios. Among these are:

1. *Hydrocodes (such as ANSYS AUTODYN [2]):* That employs TNT equivalencies for detonation initiation and solves inviscid (Euler) equations with a real gas equation of state to quickly resolve the propagation of a detonation wave. Heats of reactions and radiative losses are ignored in this framework.

2. *Multiphysics CFD codes (such as ANSYS FLUENT [3]):* That have the ability to include the effects of turbulence, gas-phase reactions and radiative losses in the detonation wave albeit at an increased computational cost relative to the hydro codes.

While both computational frameworks have been employed in isolation to simulate different detonation scenarios, comparing and validating their predictions against measurements from the same detonation experiment can provide insights into the importance of different models that are ignored in hydro code simulations. *Therefore, the primary goal of this manuscript is to assess the effects of after-burn chemistry, viscous and radiative losses during the propagation of a detonation wave to enable users to select appropriate modeling options and CFD frameworks for carrying out their study. The adequacy of our modeling methodology is demonstrated in this study by studying hydrogen-air systems due to the abundance of experimental measurements, well-established chemistry mechanisms and availability of radiative property models for water vapor.* However, it will be clear that the same methodology can be extended to study after-burn and radiative transfer resulting from the decomposition products of condensed-phase explosives where these effects may be more pronounced.

a) The Importance of Detailed Chemistry and Viscous Effects

Recent studies that have employed large cell sizes in conjunction with the Large Eddy Simulation (LES) methodology to model hydrogen explosions in domain sizes of practical interest have provided encouraging signs that such calculations are computationally feasible within a reasonable time frame [4, 5]. These two studies by Zbikowski et al. [4, 5] employed the progress variable formulation to simulate the propagation of the reaction front in premixed hydrogen-air mixtures. The chemical kinetics in this methodology was incorporated through the specification of a detonation velocity that goes into the source term of the progress variable equation. However, due to the dependence of the detonation velocity on the mixture equivalence ratios, extending the progress variable framework to simulate detonation in non-homogeneous mixtures is not straightforward. Nevertheless, simulation of deflagration (flame propagation) in non-homogeneous hydrogen-air mixtures using the progress variable combustion model has recently been demonstrated [6].

In spite of the lower computational cost and stability associated with the progress variable approach, a recent study reported by Feldgun et al. [7] concluded that in order to account for the residual blast pressures in confined explosions accurately, the effects of after burn chemistry needs to be taken into account. Further, the heat capacity ratio (which changes as a result of after burn chemistry) was seen to have a stronger effect on the gas pressure predictions than the internal energy of explosion. Liberman et al. [8] showed that predictions of temperature-gradient induction lengths that are thought to play a vital role in triggering detonations in deflagration-to-detonation (DDT) scenarios are sensitive to the chemistry models employed in the simulations. Minimal induction length predictions when employing detailed chemistry models along with accurate kinetic-transport models were found to be 2-3 orders of magnitude greater than those predicted employing single – step global chemistry models. Therefore, these two studies [7, 8] highlight the importance of employing detailed chemistry models during simulations of detonation scenarios whenever computationally feasible.

b) The Importance of Radiative Transfer

The importance of including the effects of radiative transfer in the context of dust explosions in hydrogen-oxygen mixtures was examined by Liberman et al [9, 10]. By considering the gas mixture to be transparent and the dispersed phase to be radiatively participating, radiative transfer was found to cause heating of the particles ahead of the flame followed by re-emission of this radiation. This radiative preheating of the mixture ahead of the flame either increased the flame velocity or triggered detonation through the Zeldovich gradient mechanism[11]. Therefore, the studies by Liberman et al [9, 10] highlight the importance of including the effects of radiative transfer in the detonation wave simulations.

While hydro codes do not include the effects of viscosity, detailed chemistry and radiative transfer, they have yielded reasonable agreement with experimental measurements of detonating hydrogen-air mixtures in small scale geometries where after-burn chemistry was not important [12]. This was accomplished by representing the heat of combustion of the hydrogen-air explosive mixtures in terms of TNT equivalencies and initiating the detonation over a point source. However, in larger geometries, viscous and radiative losses may become more important with increase in the wave propagation time. Further, if the wave propagates in a premixed hydrogen-air mixture, the heat of reaction can result in acceleration and strengthening of the wave and exacerbate the effects of radiative transfer, resulting in phenomena that cannot be taken into account easily in hydro codes. Therefore, in this study we examine hydrogen-air mixtures to:

1. Assess the validity of the approximations inherent in hydro-codes when simulating a spherical detonation wave resulting from the detonation of a gaseous charge. These approximations include: assumptions of a point source, assumptions of a perfectly spherical wave, absence of turbulence, presence of

confinements and the assumption of an energy efficiency of one where all of the chemical energy released goes towards the propagation of the pressure wave.

2. To assess the impacts of viscous and radiative losses during the propagation of a pressure wave resulting from the detonation of hydrogen-air mixtures at larger scales.
3. Investigate the effects of heat of reaction towards strengthening or weakening a detonation wave as it propagates through a premixed hydrogen-air mixture.

In contrast to the dust explosion study by Liberman et al [9, 10], we consider a radiatively participating gas phase (air or water vapor). Since the shock layer was determined to be optically thin ($kL << 1$), where k is the absorption coefficient (in m^{-1}) and L the path length (in m), a spectrally averaged Planck mean absorption coefficient for the radiative properties of water vapor [13] and air [14] were computed for the scenarios and employed in conjunction with an optically thin radiation modeling approximation. As per this approximation, the temperature and pressure dependent absorption coefficients were computed as:

$$K_{air} = 3.7516 \times 10^{-6} \cdot (P)^{1.31} \cdot \exp(5.18 \times 10^{-4} T - 7.13 \times 10^{-9} T^2) \quad (1)$$

$$K_{H2O}(g) = 5.4 \times 10^{7} \cdot (T)^{-2.35} \cdot P_{H2O} \quad (2)$$

These were then employed to compute the radiative source term (divergence of the radiative flux q) in the energy equation at each spatial location as:

$$\nabla \bullet q = 4\sigma K(T^4 - T_\infty{}^4) \quad (3)$$

where σ is the Stefan-Boltzmann constant, K the absorption coefficient, T and T_∞ are the local and surrounding temperatures respectively. Equations 1 through 3 were implemented as a User-Defined Function in ANSYS FLUENT. The optically thin radiation approximation has previously been used in estimating radiation from air in hypersonic shock layers [15] as well as from radiatively participating combustion products in mildly radiating combustion flames [16].The adequacy of our modeling procedures are first establishedby comparing our numerical predictions using both computational frameworks against reported measurements from a small-scale explosion study [17].

The modeling methodology was then extended to other scenarios encompassing changes to the domain size and premixed hydrogen-air mixtures.

II. Methods

Our hydro code prediction methodology for the small scale (Case 1) explosion study followed closely the procedure adopted by Zyskowski et al [12] and is summarized in brief. The containment is a parallelepiped wooden box of length, width and height 500, 400 and 300 mm respectively with twelve pressure sensors located at various points on the containment surface (Figure 1a). During the experiments, detonation was initiated by igniting an explosive gaseous hydrogen-oxygen mixture at stoichiometric conditions within a hemispherical soap bubble of radius 30 mm. Since ANSYS AUTODYN cannot simulate the energy released during hydrogen-oxygen detonations directly, the energy released during the combustion process was represented through an equivalent amount of TNT detonation and patched over a radius of 30 mm. The initial phases of the blast wave propagation were simulated in 1D (radial direction only) assuming spherical symmetry in the shock wave development. The subsequent phases (after 0.1 ms of elapsed time) of the blast waves were carried out in 3D through a mapping of the 1D solution into a 3D domain. By utilizing the thermodynamic properties in the ANSYS AUTODYN library, air was modeled employing the ideal gas equation of state (Eq.4) whereas the Jones-Wilkins-Lee (JWL) equation of state was employed to model TNT (Eq. 5):

$$p = (\gamma - 1) \cdot \rho \cdot \varepsilon \quad (4)$$

$$P = C_1 * \left(1 - \frac{\omega}{r_1 \vartheta}\right) * e^{-r_1 \vartheta} + C_2 * \left(1 - \frac{\omega}{r_2 \vartheta}\right) * e^{-r_2 \vartheta} + \frac{\omega \varepsilon}{\vartheta} \quad (5)$$

In Eqs (4) and (5) p, ρ and γ represent the pressure, density and specific heat ratios respectively. ε is the internal energy, C_1, C_2, r_1, r_2 are constants, ω is report of the specific heat and $\vartheta$the specific volume.

In the CFD simulations using ANSYS FLUENT, a 3D representation of the parallelepiped geometry of the small-scale geometry (Case 1) was created and a hemispherical bubble of 30 mm was patched with the thermodynamic state associated with the combustion products resulting from combustion of a stoichiometric hydrogen-oxygen mixture in a constant volume reactor. In Case 2, the domain was enlarged 10 times in each direction and a hemispherical bubble of radius 300 mm was patched with TNT. In order to run the detonation scenarios successfully, we had to create a spherical indentation of radius 30mm (for Case 1) and 300mm (for Case 2) as shown in Figure 1b. The domain was meshed with 63,300 quadrilateral elements resulting in nearly the same sizes as those employed in the AUTODYN simulations. In order to initiate the detonation, 3 computational cells normal to the hemispherical surface were patched with a temperature of 3473 K (as shown in Figure 1b) corresponding to the adiabatic flame temperature of stoichiometric hydrogen-

oxygen mixtures. Next, based on the volume of the detonation kernel and the patched temperature, the ideal gas equation of state was employed to compute the pressure within the detonation volume.

Table 1 summarizes the initial conditions within the detonation kernel in the two computational frameworks when simulating detonation of a stoichiometric hydrogen-oxygen mixture. The propagation of the detonation wave in air (non-reacting) as well as lean and rich premixed hydrogen-air mixtures were also simulated employing ANSYS FLUENT. It was ensured that the critical radius and critical energy for detonation initiation was greater than the values reported in Liu et al [18]. The simulations were allowed to run for 2ms (for Case 1) or 20ms(for Case 2) and pressure profiles were recorded at the gauges placed throughout the geometry. The various modeling options employed in the two computational frameworks are summarized in Table 2.The Pressure-Based Coupled solver where the momentum and pressure-based continuity equations are solved together was employed in ANSYS FLUENT for the Pressure-Velocity coupling across all scenarios. It is worth noting that for these spherical detonation scenarios, the mesh resolution (~1 cm for Case 1 and ~10 cm for Case 2) have previously been deemed be adequate when employed in conjunction with the LES model [20, 21]. The minimum size of the control volume employed by Molkov et al. [20] in their study was 40 cm whereas Tomizuka et al. [21] deemed cell sizes less than 20 cm to be adequate for simulating hydrogen-air explosion in a large domain.

III. Results And Discussion

a) Small-Scale Study (Detonation wave propagation in air)

The transient pressure predictions at the different gauges in the small scale (1 X) explosion study (Case 1) are shown in Figure 2. A reasonably good agreement between the two modeling frameworks as well as the experiment is observed, indicating the adequacy of our modeling procedures. As seen in Figure 1a, Gauge 12 is located closest to the onset of detonation and therefore experiences the pressure pulse the fastest. Gauge 1 on the other hand is located the farthest and this is reflected in the pressure pulse arrival time. Since Case 1 corresponds to the detonation of a shock wave arising from high-pressure water vapor (the combustion product of a stoichiometric hydrogen-oxygen mixture) through air, there is no after-burn chemistry involved in this scenario. Further, the temperature increase across the shock wave was modest (~30 K) that accounting for the effects of radiative transfer in air by computing absorption coefficients and radiative source terms through Eqs. 1 and 3 had no impact on the results.

b) Large-Scale Study 10x (Detonation wave propagation in air)

Next, the propagation time of the pressure wave before it encountered the containment surface was increased ten-fold by making the domain ten times larger. The contours of gauge pressure, velocity and viscosity ratios (turbulent viscosity/molecular viscosity) after 3 ms in the large scale explosion study are shown in Figure 3. As seen in Figure 3c, the turbulent sub-grid viscosity computed using the Smagorinsky LES model [3] is four orders of magnitude greater than the molecular viscosity. It was envisioned that the increase in viscosity in conjunction with the increase in propagation time would slow down the propagation of primary and secondary shocks. To ascertain this, Case 2 was also simulated using both the ANSYS AUTODYN and ANSYS FLUENT frameworks. The transient pressure predictions at the different gauges comparing the LES calculations (ANSYS FLUENT) against the in viscid Euler calculations (ANSYS AUTODYN) are shown in Figure 4.

The magnitudes of the first peak of the reflected over-pressures at the different gauges are similar to those observed in the small-scale study (cf. Figure 2) albeit the shock wave arrival time has increased by a factor of ten due to the enlarged domain. This confirms the adherences to Hopkinson's similitude since the reduced distance of the pressure sensor ($R/E^{1/3}$) is the same in both cases, where R is the distance from the explosion center and E the energy released during the reaction. There are discernable differences between the results from the two modeling frameworks with the pressure wave from the inviscid AUTODYN calculations travelling faster than the LES calculations using ANSYS FLUENT. Again, the effects of radiative transfer did not have any bearing on the predictions (LES calculations without radiative transfer were identical to those with radiative transfer and not shown in Figure 4 for brevity).

The temperature increase across the shock wave was found to be only 30 K and this is reflected in the radiative source term magnitude of about 1 W/m^3. Our previous study of radiative transfer across shock waves in air during atmospheric re-entry [15] showed that the radiative source terms need to have magnitudes of 4,000 to 10,000 $W/m^3$to have an impact on the density and velocity profiles.

c) Pressure wave propagation in lean and rich hydrogen-air mixtures

The propagation of the detonation wave in fuel-lean and fuel-rich premixed hydrogen air mixtures within the domain was simulated next. The domain compositions corresponding to these two scenarios are shown in Table 1. The chemistry was accounted for employing a 21-step detailed chemistry mechanism for hydrogen-air combustion [19]. The equivalence ratios/compositions for the fuel-lean and fuel-rich conditions were intentionally chosen based on the large

differences in the laminar burning velocities observed in closed vessel gas explosion experiments by Dahoe [22].The peak flame speeds were observed at the fuel-rich composition of 40 mol % H_2 whereas the flame speed at the fuel lean composition of 20 mol% H_2 were lower by a factor of nearly three. Eq. (2) was employed to compute the radiative properties of water vapor. Eq. (2) in fact represents a curve-fit to the Planck mean absorption coefficients computed from line-by-line data reported in Rivière and Soufiani [13]. The goodness of this fit is shown in Figure 5. The contours of Planck mean absorption coefficient in m^{-1} and the radiative source term after 0.5 ms in the large scale explosion study at fuel-rich and fuel-lean domain conditions are shown in Figure 6. While the magnitudes of the absorption coefficient are identical in both scenarios, the radiative source term magnitude in the fuel-rich condition is nearly twice that under fuel-lean conditions. Further, the wave propagation is faster under fuel-rich conditions and about 5 times faster than the non-reacting case (comparing the positions of the shock wave in Figures 3 and 6).

Figure 7 shows contours of gauge pressure, velocity and reaction source terms after 0.5 ms in the fuel-lean and fuel-rich condition scenarios. Although the gauge pressures are identical, the velocities are 20% lower in the fuel-lean condition which qualitatively correlates with the observations of Dahoe [22] for hydrogen-air deflagration scenarios. The differences in the detonation velocities are more evident when looking at the transient pressure profiles at two of the gauges shown in Figure 8. While the over-pressures are identical in both cases, the detonation velocity is clearly higher during fuel-rich conditions.

In order to discern the effects of viscosity during the propagation of the reacting detonation wave, an additional set of calculations were carried out employing the inviscid option in ANSYS FLUENT. The transient pressure predictions at the different gauges are shown in Figure 9. It is worth noting that in Gauge 12 which is closer to the center of explosion (cf. Figure 1b), the arrival times and intensity of the pressure wave are unaffected by viscosity. However, by the time the detonation wave reaches Gauge 1, a distinct weakening of the pressure wave is noticeable in both fuel-lean and fuel-rich scenarios.

Figure 10 shows the impact of including radiative transfer effects on the detonation wave propagation. In spite of the higher magnitude of the radiative source term resulting from the higher temperatures of the reacting shock front seen in Figures (6c and 6d), including the effects of radiative transfer had no bearing on the shock wave propagation characteristics (i.e., magnitudes and arrival times). This is due to the fact that the magnitude of the reaction source term to the energy equation (Figures 7 (e, f)) were three orders of magnitude greater than the corresponding magnitudes of the radiative source term (Figures 6 (c, d)), therefore minimizing the impact of radiation on the wave propagation characteristics.

IV. Conclusions

In lieu of the growing recent evidence advocating the importance of detailed chemistry models, viscous effects and radiative transfer in detonation scenarios, the primary goal of this manuscript was to assess these effects to enable users to select appropriate modeling options and CFD frameworks (hydro-codes versus complex multi-physics codes) for their study. Hydrogen-air mixtures were investigated in this study due to the availability of experimental measurements, well-established chemistry mechanisms and radiative property models for the combustion products at high temperatures and pressures.

Predictions from a hydro code were compared against combustion simulations employing CFD techniques. The hydro-code solved the inviscid Euler equations with the JWL equation of state. Detonation was initiated using established TNT equivalencies for a stoichiometric hydrogen-oxygen mixture. The CFD simulations rigorously resolved the detonation wave employing: the SRK equation of state for densities, Large Eddy Simulations for turbulence and spectrally averaged Planck mean absorption coefficients. In addition, a 21-step detailed chemistry model was employed in scenarios where the detonation wave was allowed to propagate through lean and rich premixed hydrogen-air mixtures. In the CFD simulations, detonation was initiated by patching the adiabatic flame temperature in a spherical volume of gas at the center of the domain and employing the ideal gas equation of state to determine the pressure in the patched region at constant volume reactor conditions. Further, a temperature and pressure dependent Planck mean absorption coefficient for the radiative properties of water vapor and air were implemented in the CFD code as add-on functions and employed in conjunction with an optically thin approximation. As a result of comparing the predictions from these two modeling frameworks across the investigated scenarios encompassing variations in: domain size and reacting/non-reacting scenarios, the following conclusions can be drawn:

1. Predictions from the two modeling frameworks against reported measurements from a small-scale (Case 1) explosion study were in reasonable agreement, thereby establishing the adequacies of our modeling methodologies. This alleviates concerns regarding the effects of the approximations inherent in hydro codes when the explosion of a gaseous charge is simulated by converting it to TNT equivalencies when after-burn effects are not deemed important. These include:

assumptions of a point source, assumptions of a perfectly spherical wave, absence of turbulence, presence of confinements and the assumption of an energy efficiency of one where all of the chemical energy released goes towards the propagation of the pressure wave.

2. When the same methodology was extended to larger scales (Case 2), the over-pressure predictions compared well in adherence to Hopkinsons Scaling Law. While there was a ten-fold increase in the wave propagation times to reach the enclosure surface in the larger domain, the over pressure characteristics were unaffected by the effects of radiative transfer in both Case 1 and Case 2 since the temperature increase across the shock was modest (~30 K) when the wave was propagating in air.
3. When the detonation wave was allowed to propagate in rich (40 mol% hydrogen) and lean (20 mol% hydrogen) premixed hydrogen-air mixtures, the resulting heat of reaction resulted in a significant acceleration and strengthening of the wave front. Although the magnitudes of the over-pressures were similar in both lean and rich mixtures, the detonation wave propagation was faster in the rich mixture. These trends agree qualitatively with measurements from closed vessel gas explosion experiments. Further, comparing inviscid calculations with those employing a turbulence model showed viscous losses to result in a noticeable weakening of the detonation wave during its propagation.
4. The magnitude of the radiative source was three orders of magnitude lower than that of the chemical heat release source term. Therefore, including the effects of radiative transfer had very little bearing on the over-pressure amplitudes and arrival times in the reacting flow scenarios. While the current study was limited to hydrogen-air mixtures, the proposed methodology can now be extended to study the effects of after-burn and radiative transfer during the detonation of condensed phase explosives where their impacts may be more significant.

Acknowledgement

This work was partially supported by a seed grant awarded to Gautham Krishnamoorthy by the School of Graduate Studies at the University of North Dakota, Grand Forks, ND.

Conflict of Interest

The author(s) declares no conflict of interest.

References Références Referencias

1. JANNAF(1972)Hazard of chemical rockets and propellants handbook, General safety engineering design criteria, I, National Technical Information Service, Silver Spring, Maryland, pp. 2–26.
2. AUTODYN, ANSYS (2005) Theory manual revision 4.3. Century Dynamics, Concord, CA.
3. FLUENT, ANSYS(2011)14.0: Theory guide, ANSYS. Inc., Canonsburg, PA.
4. Zbikowski, Mateusz, Dmitriy Makarov, and Vladimir Molkov (2010)Numerical simulations of large-scale detonation tests in the RUT facility by the LES model. Journal of hazardous materials 181, no. 1: 949-956.
5. Zbikowski, Mateusz, Dmitriy Makarov, and Vladimir Molkov (2008)LES model of large scale hydrogen–air planar detonations: Verification by the ZND theory. international journal of hydrogen energy 33, no. 18: 4884-4892.
6. Sathiah, Pratap, Ed Komen, and Dirk Roekaerts (2015)The role of CFD combustion modeling in hydrogen safety management–IV: Validation based on non-homogeneous hydrogen–air experiments. Nuclear Engineering and Design.
7. Feldgun, V. R., Karinski, Y. S., Edri, I., Yankelevsky, D. Z.(2016)Prediction of the quasi-static pressure in confined and partially confined explosions and its application to blast response simulation of flexible structures. International Journal of Impact Engineering. 90:46-60.
8. Liberman M A, Kiverin A D, Ivanov M F(2011) On detonation initiation by a temperature gradient for a detailed chemical reaction models. Physics Letters A 375:803-1808.
9. Liberman, M. A., Ivanov, M. F., Kiverin, A. D.(2015)Effect of thermal radiation heat transfer on flame acceleration and transition to detonation in particle-cloud hydrogen flames. Journal of Loss Prevention in the Process Industries. 38:176-186.
10. Liberman, M. A., Ivanov, M. F., Kiverin, A. D. (2015)Radiation heat transfer in particle-laden gaseous flame: Flame acceleration and triggering detonation. Acta Astronautica. 115:82-93.
11. Ya.B. Zeldovich, V.B. Librovich, G.M. Makhviladze, G.I. Sivashinsky(1970) Astronautica Acta 15:313
12. Zyskowski, A ., Sochet, I., Mavrot, G., Bailly, P., Renard, J.(2004)Study of the explosion process in a small scale experiment-structural loading. Journal of Loss Prevention. 17:291-299.
13. Rivière, Philippe, and Anouar Soufiani (2012)Updated band model parameters for H2O, CO2, CH4 and CO radiation at high temperature. International Journal of Heat and Mass Transfer 55, no. 13: 3349-3358.
14. Scala, S. M., Sampson, D. H.(1963)Heat Transfer in Hypersonic Flow with Radiation and Chemical Reactions. General Electric Co., Phidelphia, PA Missile and Space Division.
15. Krishnamoorthy, Gautham, and Lauren Elizabeth Clarke (2016)Computationally Efficient Assessments of the Effects of Radiative Transfer, Turbulence Radiation Interactions, and Finite Rate Chemistry in

the Mach 20 Reentry F Flight Vehicle. Journal of Computational Engineering.
16. Barlow, R. S., N. S. A. Smith, J-Y. Chen, and R. W. Bilger (1999)Nitric oxide formation in dilute hydrogen jet flames: isolation of the effects of radiation and turbulence-chemistry submodels. Combustion and Flame. 117, no. 1: 4-31.
17. J. Renard, C. Desrosier, I. Sochet(2000)Benchmark experiments for the validation of numerical codes, 16th international symposium military aspects of blast and shock, Oxford, pp. 57–64
18. Liu, Qingming, Yunming Zhang, and Shuzhuan Li(2015)Study on the critical parameters of spherical detonation direct initiation in hydrogen/oxygen mixtures. International Journal of Hydrogen Energy 40, no. 46: 16597-16604.
19. O'Connaire, M., H. J. Curran, J. M. Simmie, W. J. Pitz, and C. K. Westbrook(2004)A Comprehensive Modeling Study of Hydrogen Oxidation. Int. J. Chem. Kinet. 36:603-622 (UCRL-JC-152569).
20. Molkov, V. V., D. V. Makarov, and H. Schneider (2007) Hydrogen-air deflagrations in open atmosphere: large eddy simulation analysis of experimental data. International Journal of Hydrogen Energy 32, no. 13: 2198-2205.
21. Tomizuka, T., Kuwana, K., Mogi, T., Dabashi, R., Koshi,M (2013)A study of numerical hazard prediction method of gas explosion. International Journal of Hydrogen Energy. 38: 5176-5180.
22. Dahoe, A. E.(2005)Laminar burning velocities of hydrogen–air mixtures from closed vessel gas explosions. Journal of Loss Prevention in the Process Industries. 18, no. 3: 152-166.

Table 1: Initialization Details for Case 1 in the Hydro code and CFD Framework

Variable	Hydro code Framework (ANSYS AUTODYN)	CFD Framework (ANSYS FLUENT)
Gauge Pressure	N/A*	1.89 x 10^6 Pascal
Detonation Kernel Temperature (K)	N/A*	3473 K
Temperature within enclosure (K)	N/A*	300 K
Composition within detonation kernel (mole fraction)	An equivalent amount of TNT	H_2O = 1.0
Enclosure composition - detonation wave propagation in air(mole fraction)	N/A*	N_2 = 0.79 O_2 = 0.21
Enclosure composition – detonation wave propagation in hydrogen(mole fraction)	N/A*	O_2 = 0.21, N_2 = 0.79 (Non-reacting) O_2 = 0.126, N_2 = 0.474, H_2 = 0.4 (Rich) O_2 = 0.168, N_2 = 0.832, H_2 = 0.2 (Lean)
Volume of the detonation kernel (m^3)	56.5 x 10^{-6}	2.22 x 10^{-5}

N/A: Not Applicable*

Table 2: A summary of modeling methodologies

Physical Model	CFD Framework (ANSYS FLUENT)	Hydro code Framework (ANSYS AUTODYN)
Fluid Mechanics	Smagorinksy Large Eddy Simulation Model, Inviscid Euler equation	Inviscid Euler equation
Equation of State	Soave-Redlich-Kwong (SRK)	Jones-Wilkins-Lee (JWL)
Chemistry	21 step chemistry [19] model with stiff chemistry solver for detonation propagation in hydrogen mixture	Non reacting
Radiative heat transfer	An optically thin approximation with a Planck mean absorption coefficient for H_2O vapor and air implemented as add-on functions (Eqs. 1- 3)	No radiative heat loss
Detonation Kernel Initialization	High temperature based on adiabatic flame temperature for H_2 - O_2 mixtures. High pressure determined from ideal gas equation of state assuming constant volume combustion within the detonation kernel.	TNT equivalencies

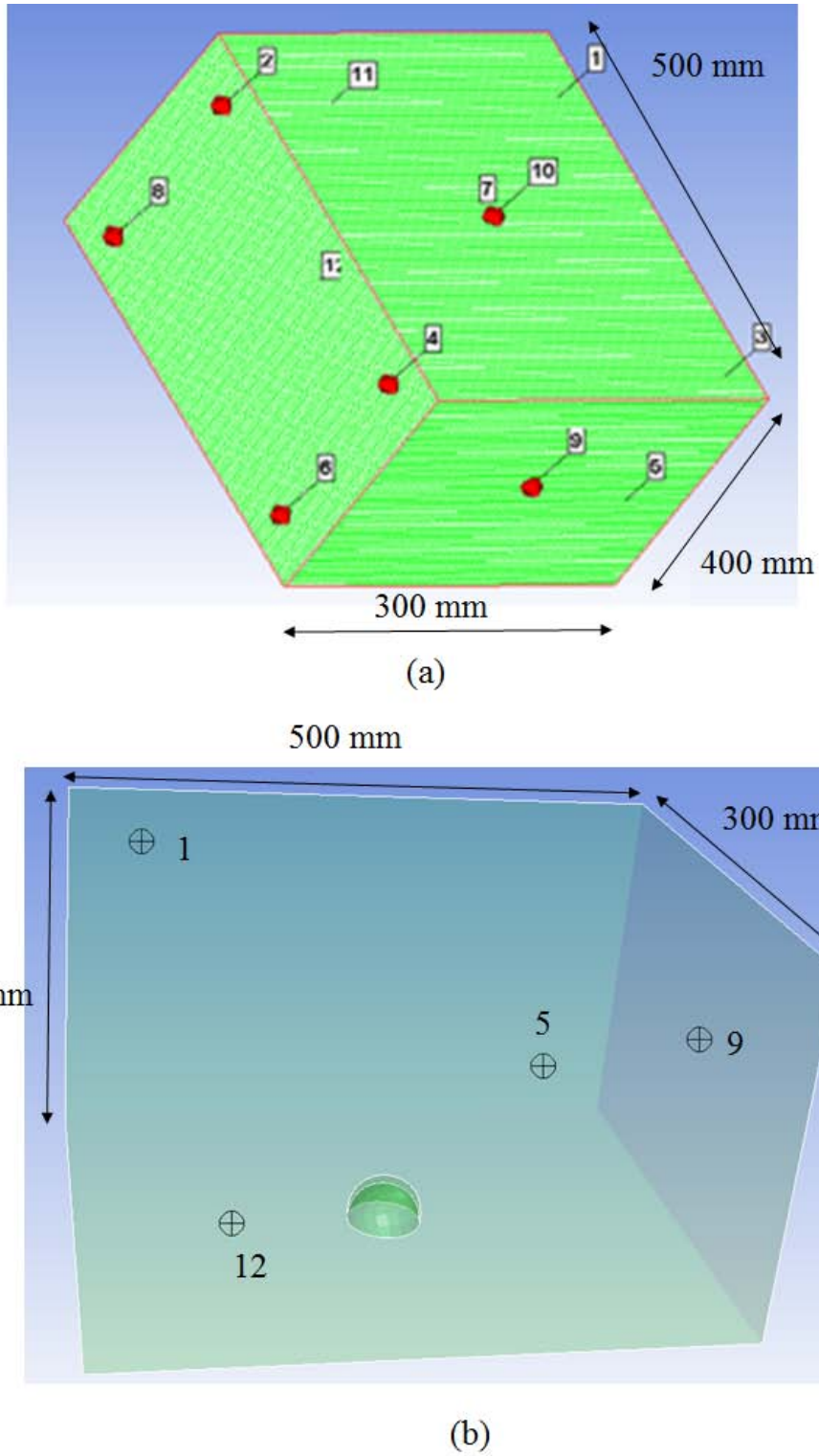

Figure 1: (a) Location of the pressure sensors in the small-scale (Case 1) geometry; (b) The detonation kernel in the CFD simulations highlighted at the center.

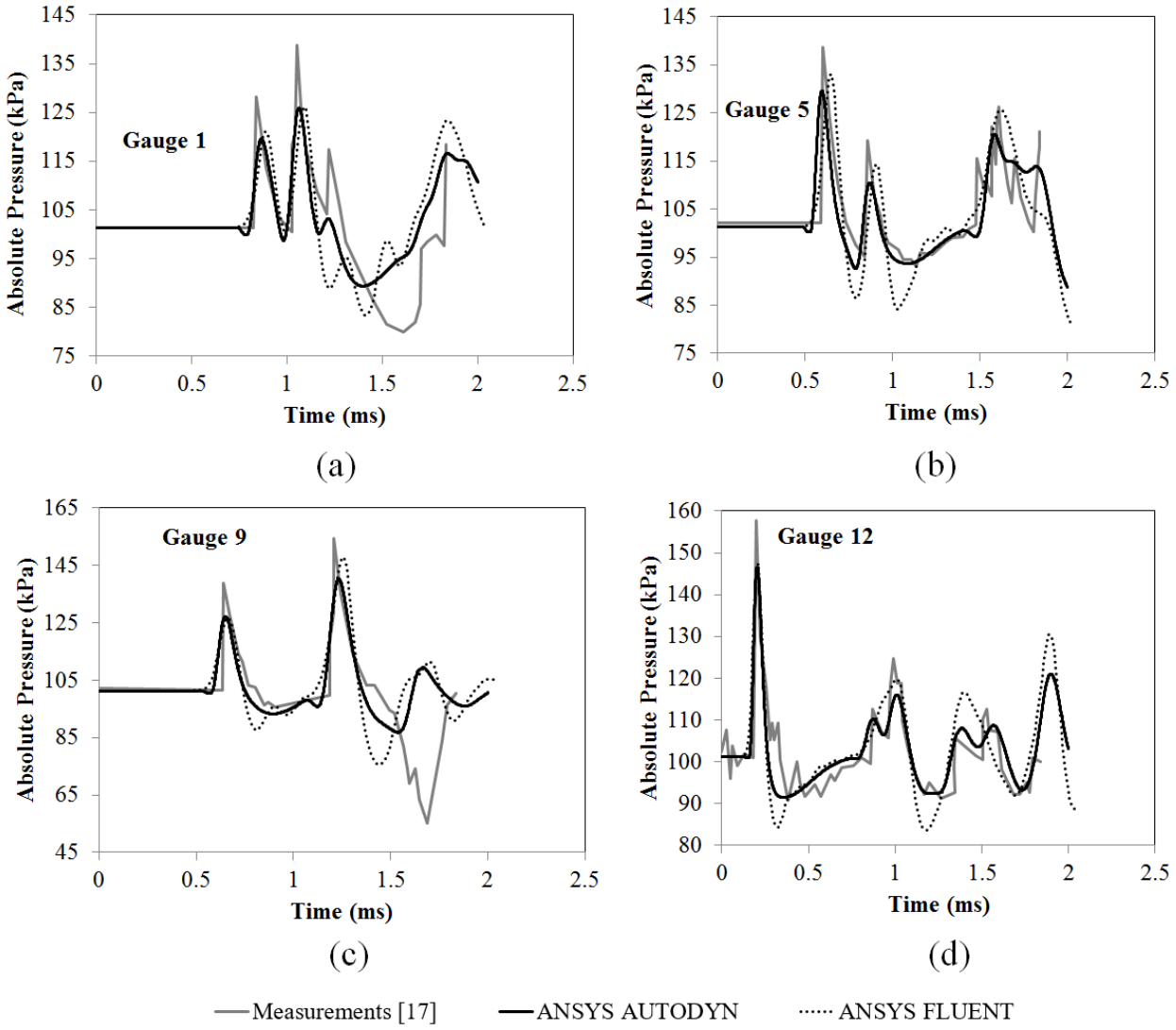

Figure 2: Transient pressure predictions at the different gauges in the small scale (Case 1) explosion study (a) Gauge 1; (b) Gauge 5; (c) Gauge 9; (d) Gauge 12.

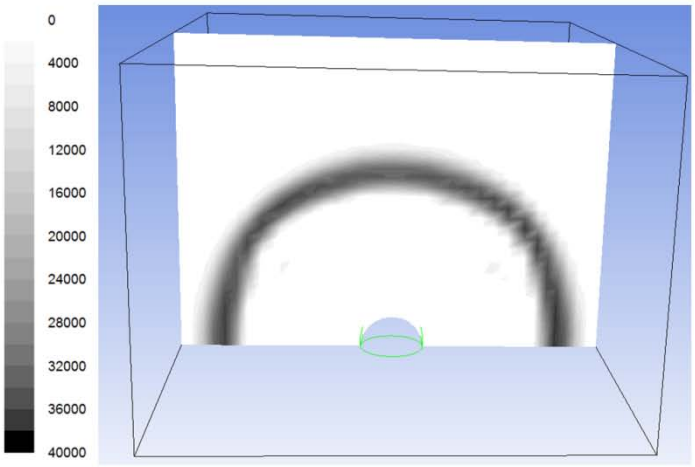

(a) Gauge pressure (Pascal)

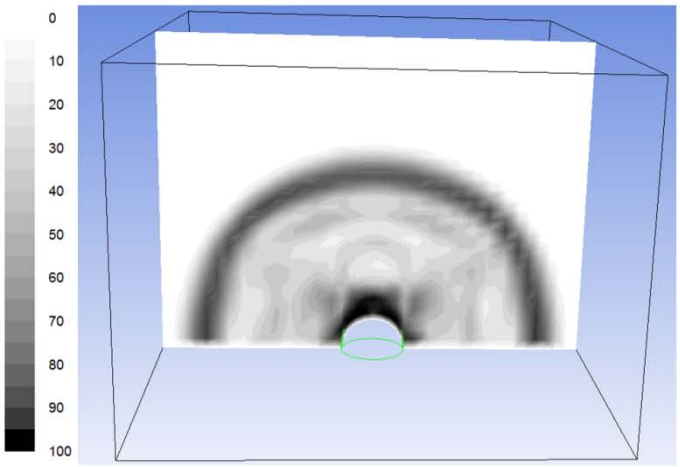

(b) Velocity (m/s)

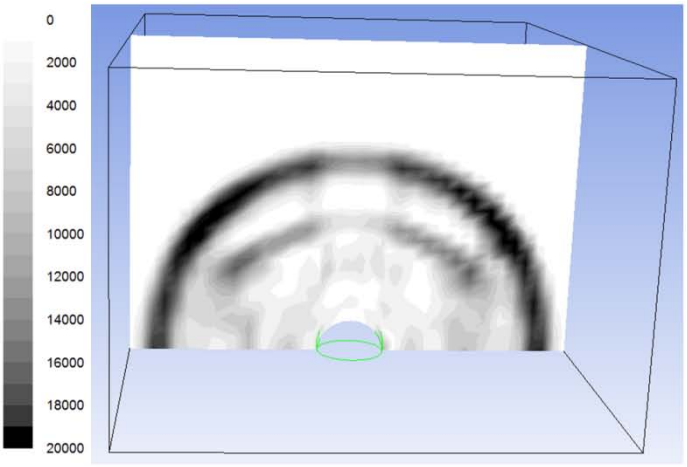

(c) Viscosity ratio

Figure 3: Contours of: (a) Gauge pressure (in Pascal); (b) Velocity (in m/s) and (c) Viscosity ratio (turbulent viscosity/molecular viscosity) after 3 ms in the large scale (Case 2) explosion study.

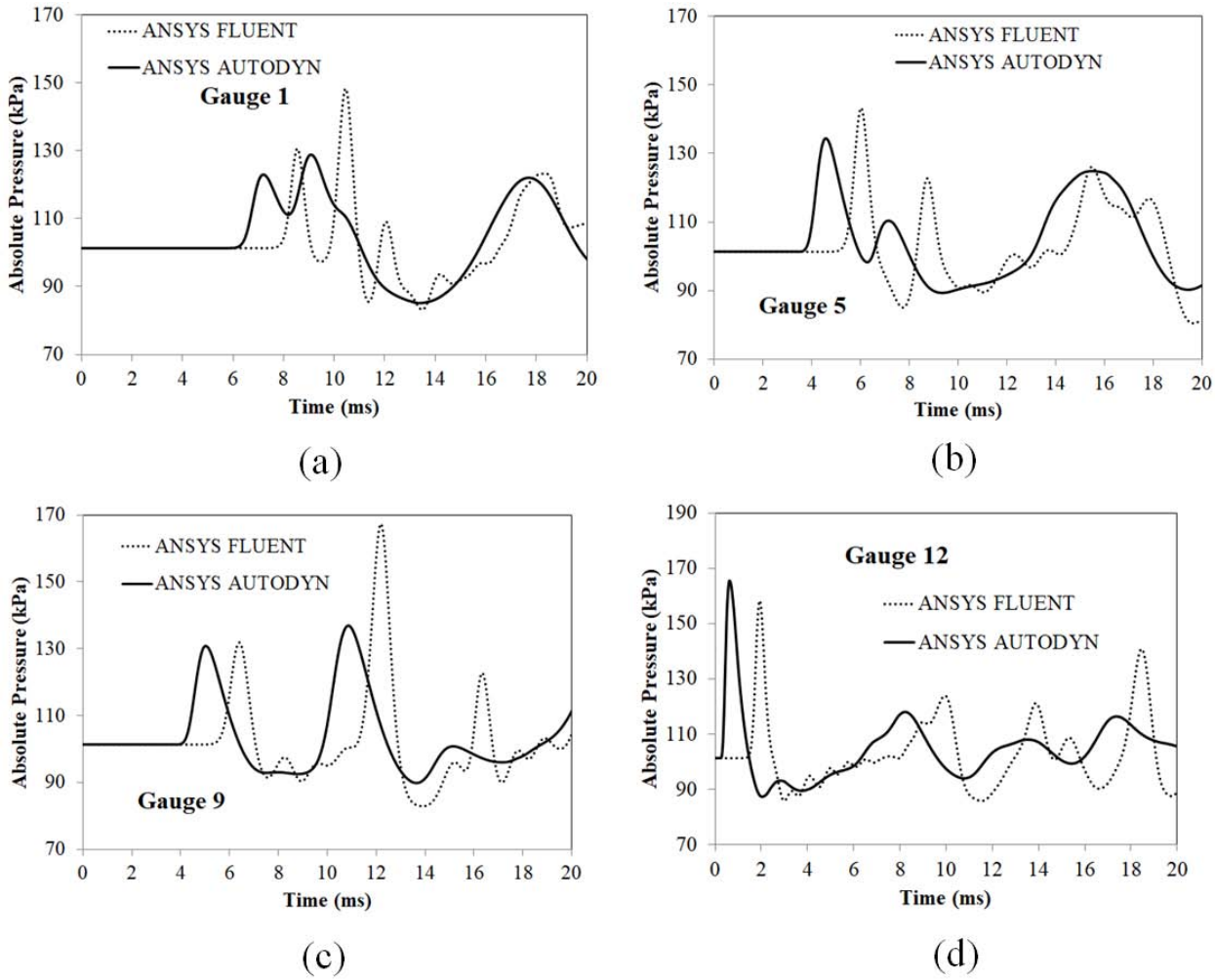

Figure 4: Effects of viscosity - Transient pressure predictions at the different gauges in the large (Case 2) scale explosion study (a) Gauge 1; (b) Gauge 5; (c) Gauge 9; (d) Gauge 12.

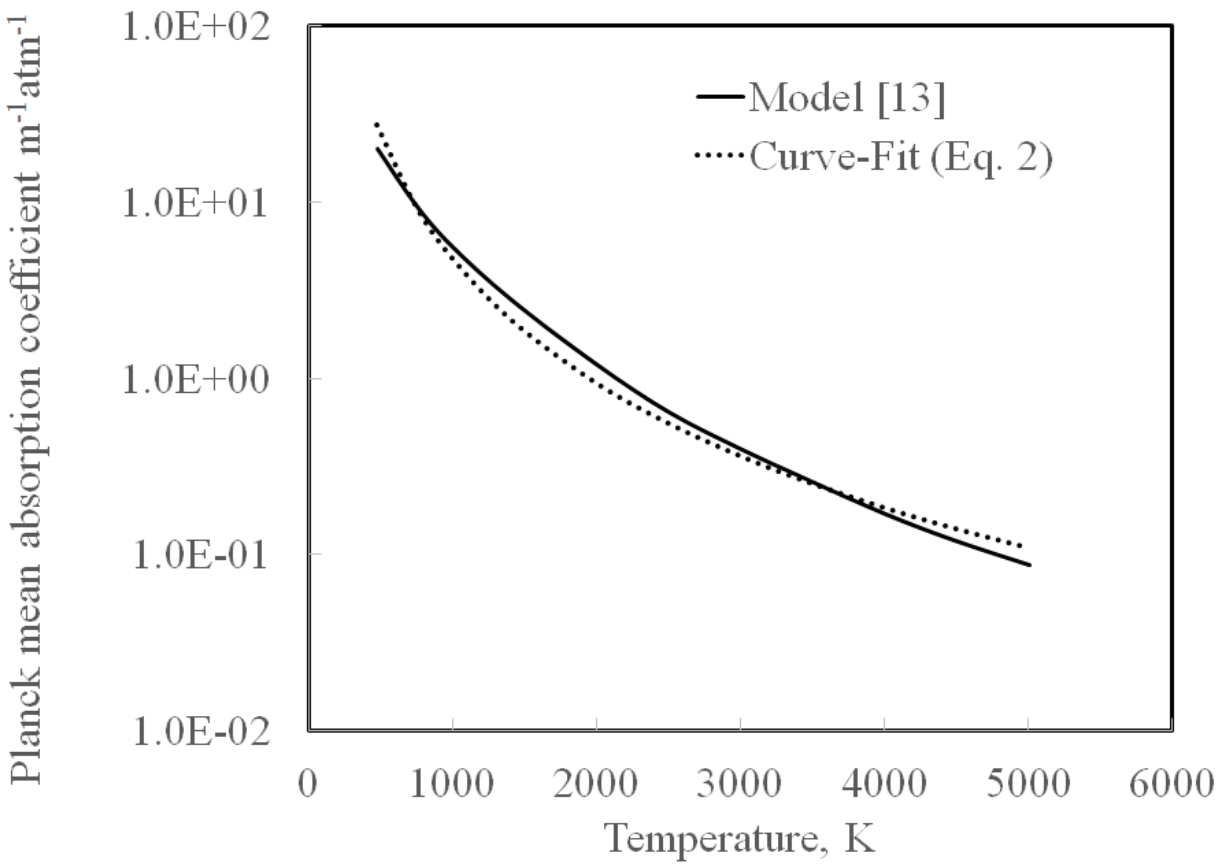

Figure 5: Planck mean absorption coefficient (in m^{-1}) of water vapor utilized in the simulations.

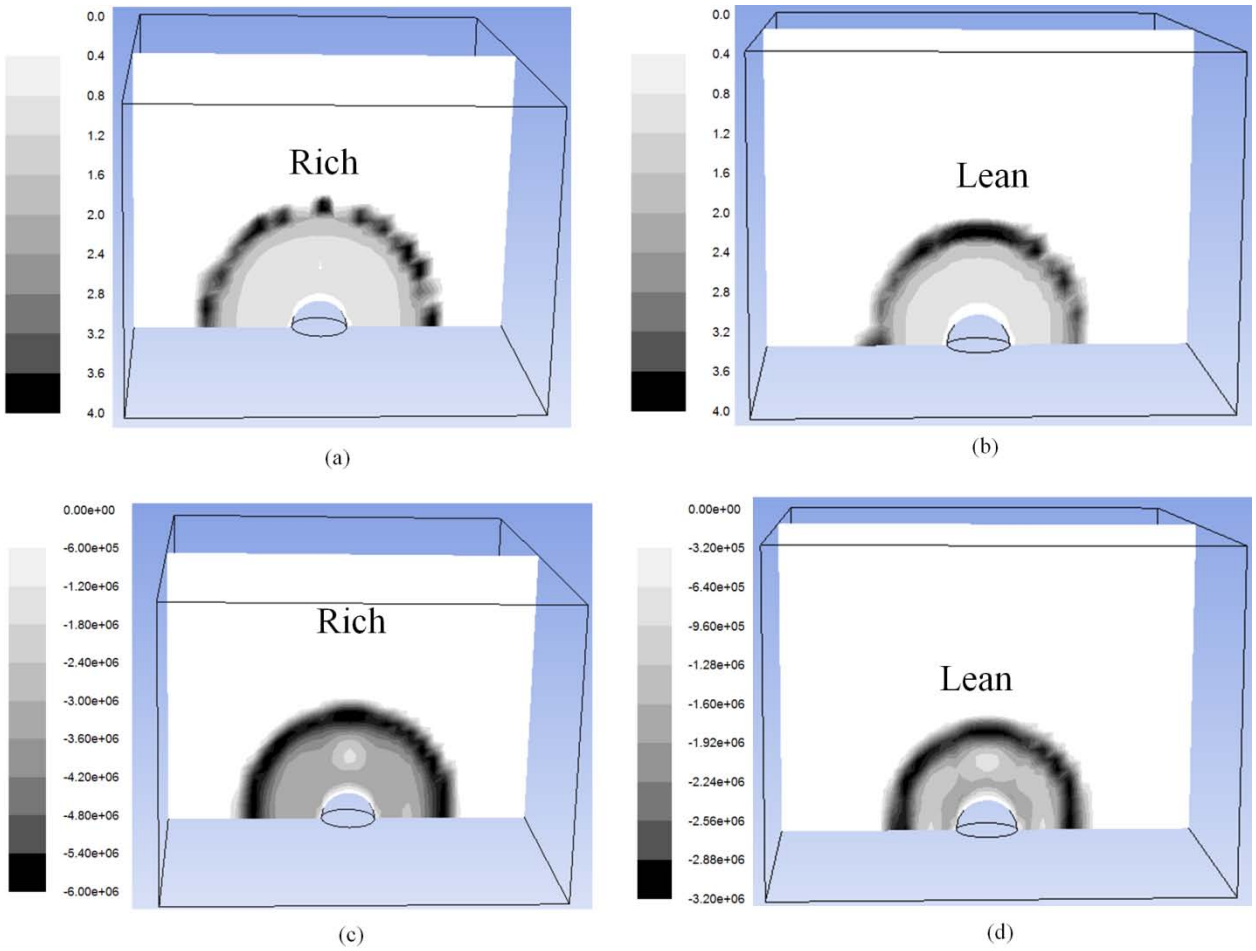

Figure 6: Contours of: (a, b) Planck mean absorption coefficient (in m^{-1}); (c, d) Radiative source term (in W/m^3) after 0.5 ms in the large scale (Case 2) explosion study at fuel-rich (40 mol% H_2) and fuel-lean (20 mol% H_2) domain conditions.

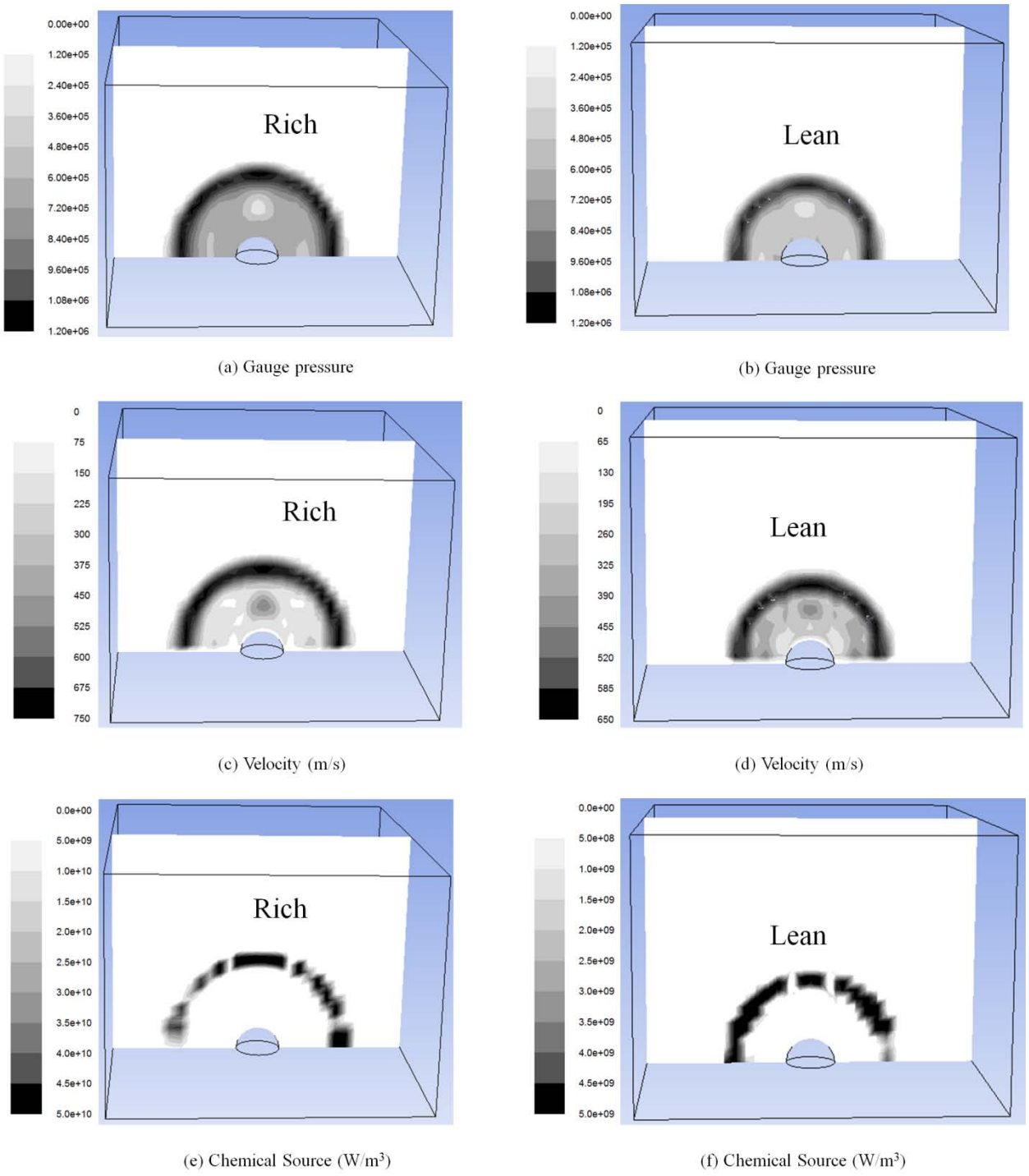

Figure 7: Contours of: (a, b) Gauge pressure (in Pascal); (c, d) Velocity (in m/s); (e, f) Reaction source term (in W/m^3); after 0.5 ms in the large scale (Case 2) explosion study at fuel-rich (40 mol% H_2) and fuel (20 mol% H_2) domain conditions.

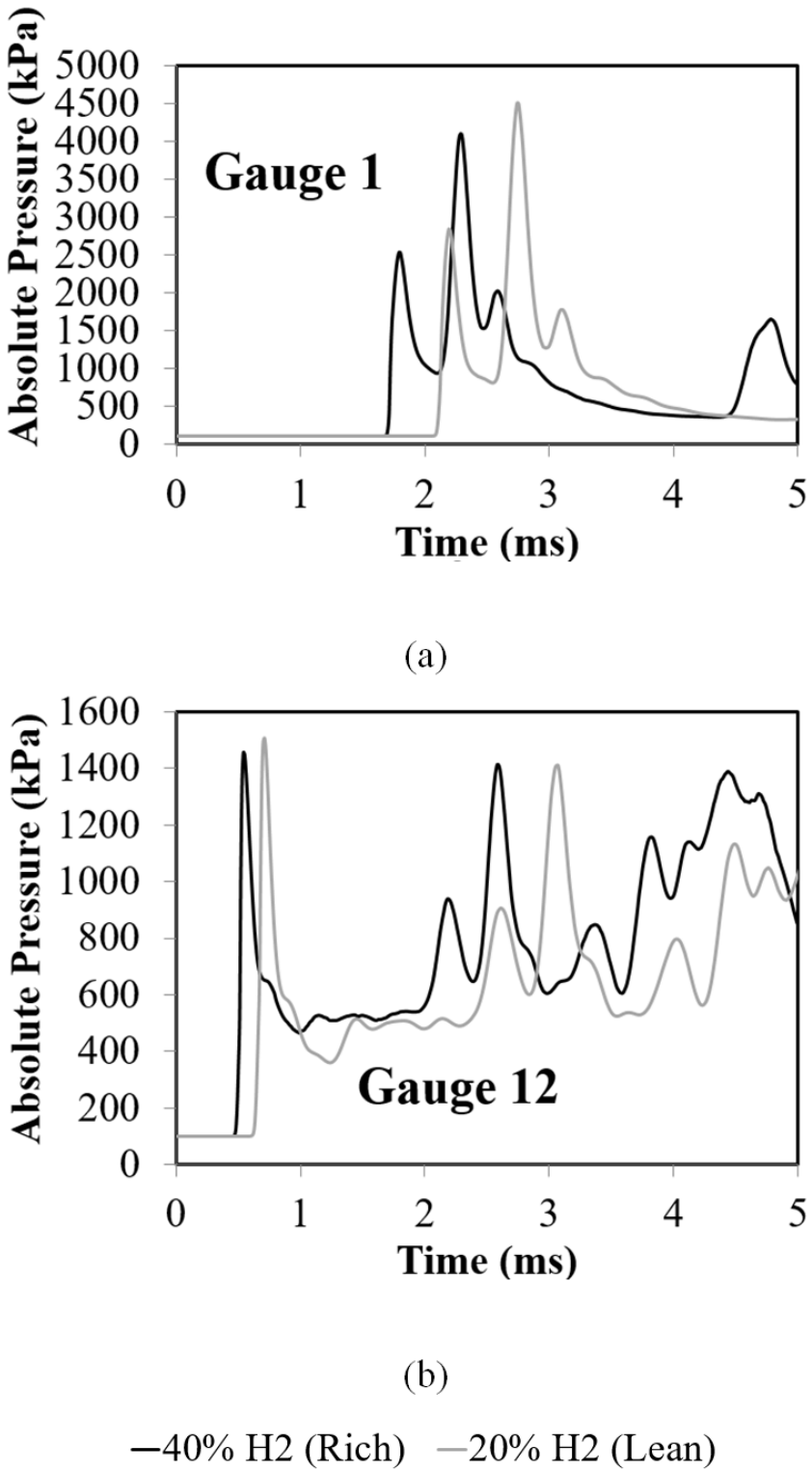

Figure 8: Effect of equivalence ratio: Transient pressure predictions at the different gauges in the large scale (Case 2) explosion study at fuel-rich (40 mol% H_2) and fuel-lean (20 mol% H_2) domain conditions.

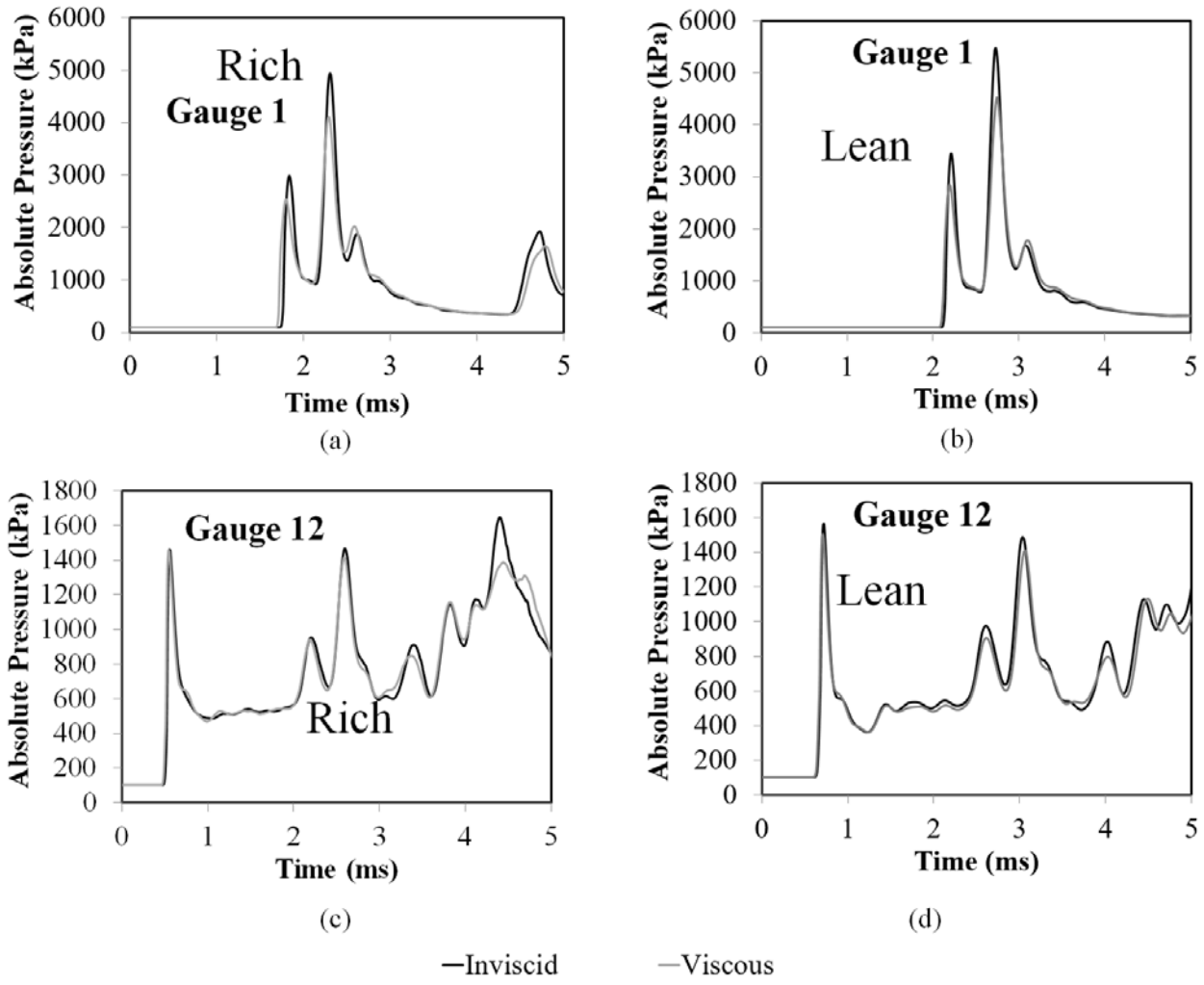

Figure 9: Effect of viscosity: Transient pressure predictions at the different gauges in the large scale (Case 2) explosion study at fuel-rich (40 mol% H_2) and fuel-lean (20 mol% H_2) domain conditions.

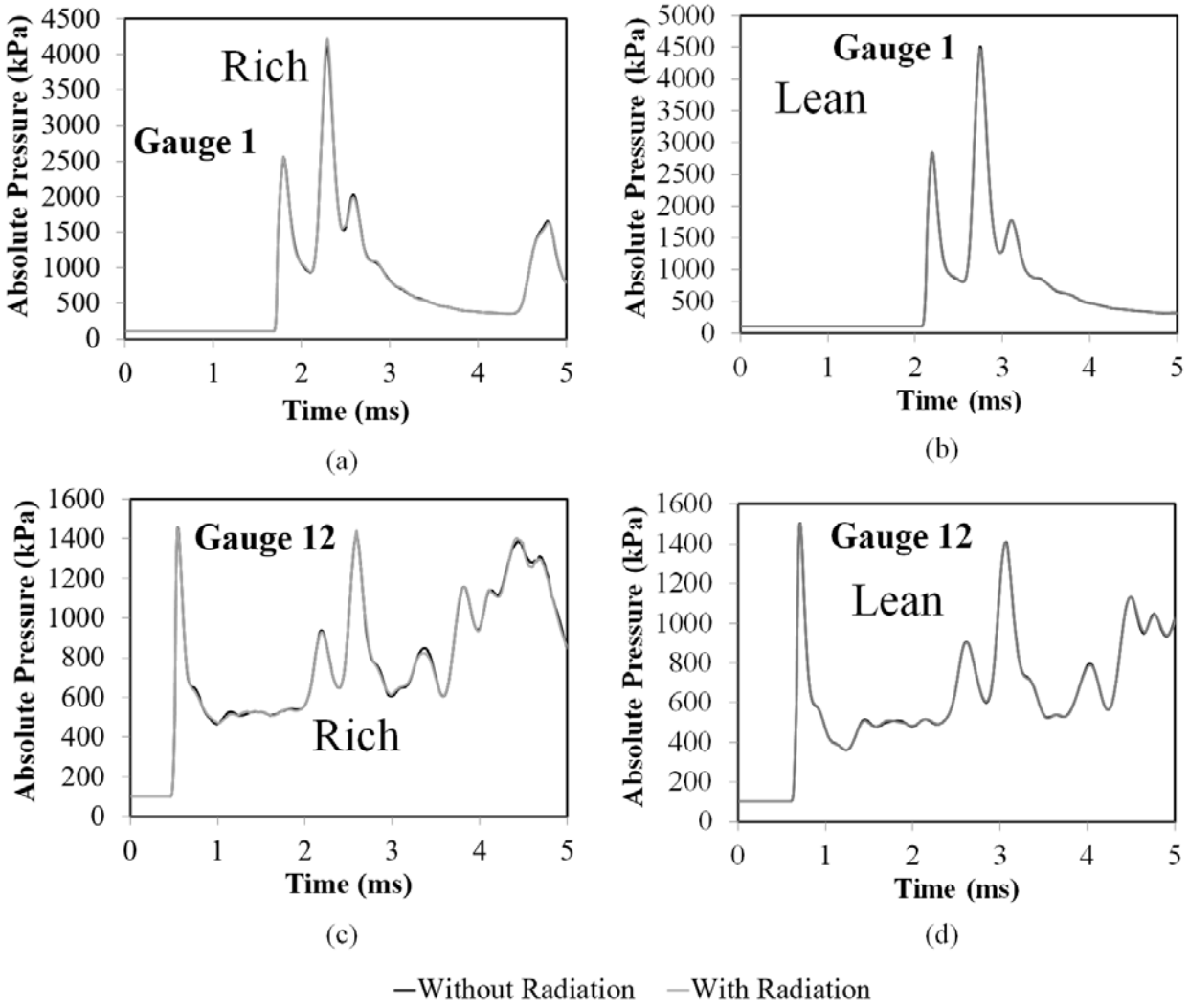

Figure 10: Effect of radiative heat transfer: Transient pressure predictions at the different gauges in the large scale (Case 2) explosion study at fuel-rich (40 mol% H_2) and fuel-lean (20 mol% H_2) domain conditions.

Global Journal of Researches in Engineering: C
Chemical Engineering
Volume 17 Issue 3 Version 1.0 Year 2017
Type: Double Blind Peer Reviewed International Research Journal
Publisher: Global Journals Inc. (USA)
Online ISSN: 2249-4596 & Print ISSN: 0975-5861

Effect of Chemical Pretreatment on the Seawater Fouling Potential

By Meshal Kh. Aldaihani, Sabah A. Alali & Radhi Alazmi
College of Technological Studies, Public Authority for Applied Education and Training

Abstract- In this research, three pretreatment chemicals, ferric chloride, aluminum chloride, and powdered activated carbon, were applied at different concentrations to a raw seawater feed. Five different concentrations (2, 5, 10, 15, and 20 ppm) of each chemical were used to examine the effect on reducing the silt density index (SDI) of raw seawater. The best overall reduction in SDI, 10.05, was obtained with ferric chloride at a concentration of 10 ppm. At higher concentrations of ferric chloride, the SDI did not improve and instead increased. The same behaviorwas observedwith powdered activated carbon (PAC), where a higher concentration resulted in a higher SDI. The SDIsof seawater treated with 2 and 20 ppm aluminum chloride were almost the same – 12.7 and 12.1, respectively. The study shows that using higher concentrations of chemical coagulant may produceadverse results rather that improving the SDI of seawater. Chemical pretreatment should be optimized according to the type and quality of the feed water.

GJRE-C Classification: *FOR Code: 090410*

Strictly as per the compliance and regulations of:

Effect of Chemical Pretreatment on the Seawater Fouling Potential

Meshal Kh. Aldaihani [α], Sabah A. Alali [σ] & Radhi Alazmi [ρ]

Abstract- In this research, three pretreatment chemicals, ferric chloride, aluminum chloride, and powdered activated carbon, were applied at different concentrations to a raw seawater feed. Five different concentrations (2, 5, 10, 15, and 20 ppm) of each chemical were used to examine the effect on reducing the silt density index (SDI) of raw seawater. The best overall reduction in SDI, 10.05, was obtained with ferric chloride at a concentration of 10 ppm. At higher concentrations of ferric chloride, the SDI did not improve and instead increased. The same behavior was observed with powdered activated carbon (PAC), where a higher concentration resulted in a higher SDI. The SDIs of seawater treated with 2 and 20 ppm aluminum chloride were almost the same – 12.7 and 12.1, respectively. The study shows that using higher concentrations of chemical coagulant may produce adverse results rather that improving the SDI of seawater. Chemical pretreatment should be optimized according to the type and quality of the feed water.

I. Introduction

Although 70% of our plant is covered with water, only 3% is fresh water, and only one-third of the 3% is available for use (approximately 60% is locked in glaciers as ice). As a result of the water shortage, approximately 2.7 billion people world wide experience water scarcity at least one month of the year [1]. As a direct result of the water shortage, proper sanitation is unavailable to billions of people. Waterborne diseases, such as cholera and typhoid fever, affect approximately two million people every year, most of them children [2].

The world water consumption rate increased six-fold from 1900 to 1995, more than double the rate of population increase over the same period [3]. Increasing population growth, climate change, and the construction of large agricultural projects exacerbate the water shortage problem. It is estimated that by 2025, two-thirds of the world's population will suffer water shortages.

About one-third of the world's population lives 100 kilometers from the seashore. Therefore, seawater desalination is considered an important solution for the world water shortage. Seawater reverse osmoses (RO) membranes can be used to treat seawater containing total dissolved solids in the range of 10,000 – 60,000 mg/L [4].

Author α σ ρ: Chemical Engineering Technology Department, College of Technological Studies, Public Authority for Applied Education and Training, P.O. Box 42325, Shuwaikh 70654, Kuwait.
e-mails: mk.aldaihani@paaet.edu.kw, sas.alali@paaet.edu.kw, rh.alazmi@paaet.edu.kw

Presently, seawater desalination has become an important source of fresh water production [5]. The salt concentration in seawater ranges from 15,000 – 50,000 mg/L total dissolved solids. The desalination of seawater can be achieved though several methods, such as multi-effect desalination (MED), multi-stage flash (MSF) distillation and RO. RO desalination has become the technology of choice recently because it is much less energy intensive than MSF technology. Fifty-one percent of the newly installed desalination capacity in 2001 and seventy-five percent of the new production capacity in 2003 are RO desalination systems [6]. The new, improved RO technology is considered to be the best choice for future desalination projects [7].

One major drawback of RO desalination technology is the susceptibility of the membrane to fouling, especially when the feed has a silt density index (SDI) larger than 3. RO membrane fouling can occur due to scaling by silica, $CaCO_3$, $CaSO_4$, $BaSO_4$, organic molecules, and suspended solids [8]. To ensure the successful implementation of RO desalination, a good pretreatment system must be used. A poor pretreatment system would result in lower permeate output, lower permeate quality, increased cleaning frequency, higher operating cost and, finally, membrane failure [9].The pretreatment process is critically important to ensure the successful operation of a RO desalination system [10].

Pretreatment can be done physically, using screening, sand filters, and/or cartage filters, or chemically, using anti-scale agents, coagulants, and disinfectants.

Ferric chloride, alum, and cationic polymers are regularly used as chemical coagulants in water desalination pretreatment systems to remove particles from raw water feeds [11].Ferric salts, especially ferric chloride, are among the most widely used chemicals for the pretreatment of seawater [12].

Furthermore, activated carbon is very effective and is the favored pretreatment for the removal of dissolved organic matter [13-14]. Gur-eznik et al. reported 80 – 90% removal of dissolved organic matter from membrane bioreactor effluents treated with activated carbon [15].

The SDI can be utilized to measure the success of the pretreatment method in reducing the fouling potential of the water fed to the desalination system.

The SDI is a parameter characterizing the fouling potential of water. Particulates, colloidal matter

and microorganisms have a natural tendency to deposit on membranes, thus impairing their effectiveness. SDI is one of the most important parameters for the design and operation of reverse osmosis membrane processes.

The SDI is determined by measuring the plugging rate of a 0.45 μm microfiltration (MF) membrane using a constant 207 KPa feed pressure for a specified period of time. The SDI can be defined as the elapsed filtration time t_f. The ASTM describes this test as a standard test for determining the fouling potential of a feed water due to the presence of particles [16]. From a practical point of view, the SDI of a fine hollow-fiber RO feed water must be below 3.

$$SDI = \frac{1-(t_i/t_f)}{t_t} X\ 100 \qquad / \text{min}) \qquad (1)$$

where:

t_i is the initial filtration time to filter a fixed volume (500 mL) in seconds

t_f is the final filtration time to filter a fixed volume (500 mL) in seconds

$t_t$is the total elapsed time of the experiment in minutes (5, 10, or 15 mins)

II. Materials And Methods

The procedure for measuring the SDI has been standardized by the ASTM [14]. The equipment and procedure used are as follows:

The apparatus was assembled as shown in Fig. 1, in which the feed pump was automatically controlled to provide a constant feed pressure of 207 ± 7 kPa (30 ± 1 psi).

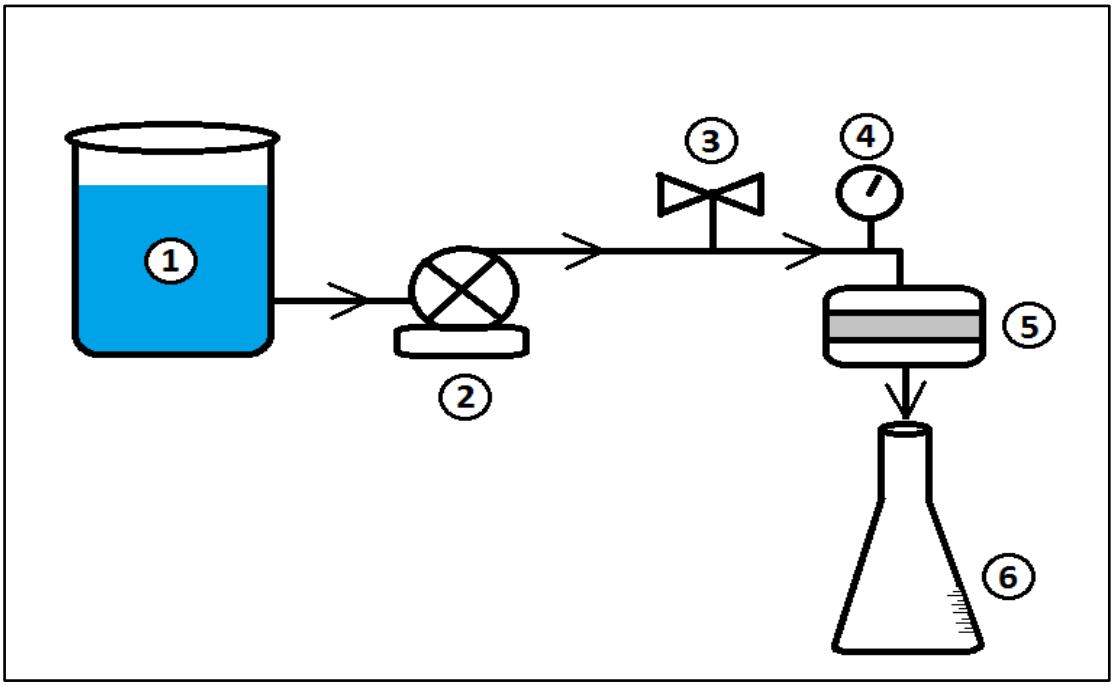

Fig. 1: SDI filtration apparatus setup. 1. treated sweater feed tank, 2. pump, 3. valve, 4. pressure gauge, 5.0.45 μm filter holder, 6. graduated cylinder.

Before installing the membrane filter, the water to be tested was flushed through the apparatus to remove entrained contaminants. The silt density index (SDI-5) was measured for sea water from Shuwaikh beach in Kuwait City. The total dissolved solids, electrical conductivity, and pH were measured for all sea water samples.

An Applied Membrane, Inc., Automatic SDI System (Y-SIMPLESDI-220) was used to measure the SDI of the seawater sample. Millipore cellulose acetate 0.45 μm micro filters were used for all filtration experiments. The pH of each sample was measured using a HANA INSTRUMENTS HI 8010 Basic Portable pH Meter. The electrical conductivity and total dissolved solids were measured using a HANN INSTRUMENTS HI 9835 EC/TDS/NaCl Meter.

It was impossible to complete the traditional 15-minute SDI tests (or even the 10-minute SDI test). The seawater samples were treated with power activated carbon (PAC), aluminum chloride ($AlCl_3$), and ferric chloride ($FeCl_3$). All of the chemicals used in this study were of ACS grade. The appropriate amount of each chemical was measured using a sensitive balance. In each pretreatment experiment, a 30 L solution was prepared with a concentration of 5,10 or15 ppm. The seawater was mixed with the pretreatment chemicals for 30 minutes at 500 RPM using a Servodyne mixer (Cole-Parmer Instrument, Vernon Hills, IL) with a high-lift blade. The treated water was allowed to settle overnight, and the clear supernatant water from the top was used for the SDI experiments. For each concentration of the pretreatment chemical, the experiment was repeated

three times, and the average SDI-5 was calculated. The temperature was maintained at approximately 20 °C during all experiments.

III. Results and Discussion

The primary aim of the work presented here is to evaluate the fouling tendency of different types and concentrations of chemicals. The sensitivity of the SDI to wards the variation in the particle concentration and the testing parameters is described in (Table 1).

Table 1: Pretreated seawater analysis for different pretreatment chemicals and SDI-5 results.

	Ferric chloride (ppm)					Powder activated carbon (ppm)					Aluminum chloride (ppm)				
Concentration (ppm)	2	5	10	15	20	2	5	10	15	20	2	5	10	15	20
TDS (g/L)	33.1	29.6	29.7	30.1	31.3	32.3	28.16	30.23	29.36	32.1	32.7	32.3	32.3	30.9	30.2
pH	8.02	7.27	7.26	7.28	7.66	7.98	7.2	7.47	7.63	8.15	7.78	8.02	7.88	7.65	7.38
Conductivity (mS/cm)	66.2	59.1	59.3	60.3	62.6	65.0	58.1	60.6	58.7	64.2	65.4	64.6	64.7	61.8	60.4
Turbidity (NTU)	0.40	0.50	0.33	1.23	0.90	0.63	0.93	0.30	0.50	3.23	0.30	0.70	0.76	0.86	1.30
SDI-5	15.80	13.36	10.05	17.99	15.30	14.60	15.67	11.29	11.88	15.00	12.70	14.18	17.46	14.48	12.10

a) Untreated Seawater Analysis

It was impossible to complete the traditional 15-minute SDI test or even the 10- or 5-minuteSDI tests without treatment.

b) Pretreatment Experiments

i. *Ferric Chloride Pretreatment Experiments*

The average SDI-5 of seawater pretreated with 2, 5, 10, 15 and 20 ppm ferric chloride($FeCl_3$) was15.8, 13.4, 10.1, 18.0, and 15.3, respectively (Fig. 2). The best result was obtained with a $FeCl_3$ concentration of 10 ppm. The results show that 10 ppm $FeCl_3$ is better than 2 or5 ppm, and the SDI-5 was lowered from15.8 and 13.4 to 10.1 for 2 and 5 ppm $FeCl_3$, respectively; nevertheless, increasing the $FeCl_3$ concentration over 10 ppm had an adverse effect, increasing the SDI-5 value. Treatment with a higher dose of $FeCl_3$(15 and 20 ppm)did not improve the SDI-5. The SDI-5 increased to 18.0 and 15.3 for $FeCl_3$ concentrations of 15 and 20 ppm, respectively.

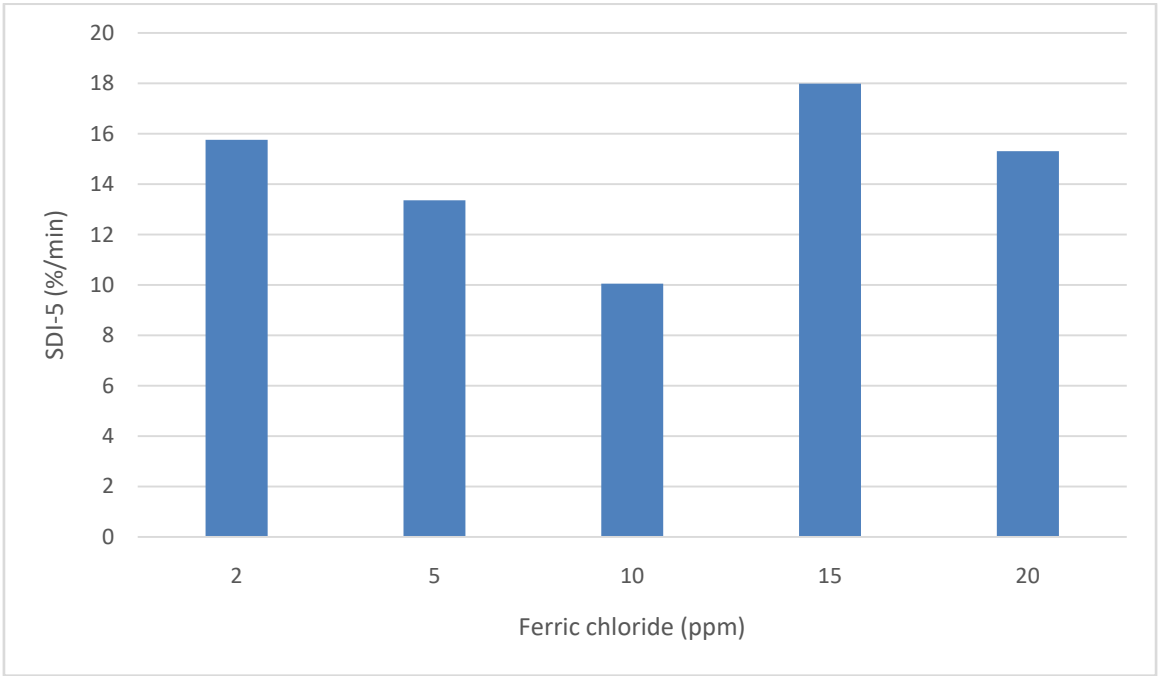

Fig. 2: Effect of pretreatment with ferric chloride on the SDI-5 of seawater.

ii. *Powder Activated Carbon Pretreatment Experiments*

The average SDI-5 of seawater pretreated with 2, 5, 10, 15, and 20 ppm PAC was14.6, 15.7, 11.3, 11.9, and 14.9, respectively (Fig. 3). The best result was obtained with a PAC concentration of 10 ppm (Fig. 3).

The SDI-5 results at different PAC concentrations are displayed in Fig. 3. The results show that 10 ppm PAC is better than 2 or5 ppm. Treatment with a higher dose of PAC resulted in a higher SDI-5. Treatment with 15 and 20 ppm PAC did not improve the SDI-5.

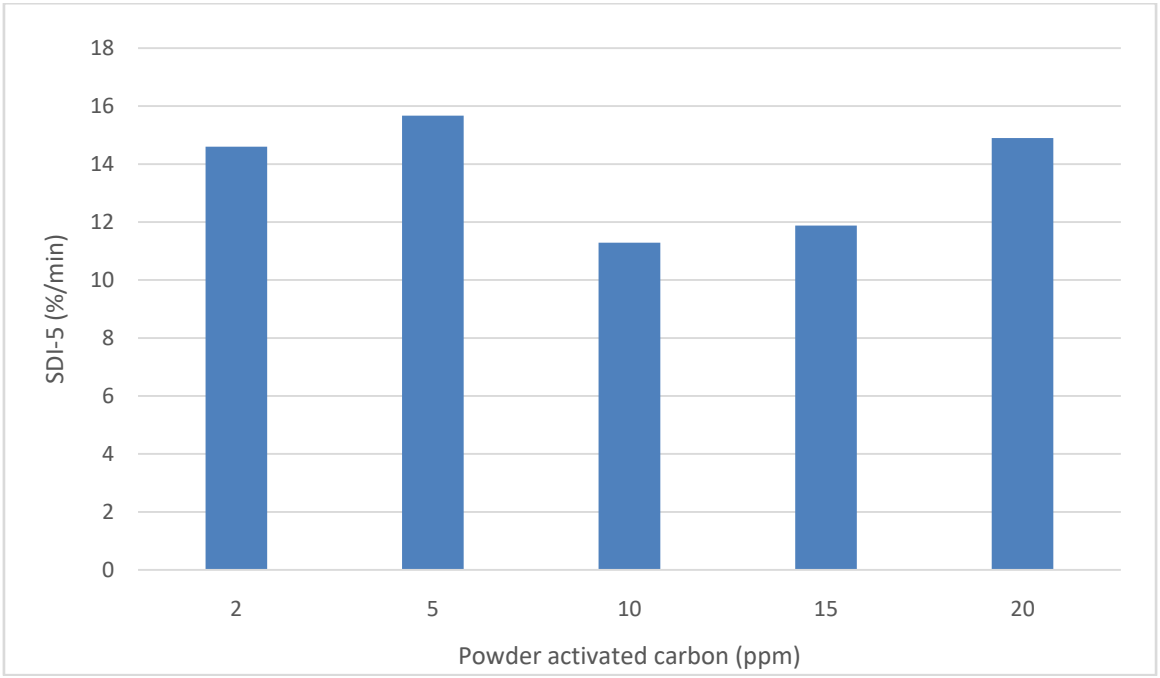

Fig. 3: Effect of pretreatment with PAC on the SDI-5 of seawater.

iii. *Aluminum Chloride Pretreatment Experiments*

The average SDI-5 of seawater pretreated with 2, 5,10,15, and 20 ppm $AlCl_3$ was 12.7, 14.2, 15.9, 14.5, and 12.1, respectively (Fig. 4). The best result was obtained with an$AlCl_3$ concentration of 20 ppm (Fig. 4); nevertheless, using the lowest $AlCl_3$ concentration of 2 ppm gave a SDI- 5 close to that of the 20 ppm sample. The SDI-5 results at different $AlCl_3$ concentrationsare displayed in Fig. 4. There is no clear behavior for different concentrations of $AlCl_3$, and using 10 ppm $AlCl_3$ increased the SDI-5 to 15.9.

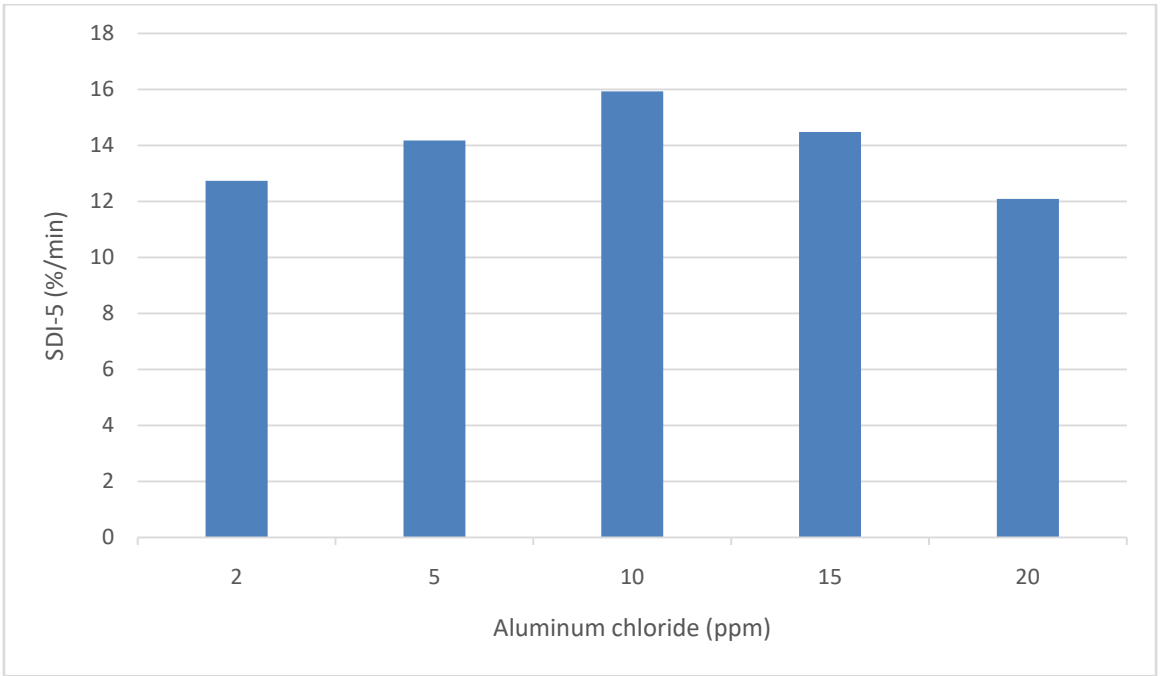

Fig. 4: Effect of pretreatment with aluminum chloride on the SDI-5 of seawater.

IV. Conclusions And Recommendations

The study indicates the important of optimizing the chemical coagulant dose in the pretreatment of seawater for desalination using RO systems. From the three pretreatment chemicals used in this study, i.e., ferric chloride, PAC, and aluminum chloride, ferric chloride gave the best reduction in SDI. The best overall reduction in SDI, 10.05, was obtained with ferric chloride at a concentration of 10 ppm. It is worth noting that a higher SDI was obtained using ferric chloride concentrations of 2, 5, 15, and 20 ppm, which were 15.8, 13.36, 17.99 and 15.30, receptively. It is hypothesized that at low coagulant concentrations, the particles do not sufficiently precipitate, and at higher coagulant concentrations, smaller-sized particles that usually pass through the filter are aggregated to a size sufficient to clog the filter but not large enough to precipitate. This type of behavior is also observed with PAC, where the best reduction in SDI was obtained at a concentration of 10 ppm and at higher and lower PAC concentrations the SDI was higher. It is very clear from the result that the chemical coagulant concentration should be optimized according to the feed seawater quality and that using a higher concentration of chemical coagulant may gave adverse results rather than improving the SDI of the feed seawater.

References Références Referencias

1. World wild life organization. https://www.worldwildlife.org/threats/water-scarcity
2. WHO, World Health Organization: 10 facts about water scarcity, http://www.who.int/features/factfiles/water/en/, 2010 (March 2009).
3. UNEP. (1999). *GEO-2000. Global Environmental Outlook*. United Nations Envirnment Programme, Nairobi, Kenya.
4. Mickley, M.C., (2001). Membrane Concentrate Disposal: Practices and Regulation. U.S. Department of the Interior, Bureau of Reclamation, Mickley & Associates.
5. Gaid, K. (2011). A large review of the pre treatment. In *Expanding Issues in Desalination*. In Tech.
6. Wolfe, P. (2005). Fujairah marks major milestone for desalination in middle east. Water and Wastewater International.
7. Greenlee, L. F., Lawler, D. F., Freeman, B. D., Marrot, B., & Moulin, P. (2009). Reverse osmosis desalination: water sources, technology, and today's challenges. Water research, 43(9), 2317-2348.
8. Van der Bruggen, B., & Vandecasteele, C. (2002). Distillation vs. membrane filtration: overview of process evolutions in seawater desalination. *Desalination*, 143(3), 207-218.
9. Fritzmann, C., Löwenberg, J., Wintgens, T., & Melin, T. (2007). State-of-the-art of reverse osmosis desalination. *Desalination*, 216(1-3), 1-76.
10. Kumar, M., Adham, S. S., & Pearce, W. R. (2006). Investigation of seawater reverse osmosis fouling and its relationship to pretreatment type. Environmental science & technology. 40(6), 2037-2044.
11. Gabe lich, C. J., Yun T. I., & Coffey, B. M. (2002). Effects of aluminum sulfate and ferric chloride coagulant residuals on polyamide membrane performance, *Desalination*, 150(1), 15-30.
12. Edzwald, J. K., & Haarhoff, J. (2011). Seawater pretreatment for reverse osmosis: chemistry, contaminants, and coagulation. *Water research*, 45(17), 5428-5440.
13. Ahmad, A. L., Ismail, S., & Bhatia, S. (2003). Water recycling from palm oil mill effluent (POME) using membrane technology. *Desalination*, *157* (1-3), 87-95.
14. DeSilva, F. J. (2000) Activated carbon filtration, water quality products, 16.
15. Gur-Reznik, S., Katz, I., & Dosoretz, C. G. (2008). Removal of dissolved organic matter by granular-activated carbon adsorption as a pretreatment to reverse osmosis of membrane bioreactor effluents. *Water research*, *42*(6), 1595-1605.
16. Standard, A. S. T. M. (2007). Standard Test Method for Silt Density Index (SDI) of Water. D19, 8, 4189-07.

This page is intentionally left blank

Global Journal of Researches in Engineering: C
Chemical Engineering
Volume 17 Issue 3 Version 1.0 Year 2017
Type: Double Blind Peer Reviewed International Research Journal
Publisher: Global Journals Inc. (USA)
Online ISSN: 2249-4596 & Print ISSN: 0975-5861

Kinetic Models of Adsoption on Active Carbon DSAC36-24

By Khaoulahidouri, Ali Benhmidene, Bechir Chouachi & Ammar Houas

Abstract- Activated carbon is one of the highly adsorbent materials, characterized by a specific surface area of 548.13m^2g^{-1}. Their manufacture uses the natural raw material such as date cores. Several models have been used to monitor the adsorption kinetics. Lager green model, for the determination of the apparent velocity constant (kad) and the order of the reaction. Model of Weber and Morris to approximate the kinetic constant of intra particular diffusion (kid).Mc Kay model, to determine the external mass transfer coefficient (kf). The interpolation by the three models above is carried out for each compound for the different initial concentrations and different pH. That all the models used well describe the experimental results of diffusion adsorption. All the models used describe well the experimental results of the adsorption and that of Langmuir-Freundlich (with three constants) gives a more precise description. A classification of the adsorption of four phenolic compounds according to the maximum adsorption capacity at different of solution(pHs), and according to the pH for each compound.

Keywords: *adsorption of phenolic compounds, effect of initial concentration to adsorption, effect of ph to adsorption.*

GJRE-C Classification: *FOR Code: 090499*

Strictly as per the compliance and regulations of:

Kinetic Models of Adsoption on Active Carbon DSAC36-24

Khaoulahidouri [α], Ali Benhmidene [σ], Bechir Chouachi [ρ] & Ammar Houas [ω]

Abstract- Activated carbon is one of the highly adsorbent materials, characterized by a specific surface area of 548.13m^2g^{-1}. Their manufacture uses the natural raw material such as date cores. Several models have been used to monitor the adsorption kinetics. Lager green model, for the determination of the apparent velocity constant (kad) and the order of the reaction. Model of Weber and Morris to approximate the kinetic constant of intra particular diffusion (kid).Mc Kay model, to determine the external mass transfer coefficient (kf). The interpolation by the three models above is carried out for each compound for the different initial concentrations and different pH. That all the models used well describe the experimental results of diffusion adsorption. All the models used describe well the experimental results of the adsorption and that of Langmuir-Freundlich (with three constants) gives a more precise description. A classification of the adsorption of four phenolic compounds according to the maximum adsorption capacity at different of solution(pHs), and according to the pH for each compound.

Keywords: adsorption of phenolic compounds, effect of initial concentration to adsorption, effect of ph to adsorption.

I. Introduction

Phenols are aromatic organic compounds of great environmental interest; their determination has increased over the last few years because of their toxicity. Phenolic compounds are often derived from various manufacturing processes such as pharmaceuticals, petroleum refineries, coke plants, and phenolic resin plants [1,2]. They emit an unpleasant odor and taste at a concentration of 5µ.L1 and are toxic to aquatic life, plants and humans. [3]Kumar et al gives the ingestion of phenols whose concentration varies between 10 and 240 mg L for long periods causes irritation of the mouth, impaired vision, and diarrhea [3]. They are considered one of the priority pollutants by the US Environmental Protection Agency [4]. The maximum permissible concentration of phenol in drinking water is 1µg.L (World Health Organization) [5] as a result; various studies have been carried out for the removal of phenolic compounds before being released to the receiving medium.

In Tunisia the dates for centuries have been the staple food of the desert populations. With its dietary properties, it is now on the way to becoming a strategic agricultural product for export, as much as olive oil. In Tunisia, the production of dates continues to increase. It is estimated annually at 105 thousand tons of which 70 thousand tons of Degletnour (finger of light), variety considered the best. This product is very successful in the domestic and foreign markets. The major production of dates involve the existence of large quantities of date waste among them their nuclei. In this way, the idea to produce activated carbon (by chemical and physical activation) was found from dates nuclei characterized by a high surface area.

The aim of this study was to investigate kinetics and equilibrium aspects of the adsorption of phenol onto date cores activated carbon. Three kinetics models including pseudo-first order, pseudo second order and intra-particle diffusion models were used to discuss adsorption mechanisms. Lager green[6] model, for the determination of the apparent velocity constant (kad) and the order of the reaction. Model of Weber and Morris[7]to approximate the kinetic constant of intra particular diffusion (kid).McKay [8], determine the external mass transfer coefficient (kf)

II. Materials And Experimental Methods

In Tunisia there is a natural, inexpensive and very abundant material. These are dates nuclei which can, after a suitable treatment, give rise to an active charcoal. The date nuclei are first washed with tap water to remove traces of the pulpit from dates and then rinsed with distilled water. They are then dried in an oven (110 ° C.) for one day in order to remove traces of water and volatile matter. Once crushed to a size of 2 to 5 mm, they give rise to the useful precursor in the rest of the preparation.

a) Chemical Activation

A well-determined quantity of H_3PO_4 (36%) is brought into contact with a mass m of precursor obtained, for 1 hour. Once filtered, this mass is washed with distilled water to pH = 6 and dried in an oven (110 ° C.) for 24 hours.

b) Pyrolysis and gasification

The next step is carbonization. The purpose is to eliminate the volatile products trapped in the carbon skeleton. The organic matter is removed, and is preserved in addition to the mineral matter, only the carbon skeleton. Thus, this pyrolysis takes place under

Author α: Engineers National of Gabès, Omar Ibn El Khattab Street, Gabès 6029, Tunisia.
Author σ: Faculté des Sciences de Gabès Catalyse et Matériaux pour l'Environnement et les Procédés. e-mail: khaoula2013@yahoo.fr

a stream of nitrogen (3.6L/h) with a heating rate of 7.5°C/min to 400°C. and maintained for 1 hour at this temperature. Finally, gasification (physical activation) by carbon dioxide for 24 hours at 900 °C. Allows the internal surface of the carbonized material to be developed by eliminating the residues of the pyrolysis responsible for the clogging of the pores. After cooling under CO_2, the activated carbon is recovered, washed with distilled water to pH = 6-7, dried, weighed and stored in hermetic bottles.

III. Determination of the Physico-Chemical Characteristics of Active Coal Dsac36-24

a) Measurement of the specific surface area and porous distribution

Among the essential characteristics of an activated carbon, the specific surface and the pore volume greatly influence the adsorption capacities and condition the mechanisms of the adsorption.

The study of the specific surface and of the pore distribution is carried out from the nitrogen gas adsorption isotherm. The gas adsorption isotherm of nitrogen (molecular surface area equal to 16.2 $10^{-20}m^2$) is carried out for a range of relative pressures between 0 and 1 μm. The isothermal adsorption desorption curve of N_2(Figure (1)) can allow us to derive two information by its form:

- The type of solid by the type of isotherm
- The shape of the pores by the shape of the hysteresis

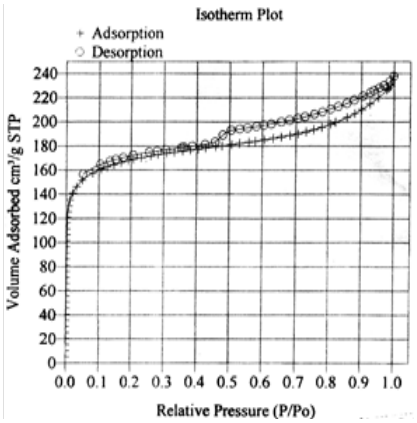

Figure 1: The isothermal adsorption desorption curve of N_2

It is there fore a coal which can present both micropores and mesopores and the hysteresis obtained shows that the pores are open slit. The specific surface area is calculated from the linear BET transform shown in Figure (2). The slope of the line is the essential parameter that makes it possible to calculate the specific surface area.

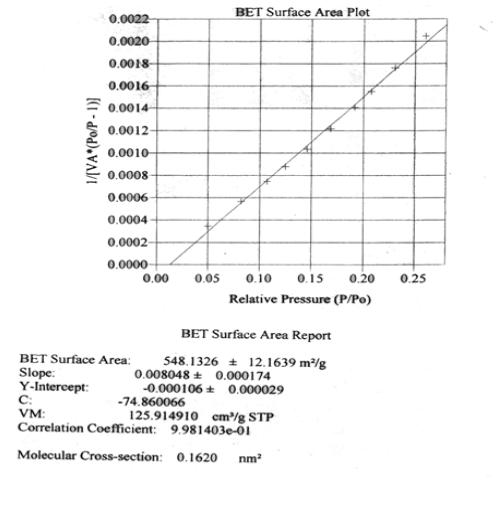

Figure 2: BET

The ash rate, bulk density and iodine value found for DSAC36-24 activated carbon are summarized in the summary table of its physico-chemical characteristics (Tab (1)). These results show that the DSAC36-24 coal has a low ash content indicating that it consists essentially of organic matter. Its iodine value and apparent density are comparable to those of commercial activated carbon F400[9].

Table 1: Physico-chemical characteristics

Origine	Date nuclei
Type Activation	Activation (Chemical+Physical)
Specific surface area (m^2/g)	548.13
Average pore diameter (A°)	25.55
Pore volume (cm^3/g)	0.35
Granulometry (µm)	< 50
Iodine value (mg/g)	849.839
Bulkdensity (g/cm^3)	0.37
Acid surfce function (meq/g)	1.57
Fonctions de surface acides (meq/g)	0.25
pH_{PZC}	8.37

The concentrations of functional groups (Table 1, lines 10 and 11) correspond to the neutralization with 0.1N concentration for NaOHacid groups and the neutralization with 0.1N HCl for the basic groups. As can be seen from the values found, the activated carbon DSAC36-24 contains mainly basic functions (1.57meq/g). It is therefore a coal with a rather basic character. This is confirmed by the found value of pH_{PZC}(8.37). SEM analysis of DSA36-24 is presented on the micrographs (Figure 3) at two different extensions respectively 497 and 2011, showing that it has a more or less uniform spongy structure.

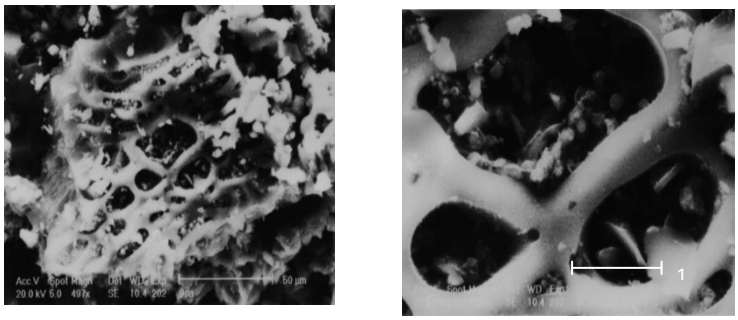

Figure 3: SEM analyses

b) Phenolic compounds used

In Table (2), the main characteristics of the molecules studied are grouped together. Other more conventional characteristics such as melting and boiling temperatures are also given in this table. These give information about the strength of the bonds that exist between the molecules. The dipole moment makes it possible to account for the polarity of the molecule and therefore the most active sites electrically.

Table 2: Main physico-chemical characteristics of the organic compounds used

Phenoliccompounds	HYDRO	PNP	2,4¯DNP	2,4,6-TNP
pKa	9.69	7.16	4	0.8
Molar mass (g/mol)	110.11	139.1	184.11	239. 11
Solubility in water (g/l) Solubility in water (mmol/l)	80 0.72	17 0.122	6 0.032	1.23 0.0053
Fusion temperature (°C)	173	114	113	122
boiling temperature (°C)	286	279	-	300
Dipolar momentµ (deby)	0	5.6	3.4	1.5
Naturel pH	5.65	5.62	4.82	3.85
Chemical displacementδ_{ortho} (ppm)	0.74	-0.6	-1.57	-1.94

The choice of these chemical compounds also makes it possible to obtain molecules in solution in distilled water with electrically different chemical forms (acids, conjugated mesomeric forms, etc.). The isotherms and kinetics of adsorption of these molecules are carried out at different pHs. The choice of the pH value depends on the pKa of these different molecules(figure 4). It allows us to have solutions in which one or the other or both forms, molecular (non-dissociated) form and ionized (dissociated) form exists.

The pH is adjusted by adding a few drops of concentrated sulfuric acid or soda.

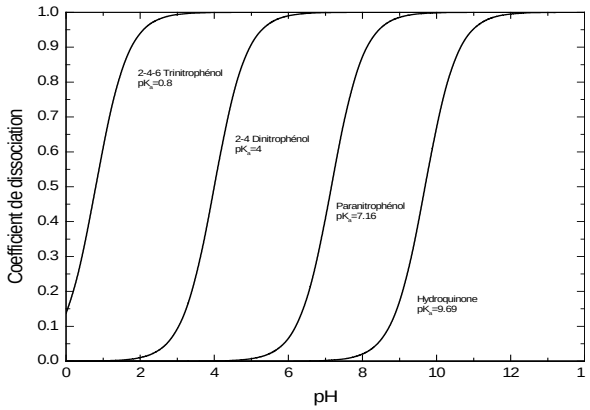

Figure 4: Evolution of the rate of dissociation of molecules as a function of pH

IV. Relationship Between Bohart-Adams and Mckay

The adsorption capacity, the rate constant and the external mass transfer coefficient of a solute on an adsorbent material can be calculated from the adsorption kinetics. For activated carbon, it is assumed that the solute is transferred from the solution to the liquid film and then a transfer of the solute to the solid. After these steps, the phenomena of adsorption and diffusion in the material will take place. Thus, Thomas [10] shows that the rate of adsorption of a solute on a porous solid support can be written:

$$\frac{d(Cad/m)}{dt} = k_{ads} C_r[(\frac{Cad}{m})_0 - (\frac{Cad}{m})] - k_{des}(\frac{Cad}{m}) \quad (1)$$

The equation can be exploited using adsorption kinetics: when equilibrium is established $\frac{d(Cad/m)}{dt} = 0$

$$k_{ad} C_r[(\frac{C_{ad}}{m})_0 - (\frac{C_{ad}}{m})] = k_{des}(\frac{C_{ad}}{m}) \quad (2)$$

$$\frac{k_{ad}}{k_{des}} C_r[(C_{ad}/m)_0/(C_{ad}/m)] - [k_{ad}/k_{des}]C_r = 1 \quad (3)$$

By asking: $k_{ad}/k_{des} = b$; $q = C_{ad}/m$ and $q_o = (C_{ad}/m)_0$
We obtain a relation of type Langmuir

$$q_e = q_m \frac{b C_e}{1 + b C_e} \quad (4)$$

Bohart and Adams [11]estimate that in the rapid phase of adsorption kinetics the desorption of the solute is very small, we obtain:

$$\frac{d(Cad/m)}{dt} = k_{ads} C_r[(\frac{Cad}{m})_0 - (\frac{Cad}{m})] \quad (5)$$

The slope of the line $\frac{1}{C_r}\frac{d(C_{ad}/m)}{dt} = f(\frac{C_{ad}}{m})$

Gives k_{ad} and the ordinate at the origin gives and $k_{ads}\left(\frac{C_{ad}}{m}\right)_0$, which makes it possible to have an estimate of the maximum capacity of adsorption. From the kinetic equation used byMcKay et al [12]we obtain:

$$\frac{Cr}{Co} = \frac{1}{1+mK_L} + \frac{mK_L}{1+mK_L}\exp(-\frac{1+mK_L}{mK_L}k_f.S.t) \quad (6)$$

A passage in the logarithm gives us:

$$\ln(\frac{C_r}{C_o} - \frac{1}{1+mK_L}) = \ln(\frac{mK_L}{1+mK_L}) - (\frac{mK_L+1}{mK_L})k_f.S.t \quad (7)$$

Where $\ln(\frac{Cr}{Co} - \frac{1}{1+mK_L})$ As a function of time, the external mass transfer coefficient k_f is calculated from the slope and the ordinate at the origin by knowing S.

V. Relation Of Lagergreen

The Lagergreen relation allows us to study the adsorption kinetics as a whole. It therefore makes it possible to determine an apparent kinetic constant k_{ad}. The rate of adsorption therefore depends in this case on:

- The concentration of absorbable solute,
- The surface area of the adsorbent and its surface functions,
- The conditions of transfer of the molecules to be adsorbed to the liquid from the liquid to the surface of the adsorbent: the diffusion rate of the molecule and the conditions of turbulence prevailing in the medium. This relation is of the form:

$$Ln(q_e - q) = Lnq_e - k_{ad}t \quad (8)$$

VI. Relation By Weber And Morris

In static reactors, transport of the adsorbate within the pores of the adsorbent may be the limiting stage of the adsorption rate. This has been observed for several adsorption processe. In order to verify the intervention of this phenomenon, Weber and Morris studied the evolution of the quantity adsorbed in the solid phase or the conversion rates as a function of the square root of time

$$\frac{C_{ad}}{C_o} = 1 - k_{id}.t^{1/2} \quad (9)$$

It often happens to find curves in the form of two portions, which can be explained by the fact that the first portion of the curve is attributed to the effect of diffusion in the boundary layer, whereas the final portion, which is linear, is attributed to the effect of intarparticular scattering. The slope of the linear portion of such curves has been defined as a kinetic parameter kid note, characterizing the rate of adsorption in the region where intraparticular diffusion is the limiting factor of the kinetics of adsorption

VII. Adsorption Kinetics

The kinetic study is carried out for duration of one hour for each compound, at different initial concentrations or different pHs.

a) Influence of initial concentration

The adsorption kinetics were carried out by introducing 100 mL of an adsorbate solution to a concentration and 0.1 g of activated carbon in several stirred reactors controlled at 25 ° C ± 0.2 ° C. AT The adsorbent is separated from the solution by filtration (0.45 µm).

The analyzes of solutions are carried out by HPLC. The equipment used is a Hewlett-Packard 1050 series. Consisting of a Shimadzu SPD-6A UV detector (268 nm) and a Supelcosil C18 column (250 mm × 4 Mm d.i. ; Particle size 5 µm). All analyzes were carried out in isocratic mode with a phase mobile composition: methanol: water (1% acetic acid) (20:80) at a flow rate of 1 mL.min^{-1}.

For adsorption kinetics and adsorption isotherms studies, adsorption capacities (q_t) at time t (q_t (g\g)) are calculated by the following relation:

$$q_{t=}\frac{(c_0-c_t)}{m_i}V \quad (10)$$

Where C_0, C_t represents the concentration of the phenolic compound in the initial solution and at time t, m_i the mass of activated carbon (g) and V is the volume of the solution in the reactor (L).

By analogy, equilibrium adsorption capacities (q_e (g/g)) are calculated from this same Relationship.

Figure 5 (a), (b), (c) and (d) shows the evolution of residual concentration as a function of time for different initial concentrations, respectively for HYDRO, PNP and 2,4-DNP 2,4,6-TNP.The kinetic exploitation of these results is carried out by different models: Lagergreen model, for the determination of the apparent velocity constant (k_{ad}) and the order of the reaction.

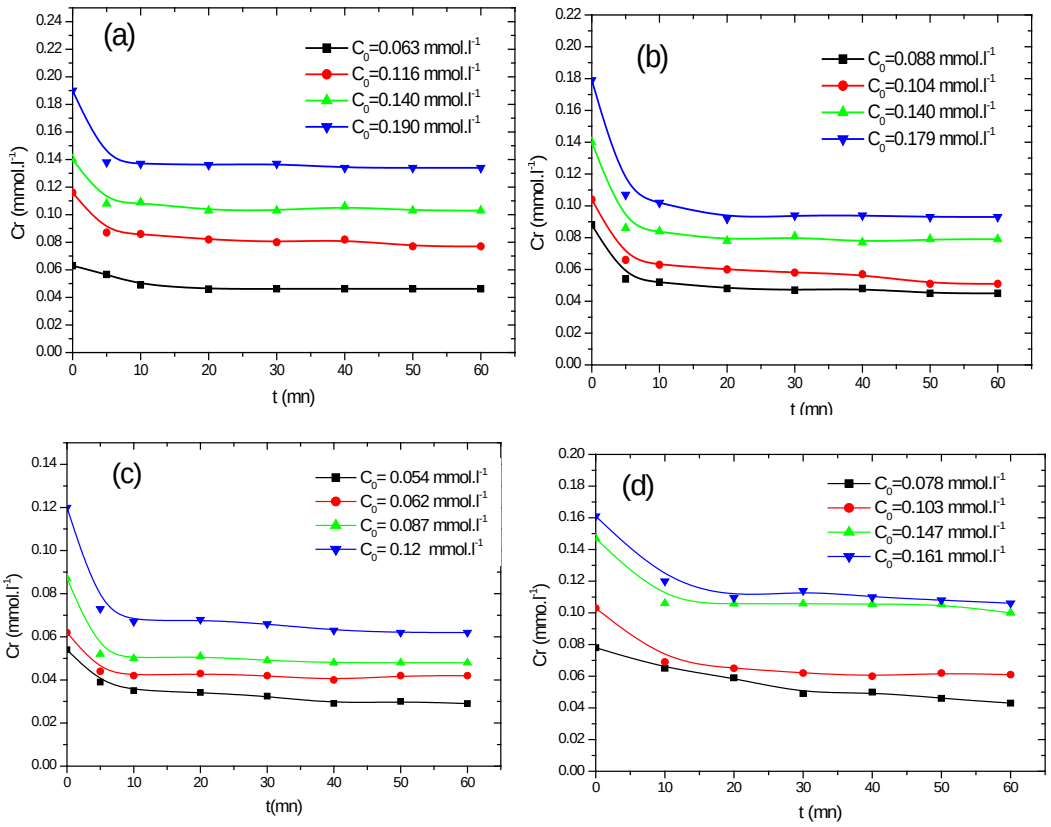

Figure 5 (a,b,c,d): Evolution of residuel concentration in function of time

Model of Weber and Morris to approximate the kinetic constant of intraparticular diffusion k_{id}. Mc Kay model, to determine the external mass transfer coefficient k_f. The interpolation by the three models cited above is carried out for each compound for the different initial concentrations. The Effect of initial concentration:

The lines obtained with the Lager green model show that whatever the initial concentration or the pH, the kinetics of adsorption of the various compounds is of order 1.

The values of the various kinetic constants determined, the errors on the values and the coefficients of correlations are grouped, for the different initial concentrations, in the Table (3) The apparent rate constant k_{ad} varies with the initial concentration, it decreases for Hydroquinone, paranitrophenol and 2,4,6-trinitrophenol when the initial concentration increases. On the other hand, it increases with 2,4-dinitrophenol. Decay is exponential for HYDRO, but linear for PNP. In the case of 2,4, -DNP, k_{ad} grows exponentially with the initial concentration.

Table 3: Values of the various kinetic constants

pH naturel	Co(mol/l)	$k_{ad}(mn^{-1})10^3$	$k_{id}(mn^{-1/2})\ 10^3$	$k_f(m.mn^{-1}10^7)$	$k_f.S(mn^{-1})10^3$
HYDRO (pHn=5.62)	0.063	12.95	23.4	1.02	3.35
	0.116	5.06	15.85	6.87	3.68
	0.14	2.18	6.87	0.368	1.21
	0.19	1.932	3.98	0.307	1.01
PNP (pHn=5.65)	0.088	5.66	18.11	1.13	3.729
	0.104	5.2	25.96	1.81	5.964
	0.14	3.24	9.1	5.06	1.66
	0.179	8.53	13.07	0.769	2.53
2,4-DNP (pHn=4.82)	0.054	0.759	32.15	1.9	6.25
	0.062	4.57	11.72	1.45	4.77
	0.087	3.105	8.33	0.75	2.48
	0.12	5.625	15.22	1.07	3.52
2,4,6-TNP (pHn=3.85)	0.078	22.356	61.04	2.947	9.69
	0.103	8.418	16.66	0.871	2.86
	0.147	0.644	0.97	0.0467	0.153
	0.161	8.533	19.23	0.709	2.334

The equation of K_{ad} in function of C_0 it show in this figure 6. From these equations obtained and for an identical initial concentration (0.15 mmol /l), the k_{ad} classification of the four compounds studied is as follows: 2,4-DNP > PNP > HYDRO > 2,4,6-TNP. This classification appears to be related to the shape of the molecule in solution (non-dissociated or dissociated). Indeed 2,4-DNP is in solution in both forms, which would increase the rate of adsorption, due to the presence of all types of interactions.

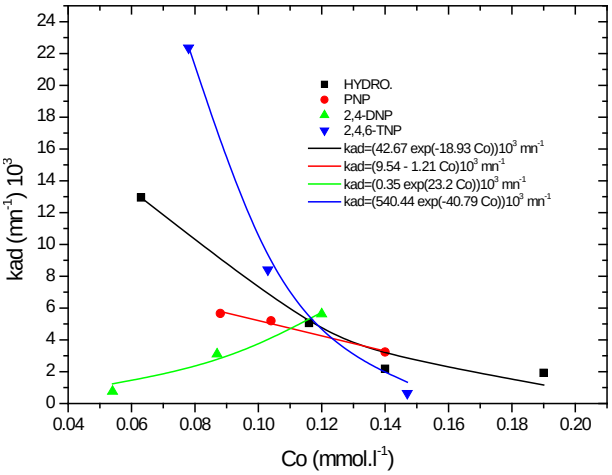

Figure 6: Variation of k_{ad} as a function of C_o for HYDRO, PNP, 2,4-DNP, 2,4,6-TNP

Moreover, the natural pHs of the different compounds, being different and more or less remote from the $pH_{PZC}$of the coal, the proportions of the acidic and basic surface functions will therefore vary, which would influence the rate of adsorption.

In conclusion, the form of the compound considered in solution, its natural pH (more or less distant from the pH_{PZC} of the coal) and the nature of the surface functions of the coal, induce the presence of the different types of interaction and therefore adsorption rates Different.

Moreover, all the straight lines obtained, giving the variation of C / Co as a function of t ^ 1/2 not exceed 1, thus showing that the intraparticular diffusion is not the only process that controls the kinetics.

The intraparticular diffusion constant (k_{id}) also depends on the initial concentration. Its variation as a function of this is shown in figure (7).

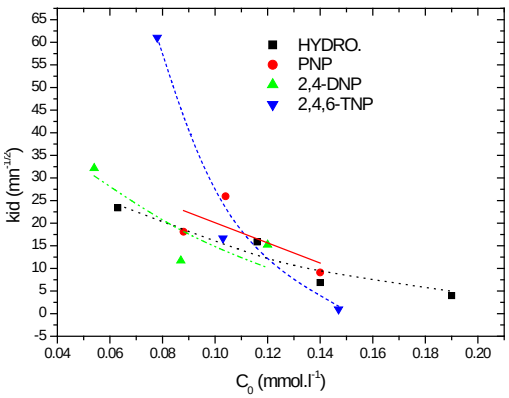

Figure 7: Variation de k_{id} en fonction des concentrations initiales pour HYDRO, PNP, 2,4-DNP, 2,4,6-TNP

The kid constant appears to decrease when the initial concentration increases. In fact, the more it increases, the greater the thickness of liquid film surrounding the particles of the coal, the lower the rate of diffusion in the pores.

b) Effect of pH

The values of the mass transfer coefficient k_f grouped in Table (4) appear to be very complex to discuss. Indeed, k_f depends mainly on the hydrodynamic conditions, which have not been considered in our work. The products k_f. S presented in Table (4) have the same unit as the apparent constant $k_{ad}(mn^{-1})$ and are generally of the same order of magnitude as this, indicating that the adsorption rate is controlled By diffusion.

Table 4

pH	Composés	$k_{ad}(mn^{-1})*10^3$	$k_{id}(mn^{-1/2})*10^3$	$k_f(m.mn^{-1})*10^7$	$Vo=k_{ad}*co(10^3$ /mn/mol/l)
pH=2	HYDRO.	10.603	23.19	-	1.91
	PNP	21.36	18.3	3.28	3.05
	2-4 DNP	9.96	62.56	2.37	1.07
	2-4-6 TNP	18.63	19.28	0.89	2.83
pH naturel	HYDRO.	1.932	3.98	0.307	0.36
	PNP	3.24	9.1	5.06	0.45
	2-4 DNP	5.635	15.22	1.07	0.67
	2-4-6 TNP	0.644	0.97	0.0467	0.094
pH=9	HYDRO.	-	-	-	-
	PNP	1.518	8.26	0.267	0.19
	2-4 DNP	23.506	30.07	1.22	3.97
	2-4-6 TNP	16.19	27.87	1.71	2.12
pH=13	HYDRO.	25.83	4.43	2.51	4.67
	PNP	5.23	17.26	1.07	0.94
	2-4 DNP	18.33	29.78	1.239	2.47
	2-4-6 TNP	11.63	16.78	0.78	1.523

The effect of pH is shown in Table (4), the variation as a function of the pH respectively of the initial velocity v and the intraparticular diffusion constant k_{id}. It is found that the adsorption rate of hydroquinone and 2,4-DNP is faster at alkaline pH.

On the other hand, that of PNP and 2,4,6-TNP are faster at acid pH. The classification of different compounds according to the initial rate

At pH = 2 is as follows: PNP>2,4,6-NPT>HYDRO>2,4-DNP

At pH=13 it is as follows HYDRO > 2,4-DNP > PNP > 2,4,6-TNP

Intraparticular scattering is generally faster at acid pH, indicating that the undissociated form will diffuse more rapidly than the dissociated one. Indeed, the undissociated molecule seems to be less hampered by electrostatic attraction-repulsions on the surface of the particle.

VIII. Conclusion

The adsorption kinetics studied at various initial concentrations or different pHs showed that: The adsorption reaction is first order for all compounds regardless of the initial concentration or pH. The apparent rate constant k_{ad} decreases when the initial concentration increases exponentially in the case of HYDRO and 2,4,6-TNP and linearly in the PNP case, but increases exponentially with the initial concentration in the case of 2,4,6-TNP -DNP.From the equations obtained, giving the variation of k_{ad} as a function of the initial concentration, a classification following k_{ad} is deduced for an identical initial concentration. This ranking is as follows: 2,4-DNP > PNP > HYDRO > 2,4,6-NPT. Intraparticular scattering is not the only process that controls kinetics. Its k_{id} coefficient appears to decrease when the initial concentration increases.

Adsorption kinetics depend on pH; It is faster at alkaline pH for HYDRO. And 2,4-DNP and at acid pH in the case of PNP and 2,4,6-TNP. All the results obtained demonstrate the simultaneous presence of all or only certain types of interactions: nonlocalised (Van Der Waals-London Π-dispers dispersive forces), donor-acceptor, by electrostatic attraction-repulsion and hydrogen bonding. The nature of the interactions responsible for adsorption depends essentially on the pH of the solution, the nature of the surface functions of the coal and the physico-chemical characteristics of the phenolic compounds to be adsorbed.

References Références Referencias

1. Chan, C.H., Lim, P.E. Evaluation of sequencing batch reactor performance with aerated and unaerated FILL periods in treating phenol-containing wastewater. *Bioresour. Technol. 98 (7),* ***2007,*** *1333– 1338.*
2. Wang, C., Feng, Y., Gao, P., Ren, N., Li, B.L., 2012. Simulation and prediction of phenolic compounds fate in Songhua River, *China. Sci. Total Environ. 431,* ***2012****, 366–374.*
3. Kumar, S., Zafar, M., Prajapati, J.K., Kumar, S., Kannepalli, S.Modeling studies on simultaneous adsorption of phenol and resorcinol onto granular activated carbon from simulated aqueous solution. *J. Hazard. Mater. 185 (1),* ***2011*** *287–294.*
4. Calace N, Nardi E, Petronio BM, Pitroletti M. Adsorption of phenols by papermillsludges. *Environ. Pollut.* **118**, **2002**315-319.

5. Santana CM, Ferrera ZS, Torres Padrón ME, Santana Rodríguez JJ. Methodologies for the Extraction of Phenolic Compounds from Environmental Samples: *New Approaches. Molecules 14: **2009** 298-320.*
6. Langmuir, I. the adsorption of gases on plane surfaces of glass, mica and platinium, J. Am. Chem. Soc. 40, **1919** 1361.
7. Weber, J.; Morris, J.C. Kinetics of adsorption on carbon from solution. J. Sanit. Eng. Div. 89: **1963**, 31–60
8. Ho, Y., Mc Kay, G. The kinetics of sorption of divalent metal ions onto sphagnum moss peat, *Water Research 34, **2000**, 735.*
9. N.T. Abdel-Ghani, E.S.A. Rawash, G.A. El-Chaghaby Equilibrium and kinetic study for the adsorption of p-nitrophenol from wastewater using olive cake based activated carbon
10. *Global J. Environ. Sci. Manage., 2(1): **2016**,11-18*
11. Thomas H.C., Am. Chem. *Soc.66 , **1944** ,1664*.
12. Bohart G.S. et Adams E.Q. Am. Chem. *Soc **1920**42 , 523.*
13. Mc Kay G., Brino M.J. et Altmemi A., *Water RES.20,4 **1986** 435.*

This page is intentionally left blank

Global Journal of Researches in Engineering: C
Chemical Engineering
Volume 17 Issue 3 Version 1.0 Year 2017
Type: Double Blind Peer Reviewed International Research Journal
Publisher: Global Journals Inc. (USA)
Online ISSN: 2249-4596 & Print ISSN: 0975-5861

Emulsion Terpolymerization of *St/MMA/Bua:* III. Modeling of Bua Backbiting, Diffusion of Monomers and Polymers in the Particle, and Bua Induced Branching

By Javier Alejandro Díaz-Ponce & Carlos Martínez-Vera
Universidad Autonoma Metropolitana Iztapalapa

Abstract- In this work, the BuA backbiting and its kp-gel effect is included in a previous published model for the simulation of the emulsion terpolymerization of St/MMA/BuA. It is then possible to evaluate the branching of this terpolymer and the average diffusion of the monomers, polymers and polymer radicals. The diffusion is evaluated through the propagation and termination coefficients with a modification of the Schmoluchowski equation. On the other hand, it is also found that the BuA propagation coefficient depends on the fraction of BuA free volume $X_{Vf,BuA}$ in the terpolymer and that the kind of model suitable for the simulation of the k_p-gel effect is determined by the rate of polymerization R_p, the number of radicals in the particle per mol of monomers #R/n and the total diffusion of the polymer radicals in the particle $n_T D^{PR}$.

Keywords: *backbiting, gel effect, diffusion, rate of polymerization, branching.*

GJRE-C Classification: *FOR Code: 290699*

Strictly as per the compliance and regulations of:

Emulsion Terpolymerization of *St/MMA/Bua:* III. Modeling of Bua Backbiting, Diffusion of Monomers and Polymers in the Particle, and Bua Induced Branching.

Javier Alejandro Díaz-Ponce [α] & Carlos Martínez-Vera [σ]

Abstract- In this work, the BuA backbiting and its k_p-gel effect is included in a previous published model for the simulation of the emulsion terpolymerization of St/MMA/BuA. It is then possible to evaluate the branching of this terpolymer and the average diffusion of the monomers, polymers and polymer radicals. The diffusion is evaluated through the propagation and termination coefficients with a modification of the Schmoluchowski equation. On the other hand, it is also found that the BuA propagation coefficient depends on the fraction of BuA free volume $X_{Vf,BuA}$ in the terpolymer and that the kind of model suitable for the simulation of the k_p-gel effect is determined by the rate of polymerization R_p, the number of radicals in the particle per mol of monomers #R/n and the total diffusion of the polymer radicals in the particle $n_T D^{PR}$.

Keywords: backbiting, gel effect, diffusion, rate of polymerization, branching.

I. Introduction

The copolymers of butyl acrylate BuA synthesized by emulsion polymerization are important as resins for the paint industry [1.2]. In particular, the increment of the branching of their chains promotes a lower swelling of the BuA copolymer by the solvent [3]. The branching also avoids the easier dispersion of carbon black [4]. Both effects modify the characteristics of the paint with technological and economical consequences. The branching is estimated through the branching density BD, to say, the fraction of branched BuA monomer units to the total number of monomer units polymerized [3].

The branching in a polymer with BuA is mostly caused by the backbiting reaction of BuA (intramolecular polymer chain transfer). The backbiting reaction is substantially carried out through a ring of six carbon atoms (abstraction 1:5), when the BuA ended secondary radical finds a BuA unit in the pen-pen-ultimate position and abstracts the hydrogen of the tertiary carbon near to the carbonyl group (See Supporting Information Section S-1) [5,6]. This abstraction of hydrogen forms a lower reactive tertiary electrophylic radical [7]. We emphasize the word electrophylic because the tertiary radical is joined to the carbonyl group of the butyl acrylate, which attracts the charge of the tertiary radical and increases its electrophylicity. This tertiary radical propagates with a branch of two inactive monomers. The penultimate effect is present in the backbiting reaction of the terpolymer of styrene/methyl methacrylate/butyl acrylate St/MMA/BuA because the presence of penultimate monomers of St or MMA decreases the backbiting reaction as a consequence of steric effects [5]. At low temperatures T < 80 °C, as it happens in the emulsion polymerization of St/MMA/BuA, the β-scission [3,8] and depropagation side reactions are negligible and they are not taken into account in the modeling of its backbiting.

A lower concentration of monomer leads to a higher degree of branching due to a higher proportion of intramolecular (backbiting) and intermolecular polymer chain transfer with respect to the propagation reaction [3]. For this reason, it is expected a higher proportion of branching in the semicontinuous processes. Besides, it has been found that a higher amount of chain transfer agent reduces the backbiting reaction in acrylics, and correspondingly their branching. There are three explanations to this phenomenon: 1. Transfer of the proton (in the case of thiols) or of the halogen (patching in the case of halogenides) to turn off the reactivity of the tertiary electrophylic radicals; 2. The chain transfer agent decreases the chain length of the polymer chain and there are lesser active sites for the radical intramolecular chain transfer to the polymer; 3. The decrement of the degree of polymerization induced by the transfer agent provokes a diminution of the value of the kinetic coefficients of BuA. This is the hypothesis of kinetic coefficients depending of the degree of polymerization. On this way, a lower value of the kinetic coefficients of BuA induces a higher lessening of the BuA backbiting kinetic coefficients and, in consequence, a decrement of the branch density BD. In the case of bulk polymerization, Agirre et al. [3] discarded the patching of the tertiary electrophylic radicals because the signals in MALDI-TOF and NMR spectra for the

Author α: Departamento de Física, Postdoctoral Position.
Author σ: Departamento de Ingeniería de Procesos e Hidráulica. Universidad Autónoma Metropolitana-Iztapalapa. Av. San Rafael Atlixco 186, Col. Vicentina, Apdo. Post. 55-534, Mexico City, C.P. 09340, México. e-mails: qjavier2002@yahoo.com, cmv@xanum.uam.mx

patched carbon were not found. Nevertheless, Ballard reported that a more careful analysis of the spectra indicates a signal related to the patching of these radicals. Ballard also found that the incertitude of the temperature in bulk polymerization does not allow determining the precise magnitude of the patching by the transfer agent [9]. In the case of solution polymerization, Ballard concluded through the fitting of computer simulations to the experimental data that the 1st hypothesis is discarded. This is due to a low value of the kinetic rate of the chain transfer agent which is not enough to avoid the backbiting of BuA. By the contraire, chains with a lesser degree of polymerization decrease the branching of the polymer. These calculations validate then the 2nd hypothesis. On the other hand, Ballard also concluded that the 3th hypothesis is not valid because the kinetic rate in degrees of polymerization greater than 3 does not appreciably depend on the degree of polymerization or the chain transfer agent CBr_4 [9]. On the other hand, there are additional kinetic rates in the emulsion polymerization in comparison to the bulk and the solution polymerization: kinetic rate of radical desorption from the particle to the aqueous phase R_f and kinetic rate of capture of radicals from the water phase into the particle R_a. So, the concentration of BuA monomeric radicals in the particles is influenced by their capture/desorption into/from the particles and then the backbiting and consequently the branching are influenced by these phenomena. Besides, the influence of the surface on the kinetic rates and the concomitant hypothesis of homogeneous reaction throughout the particle must be evaluated because the emulsion polymerization is compartmentalized in particles emulsified in water. The correct assessment of surface dependence of the radicals desorption from the particle, for example, helps to determine more accurately the branching of the St/MMA/BuA terpolymer.

The homogeneous reaction throughout the particle was first postulated by Harkins [10,11], but the presence of domains such as a core shell structure in the particle can influence the balance of polymer radicals. On this way, it has been found that the reaction on the surface influences the desorption rate of monomeric radicals R_f. This is the case when the backbiting reaction of BuA is taken into account to simulate the molecular weight of the terpolymer [12]. The influence of the surface on the balance of radicals has been found out in particles of 250 nm for PMMA at high conversions, but not in particles of 25 nm [13]. For this reason, it is necessary to determine if the other kinetic rates are surface dependent in the emulsion terpolymerization of St/MMA/BuA. The verification must be done in processes in which the consideration of polymerization in all the volume or on the surface modifies appreciably the outputs of conversion and/or molecular weight. In our experimental setup the verification was done in batch B-3 in which the higher amount of water soluble monomers led to a high desorption of the monomeric radicals from the surface:

This verification was also done in the seeded semicontinuous BS-1 in which the particle volume was high, see below. On the other hand, it has been found in the emulsion terpolymerization of St/MMA/BuA that the transfer to monomer R_m is not so important for the evaluation of the conversion and the molecular weight [12].

We consider that the evaluation of the k_p-gel effect in terpolymers in which the backbiting of BuA occurs is more sensitive for testing the hypothesis of homogeneous particle-phase polymerization. This is due to the high reactivity of BuA-ended secondary radicals ($k_{p,\ BuA0}$ = 32390 dm^3/mol/s at 55 °C) and the low reactivity of the tertiary electrophylic radicals ($k_{p,\ BuAbb}$ = 34.45 dm^3/mol/s at 55 °C) [5]. The gel effect in BuA causes a high variation of these propagation coefficients [12] and then the simulation model must be more exact in order to fit the outputs of conversion and molecular weight. On this way, the inclusion of the hypothesis of particle- phase polymerization must give outputs in accordance to the experimental results. In this context, the values of the diffusion of the monomers D^M and polymers D^P in the particle determined by the simulation model must also correspond to the values found in the literature. The behavior of these diffusion coefficients in the reaction can also help to understand the causes of the gel effect. It has been found that the diffusion of St in polystyrene PSt [14] is of the order of 10^{-6} cm^2/s at W_p = 0.5 and T = 50 °C. On the other hand, the diffusion of MMA in polymethylmethacrylate PMMA is of the order of 10^{-5} cm^2/s [13] at W_p = 0.5 and T = 50 °C. Furthermore, the diffusion of the monomers of BuA or MMA in a copolymer of MMA/BuA (20-80 wt%) is of the order of 10^{-7} cm^2/s [15] at 50 °C and W_p = 0.6. For this reason, it is expected a similar trend in the terpolymer of St/MMA/BuA. In principle, the Rouse model can be applied to evaluate the diffusion of the polymers D^P in a concentration lower than the critical concentration for the overlap of the polymer chains c* (concentration in which the polymers interpenetrate in the dilution regime). On this way, the Rouse model predicts a dependence of the polymer diffusion coefficient as $D^P \propto (N^P)^{-1}$ [16]. N^P is the degree of polymerization of the polymer and is obtained from the one and second moment of the molecular weight distribution of the dead polymer ν_1, ν_2, respectively. On the other side, in accordance to the reptation model the diffusion of the polymer D^P scales with N^P as $D^M/(N^P)^n$ [17,18] with n = 2 after the critical concentration for the entanglements c**. Griffiths et al. have pointed out that the exponent should increase progressively from n = 0.5 - 0.6 at infinite dilution to n = 2 at a concentrated solution [19]. By their part, Tulig and Tirrell have emphasized, the dependence of the diffusion of the polymer D^P on the concentration of the polymer solution "c" with a

dependence of $c^{0.75}$ at $c < c^{**}$, and $c^{1.75}$ at $c > c^{**}$ in accordance to the reptation model [20-21].

In our previous work [12], we only reported the results of the simulation of the backbiting of the BuA-ended polymer radicals. The purpose of this work is to explain in more detail the previous results and correlate the backbiting to the diffusion and the branching phenomena in the emulsion terpolymerization. First, we describe the new equations added to the previous terpolymerization model as consequence of the BuA-ended secondary polymer radicals backbiting. As a general overview, we make a comparison of the outputs of conversion and glass transition temperature between the average k_p-k_t model for the terpolymerization developed in the previous work and the model which includes the backbiting of BuA. After that, we correlate the gel effect to the diffusion of monomers and polymer radicals in order to explain the causes of the gel effect. As a last part of this work, we make an analysis of the dependence of the branching of the terpolymer to the kinetic conditions of the emulsion terpolymerization. We considerer that the key contribution of our work is the evaluation by first time of the diffusion of monomers in the particle. Also, our calculations differentiate the diffusion of the polymer radicals from the polymer molecules.

II. Review of the Experimental Data

The composition and conditions of batches B-1 to B-4, semicontinuous SC-1 to SC-4 and seeded semicontinuous BS-1 are given in our previous work. The batches B-1, B-2 and B-4 in addition to the semicontinuous SC-1, SC-2 and SC-3 have the same feed composition of St/MMA/BuA (25/50/25 wt%) near to the azeotropic unitary composition. The batch B-3 and the semicontinuous SC-4 have the feed same composition (17/33/50 wt%). The seeded semicontinuous BS-1 was near to composition of B-1 (29/45/26 wt%). The addition rate of monomers was: SC-1 (0.27 g/min), SC-2 (0.48 g/min), SC-3 (0.84 g/min), SC-4 (0.34 g/min), BS-1 (0.50 g/min). The reaction temperature was 55°C, at exception in B-4 and BS-1 in which the reaction temperature was 70°C [12]. The strategy of monomers addition and initial composition of the seed in seeded semicontinuous BS-1 tried to keep the proportion of the monomers in the terpolymer almost constant throughout the polymerization reaction. For that reason, the reaction of the batch used as seed was near the unitary azeotropic composition and was stopped at 77.5 % wt% of conversion in order to avoid a higher drift in the composition of the monomers in the terpolymer. This batch was then distilled at low pressure in order to discard the residual monomers. The conversion only increased to 79.2 wt% after the distillation. Most of the monomers in the emulsion were in the particles and the higher boiling point of the acrylic monomers with respect to water produced their lower rate of distillation. So, in accordance to the mass balance, the water was the most distilled liquid and the proportion of monomers in the emulsion slightly increased from 3.2 to 4.1 wt%. On this way, from the 150 g of the distilled emulsion that was used as seed, the mass of monomers was 6.2 g as reported in the previous work [12]. In addition, the values of the final molecular weight for the processes are: B-1: M_n = 45000, M_w = 102000; B-2: M_n = 31000, M_w = 57000, B-3: M_n = 34000, M_w = 52000: B-3: M_n = 34000, M_w = 52000; SC-1: M_n = 28000, M_w = 47000; SC-2: M_n = 34000, M_w = 65000; SC-3: M_n = 43000, M_w = 72000; BS-1: M_n = 98000, M_w = 299000 g/mol [22-23].

We have made the simulation of the transition glass temperature T_g and DSC thermograms. We have verified its results with the experimental DSC thermograms obtained in a Dupont 4210 DSC. The experimental DSC thermograms were run from -70 °C to 130 °C with a temperature rate of 10°C/min at open panel with a flux of N_2. The sample approximately weighted 10 mg. The simulation of the DSC was better for the batch processes and the variable that adjusted better the experimental range was ΔT_{gi}, as seen below (The equations for the simulation of Tgi and the DSC thermograms are given in Supporting Information Section S-6).

III. Backbiting Reaction Added to the Previous Terpolymerization Model

The simulation model for the emulsion terpolymerization given in the previous article [12] is extended to include the backbiting side reaction of BuA.

a) BuA Backbiting model considerations

- β-scission [8] and depropagation reactions are not considered.
- The total number of j-ended radicals is obtained by the Nomura's semiempirical equation for the radicals in the particle [24]. The BuA-ended tertiary electrophylic radicals have the same kinetic processes as the secondary BuA-ended radicals: propagation, termination, transfer to monomer and transfer to chain transfer agent, with exception of the rate of capture of radicals into the particle and rate of desorption. The last rate is not considered because the tertiary radicals have a degree of polymerization greater than 2 and then they are not desorbed.
- The k_p-gel effect of the BuA-ended radicals starts since the beginning of the reaction [12].
- The constants of the Hamielec model of k_p-gel effect are evaluated independently to the Ray and W_p models. The constants of the two last models are interrelated through our previous procedure [12].

– The model considers the initiation, termination and desorption of radicals in the aqueous phase in Equation (S-5) - (S-11) of Supplementary Information of the previous work [12]. The model does not consider the propagation of radicals in the aqueous phase. Through the evaluation of the experimental value of particle diameter vs conversion, the model includes the increment of the diameter by the homogeneous nucleation and the subsequent adsorption in the particle. In the previous work, the simulation of the diameter of the particle through the Langmuir adsorption curve includes the increment of the diameter by homogeneous nucleation through the adjustment of the value of the exponent x of the micelar nucleation. The exponent x is given in Table 4 of the previous work [12].

b) Materials Balance

The mass balance was the same as the previous model [12] splitting the term of BuA radicals in terms of secondary and tertiary radicals.

c) Average total number of j-ended radicals in the particle n_T

The total average number of j-ended radicals in the particle "n_T" was calculated through the semi-empirical equation of Nomura [24]. The equations for finding n_T only added the term of backbiting. In order to not be redundant with the previous work, these equations are given in Supporting Information Section S-1. The kinetic rates are also given in that section. The number of BuA-ended tertiary radicals n_{cbb} were calculated through a mass balance of the kinetic rates (#rad/part/s) of backbiting R_{ncbb}, propagation $R_{p,ncbb}$, termination $R_{t,ncbb}$, transfer to monomer $R_{m,ncbb}$ and transfer to chain transfer agent $R_{T,ncbb}$ in accordance to Table I. The probability $P_{ijk}(i,j,k)$ of existence of the j-ended radical triad ijk at time t was calculated by the product of the probabilities of the occurrence of the n_i, n_j, n_k-ended radicals (without considering the tertiary radicals of BuA) at times $t-3\Delta t$, $-t2\Delta t$ and $-t\Delta t$, respectively. Δt is the increment of time for the evaluation of the reaction kinetics, in this case 0.001 s. This procedure is different to the one of Wang and Hutchinson [5].

The total average number of j-ended radicals in the particle n_T and the average number of other radicals that the BuA- tertiary radicals "n" are given by:

$$n_T = n_a + n_b + n_c + n_{cbb} \quad (1a)$$

$$n = n_T - n_{cbb} \quad (1b)$$

With:

$$\text{If } n < 0 \text{ then } n_T = n_{cbb} \text{ and } n = 10^{-9} \quad (1c)$$

The simulation was also performed considering a proportional amount of the radicals n and n_{cbb} when $n_{cbb} > n_T$, but it did not give congruent results. The explanation of this behavior is that the formation of the tertiary BuA-ended radicals needs of the backbiting of polymer radical with a degree of polymerization at least of j = 3. For this reason, these radicals are not desorbed ($R_{fncbb} = 0$) because the model considers desorption of monomeric radicals with j = 1.

As a chemical kinetic ground, the high reactivity of the BuA secondary radicals and the corresponding lower reactivity of the tertiary BuA-ended radicals produce a lower amount of the secondary radicals in the particle, as will be seen below.

d) Reaction Kinetics

(The reason of defining the k_p-gel effect in this article is given in Supporting Information Section S.1.3.) The evaluation of the kinetic rates R_f, R_p, R_m and R_T depends on the propagation coefficient $k_{p,ij}$ (See Supporting Information, Tables S-1 and S-2), which has a k_p-gel effect. For this reason, we estimated first this variable and then we used it in the corresponding kinetic rates.

i. *Propagation rate coefficient of radical "i" to monomer "j" $k_{p,ij}$.*

We have analyzed the k_p-gel effect for this system in the previous article [12]. In this work the backbiting of the BuA secondary-ended radicals was taken into account, in which the k_p-gel effect starts since the beginning of the reaction. The apparition of the k_p-gel effect in BuA is caused by the lower free volume V_f of St and MMA than of BuA in the terpolymer (Vf_{PSt} = 0.0025, Vf_{PMMA} =0.0032, Vf_{PBuA} = 0.0605 at 55°C for the homopolymers) [12]. In principle, we have kept the values and restrictions of the k_p-gel constants for St and MMA [12]. On the other hand, we have found the values of the constants for BuA for the V_f Ray's k_p-gel model in the batch process B-1 iterating at the same time with the values of concentration of monomers in the particle $[M]_p$ and critical value of free volume for BuA V_{fcc} as explained in the section Methodology below. Then, we have matched the equations of the V_f Ray's and W_p k_p-gel models for BuA-ended radicals in order to obtain the constants A_j and V_{fcj} for the W_p k_p-gel model [12]. The equating gave very different results in the case of BuA in the equating of V_f Ray's and the V_f Hamielec's k_p-gel models. Probably, the sensitivity of the BuA backbiting reaction for the abrupt change of the value of $k_{p,BuA}$ set up this discordance of the Hamielec's k_p-gel model because this model predicts a lower k_p-gel effect (Higher R_p) in the batch processes than the W_p and V_f Ray's models [12]. On this way, the constants of the Hamielec's k_p-gel model were calculated of independently manner.

It has been realized by Sundberg et al. [25] that the constant A_1 of the exponential term for the

Hamielec's equation in the homopolymers for the propagation coefficient k_p is the critical free volume $V_f^{M,*}$ for the beginning of a monomer to jump:

$$\frac{k_p}{k_{p0}} = \exp[-A_1(\frac{1}{V_f} - \frac{1}{V_{f0}})] \quad (2)$$

V_{f0} is the critical free volume for the beginning of the k_p-gel effect.

The values of the constants $A_{1j} = V_f^{j,*}$ in the emulsion terpolymerization of St/MMA/BuA were near to the free volume of the homopolymers times 6 (we consider the value of $A_{1,BuA}$ for backbiting, see Table 3): $A_{1,St} = V_f^{St,*} = 0.015 \approx 6\ V_{f,PSt} = 6\ (0.0025)$, $A_{1,MMA} = V_f^{MMA,*} = 0.015 \approx 6\ V_{f,PMMA} = 6\ (0.0032)$, $A_{1,BuA} = V_f^{BuA,*} = 0.35 \approx 6\ V_{f,BuA} = 6\ (0.0605)$. These constants were found by iteration to fit the conversion curve [12] and the similarity is worthy, because it shows that free volume of the homopolymers is related to the k_p-gel effect. Consequently, a free volume V_f near to the j-ended radical of the terpolymer higher than 6 of the free volume of the average homopolymer "j" is necessary to do not have k_p-gel effect. We consider that the constants A_3 for the W_p model also have an equivalent meaning as in Equation (2).

It was observed a point of change of curvature of the rate of polymerization at $X_O = 0.78$ ($V_{fc2} = 0.05$ corresponding to $W_{pc2} = 0.7945$ in B-1), which was associated to an increment of the k_p value for the radicals of BuA [12]. We have associated this critical value of V_{fc2} to a critical value of the proportion of BuA free volume in the terpolymer X_{Vf} ($X_{Vfc2} = 0.84$ in B-1) for the beginning of the increment of the BuA propagation coefficient. Then, we have used the critical condition $X_{Vf} > X_{Vfc2} = 0.84$ for all the emulsion polymerization processes in the V_f k_p-gel models. In the W_p k_p-gel model, we used the condition $W_{pc2} > 0.7945$. We consider that the increment of $k_{p,BuA}$ was due to a higher free volume of the last portion of the terpolymer with a BuA-ended radical with a high proportion of BuA monomers in the terpolymer nearer to this radical given by the condition $X_{Vf} > X_{Vfc2} = 0.84$. We have associated the increment of the value of $k_{p,BuA}$ with a change of the value of the constants in the k_p-gel models, that is, from A_{1k} to A_{2k} (See Tables 2 and 3). The change of the value of the constants produces a jump in the value of $k_{p,BuA}$ with its subsequent decrement associated to the fall down of free volume V_f. On this way, this jump is associated to a catastrophic behavior in the value of $k_{p,BuA}$. This catastrophic behavior is found when one monomer has an extremely higher reactivity than the other monomers [26]. In this case, the segmental diffusion of the monomer ended radical of BuA is fast at a higher proportion of BuA in the terpolymer and then it produces an abrupt increment of the reactivity. This increment of the value of $k_{p,BuA}$ is produced by the higher free volume of BuA than that of St or MMA in the terpolymer. With this argument we support the idea that the contribution of the segmental diffusion is important to the evaluation of the k_p-gel effect [27], which is included in the diffusion of the polymer radical through its reptation. On this way, the diffusion of the monomers in the bulk of the solution is not as important in the selection of the k_p-gel model as their diffusion near to the polymer radical, because near to the polymer the friction exponentially grows up [28], and their diffusion falls down in the same way.

In Table 2 are given the corresponding equations for the Hamielec (k =1), Ray, (k = 2) and W_p (k = 3) models before and after the critical point for BuA, $X_{Vf} > X_{Vfc2} = 0.84$, and in Table 3 are given the values of the corresponding constants. It is observed in the processes batch, semicontinuous and seeded processes a critical value of V_{fc1} (W_{pc1}) associated to the beginning of the reaction ($V_{fc1} = 0.14$ corresponding to $W_{pc1} = 0.1865$ in B-1). This value of V_{fc1} is near to the value of V_f for the monomer St. At exception of batch B-3, the point of change of curvature at $X_{Vfc2} > X_{Vfc2} = 0.84$, only changed the value of the constant of the k_p-gel effect A_{1k} to A_{2k}, (k = 1,2,3 are the k_p-gel models). However, the critical value of V_{fc1} of 0.14 (corresponding to $W_{pc1} = 0.1865$ in B-1) remained the same as observed in Table 2. We consider that the original critical value of V_f ($Vf_{c1} = 0.14$, $W_{pc1} = 0.1865$) had influence over the gel effect throughout the reaction in almost all the processes.

In the case of the fitting of batch B-3 with a higher composition of BuA, it was necessary to put the value of $V_{fc2} = 0.052$ ($W_p = 0.7945$) instead of the value used before of $V_{fc1} = 0.14$ ($W_{pc1} = 0.1865$;) in the expression $(1/V_f\text{-}1/V_{fc1})$ at $X_{Vf} > 0.84$. Then, we applied Benyahia's procedure for the termination k_t-gel effect of BuA in order to write the expression of the k_p gel effect as seen in Tables 2 and 3 [29]. On this way, an increment of the proportion of BuA in the batch B-3 caused that the value of V_{fc2} in the point of change of curvature ($V_{fc2} = 0.052$ see Table 3, near to the free volume of the homopolymer PBuA, $V_{f,BuA} = 0.05$) had influence on the k_p-gel effect in batch B-3.

ii. *Diffusion coefficients in the particle*

The diffusion of the polymer without chemical reaction is given by Equation (3) [30].

$$D^P = 6\ k_B\ T \left[\frac{(2\ L_{pers} - b)}{b\ (N+1)}\right]^2 \left[\frac{(1+\cos(\tau))}{(1-\cos(\tau))}\right]^2 \frac{1}{\xi_{seg}\ \sigma_{SH}} \quad (3a)$$

$$L_{per} = \frac{b}{(1 + \cos(\tau))} \quad (3b)$$

We consider the model of wormlike chain (reptation of the polymeric radical chain with N monomers). The bond length is b and the bond angle is τ, k_B is the Boltzman constant (erg/K), T is the temperature (K), L_{pers} is the persistence length (cm) which is higher for stiff polymers and the sequence is $L_{pers,St}$ (≈9.0 X 10^{-8} cm) > $L_{pers,MMA}$ (6.9 X 10^{-8} cm) ≈ $L_{pers,BuA}$ (6.9 X 10^{-8} cm) [30], σ_{SH} is the hindrance factor which indicates the steric hindrance to rotate with the following sequence: $\sigma_{SH,St}$ (2.2)> $\sigma_{SH,BuA}$. ≈ $\sigma_{SH,MMA}$ (1.9). There is not certitude in the value of the steric hindrance of BuA because this parameter increases with the size of the short branches (probably near to 1.9, which is the value of the polybutymethacrylate PBuMA). ξ_{seg} is the friction coefficient of the segment of the polymer, in this case the monomer in the terpolymer (g/s).

As also explained below, a higher proportion of BuA in the terpolymer allows a higher diffusion of the polymer radicals and of the monomers. The lower value of the friction coefficient for the segment of BuA, $\xi_{seg, BuA}$, is caused by the branches of butyl and the two monomer branches induced by the backbiting of the secondary polymer radicals of BuA. On this way, Ferry pointed out that the branching decreases the friction coefficient [31]. In order to calculate the diffusion coefficients of the terpolymer, it was defined that the effective propagation coefficient $k_{p,Tot}$ with gel effect, has an independent contribution [32] (similar to a parallel electric circuit) of chemical reactivity and diffusion as expressed in Equation (4) [33-34]. Equation (4) is another way to express the dependence of the propagation coefficient on the diffusion phenomena (parallel expression) to the W_p and V_f Hamielec's and Ray's models given in Table 3. In the later models, the dependence is through the division of the chemical propagation rate coefficient between the corresponding coefficient which considers the diffusion (series expression).

$$\frac{1}{k_{p,Tot}} = \frac{1}{k_p^{chem}} + \frac{1}{k_p^{diff}} = \frac{1}{k_{p,Tot0}} + \frac{1}{k_p^{diff}} \quad (4)$$

Where $k_{p,Tot0}$, is the chemical propagation coefficient without gel effect ($dm^3/mol_{mon}/s$) and k_p^{diff} ($dm^3/mol_{mon}/s$) is the propagation coefficient which depends on the diffusion of the monomer D^M near the polymer radical and the reactivity the polymer radical D^{PR}. If we consider that the diffusion of a polymer radical D^{PR} (cm^2/s) is given by the diffusion of its center of mass (com) $D^{com,PR}$ [18] with a translation by reptation [17] and by the reaction diffusion induced by the propagation of the j-ended radicals $D^{rd} = D^{rd,PR}$ (also named roving head diffusion or residual termination [35]. We could calculate the diffusion coefficients through the sequence of the calculations given in Table 4. This sequence was established through a dimensional analysis of the Schmoluchowski equation for reaction of two species in accordance to Mills et al. [13], Russell et al. [35] and Stubbs et al.[18], which gives the equations given below (the corresponding deduction is given in Supporting Information Section S-2). It is important to remark that from the Schmoluchowski equation we obtained an expression specific for emulsion polymerization and, on this way, we could calculate de diffusion of the monomers D^M by using the propagation coefficients k_p^{diff}, $k_{p,Tot}$, $k_{p,Tot0,\ where}$ k_p^{diff} is given by:

$$k_p^{diff} = k_p^{rd} + k_p^M \quad (5a)$$

$$k_p^{rd} = 4\,\pi\,\frac{n_T}{[M_T]_p\ v_p}\,D^{rd}\,\left(\frac{\sigma_{LJ}^R}{2}+\frac{\sigma_{LJ}^M}{2}\right) = 4\,\pi\,\frac{\#R}{1000\ n}\,D^{rd}\,\left(\frac{\sigma_{LJ}^R}{2}+\frac{\sigma_{LJ}^M}{2}\right) \quad (5b)$$

$$k_p^{M} = 4\,\pi\,\frac{n_T}{[M_T]_p\ v_p}\,D^{M}\,\left(\frac{\sigma_{LJ}^M}{2}+\frac{\sigma_{LJ}^R}{2}\right) = 4\,\pi\,\frac{\#R}{1000\ n}\,D^{M}\,\left(\frac{\sigma_{LJ}^M}{2}+\frac{\sigma_{LJ}^R}{2}\right) \quad (5c)$$

Where $k_p^{rd} = k_p^{rd,PR}$ is the propagation coefficient dependent on the reaction diffusion of the polymer radical and k_p^M is the propagation coefficient dependent on the diffusion of the monomer.

We have considered that the number of radicals R which reacts per mol of monomers #R/n (radicals/mol) is:

$$\frac{\#R}{n} = \frac{\#M}{n} = \frac{1000\ n_T\ N_p\ V_w}{[M_T]_p\ v_p\ N_p\ V_w} = \frac{1000\ n_T}{[M_T]_p\ v_p} \quad (5d)$$

We have used #R/n instead of N_A, the Avogadro's number, because the last variable corresponds to a mol of radicals, but in emulsion polymerization the number of j-ended radicals in the

particle is n_T, which reacts with the same number of monomers in reaction of first order per mol of monomers. Commonly $n_T < 0.5$, and for example in the simulation of B-1, there were 6.9 X 10^6 molecules of monomer in the particle for one j-ended radical at X_O = 99 wt%. In this context, Chern and Poehlein have shown that the monomers are distributed homogeneously throughout the particle and in consequence there is not a gradient of concentration of monomers in the particle [36].

The frequency of jumping of the reaction diffusion coefficient D^{rd} is given by $k_{p,Tot}\,[M_T]_p$. (1/s) [37]. The square of the average radius of gyration of the polymer radical divided by the number of monomers $a^2_{PR}/6$ (see Table 4) indicates how much the polymer has diffused from its center of gravity by each reaction of the polymer radical with the monomers.

Ferry [31] and Sundberg et al. [25] have analyzed the influence of the free volume in the diffusion of the polymers and monomers with the corresponding critical point in order to change the diffusion values of k_p. These authors indicate that a higher free volume V_f of the polymer solution allows a higher diffusion of the polymer radical and monomers. This is concluded in the following equation for the wormlike chain in the case of the diffusion of a polymer radical depending on the free volume V_f [25,30-31].

$$D^{PR} = \phi_{0,seg}\ N\ b^2\ (2\ L_{pers} - b)\ \exp(-V_f^{Seg,*}/V_f) \quad (6)$$

From the equations in Table 4, it can be observed that the diffusion of the monomer D^M near the polymer radical depends directly on the volume of the particle v_p, the concentration of monomers in the particle $[M_T]_p$ and inversely on the number of radicals in the particle n_T. The dependence of D^M on the free volume is through the gel effect implicit in $k_{p,Tot}$. On this way, using the Equation (4), (5a)-(5c)) with the Hamielec and W_p formulas for the gel effect:

$$D^M = \frac{k_p^{diff}\ [M_i]_p\ v_p}{4\ \pi\ n_T\ (\frac{\sigma_{LJ}^M}{2} + \frac{\sigma_{LJ}^R}{2})} - D^{rd} \quad (7a)$$

Vg.: Hamielec's model:

$$k_p^{diff} = \frac{k_{p,ji0}}{\left(\exp[A_{1j}\ (\frac{1}{V_f} - \frac{1}{V_{f0j}})] - 1\right)} \quad (7b)$$

W_p model:

$$k_p^{diff} = \frac{k_{p,ji0}}{\left(\exp[A_{3j}\ (W_p - W_{p0j})] - 1\right)} \quad (7c)$$

As it will be shown below, D^{rd} was negligible. In Equation (7c) is shown the dependence of D^M to W_p.

In an analogous way, the termination coefficient $k_{t,Tot}$ has an independent (parallel expression) contribution of chemical reactivity and diffusion [33-34].

$$\frac{1}{k_{t,Tot}} = \frac{1}{k_t^{chem}} + \frac{1}{k_t^{diff}} = \frac{1}{k_{t,Tot0}} + \frac{1}{k_t^{diff}} \quad (8a)$$

With the expression of the Schmoluchowski equation for k_t^{diff} [38]:

$$k_t^{diff} = 4\ \pi\ N_A\ 2\ D^{PR,t}\ (\frac{\sigma_{LJ}^R}{2} + \frac{\sigma_{LJ}^R}{2}) \quad (8b)$$

We have used the following conditions for the evaluation the diffusion of the polymer radical in the termination process $D^{PR,t}$:

Condition 0: $D^{PR,t} = \frac{D^M}{(N^{PR,t})^{n_0}} + D^{rd}$

for $c < c^*$ and $N^P < N^{**}$ (9i)

Condition 1: $D^{PR,t} = \frac{D^M}{(N^{PR,t})^{n_1}\ c^{n_3}} + D^{rd}$

for $c^* < c < c^{**}$ and $N^P < N^{**}$ (9ii)

Condition 2: $D^{PR,t} = \frac{D^M}{(N^{PR,t})^{n_2}\ c^{n_4}} + D^{rd}$

for $c > c^{**}$ and $N^P < N^{**}$ (9iii)

Condition 3: $D^{PR,t} = \frac{D^M}{(N^{PR,t})^{n_2}\ c^{n_3}} + D^{rd}$

for $c < c^{**}$ and $N^P > N^{**}$ (9iv)

Condition 4: $D^{PR,t} = \frac{D^M}{(N^{PR,t})^{n_2}\ c^{n_4}} + D^{rd}$

for $c > c^{**}$ and $N^P > N^{**}$ (9v)

Specifically $D^{PR,t}$ is the diffusion coefficient (cm^2/s) of the polymer radical associated to the degree of polymerization of the radicals associated to termination $N^{PR,t}$, "c" is the concentration of polymer in the solution (g/cm^3). n_3 and n_4 are the exponents of the dependence of the diffusion coefficients $D^{PR,t}$ on the concentration "c". The concentration at the beginning of the overlap of the polymers c*, in which the polymers interpenetrate, was calculated in accordance to Brown and Zhou [39] and given in Table 4. In the reptation model, n_3 = 0.75 and n_4 = 1.75 [17,20]. We consider that the diffusion of the monomers D^M takes into account the contribution of the critical concentration for the entanglements c** and the critical value of

entanglement N** for this reason they are not present in Equation (9ii) – (9v). The critical concentration c** for the apparition of entanglements was found by the relation $c^{**} = K_c / N^{0.65}$. K_c was given by data of Tulig and Tirrell [20] The exponent 0.65 was calculated by the values of c** = 0.24 g/cm^3 and Mn = 79,000 g/mol of PMMA reported by the last authors. This correlation was also validated for the data of Callaghan and Pinder [40] and Elias [30] for PSt. In fact, Tulig and Tirrell affirmed that the exponent is between 0.5 and 1 [20]. Then, we have evaluated Equation (9i)-(9v) solving for $N^{PR,t}$, Vg. For condition 2 in B-1:

$$N^{PR,t} = \left(\frac{D^M}{\left[\frac{1000\ k_t^{diff}}{8\ \pi\ N_A\ (\frac{\sigma_{LJ}^R}{2}+\frac{\sigma_{LJ}^R}{2})} - D^{rd} \right] c^{n_i}} \right)^{(1/n_j)}$$

$$n_i = n_3 = 0.75\ ,\ n_j = n_2 = 1.59 \qquad (10)$$

The exponents n_0, n_1 and n_2, were varied in order to fit $N^{PR,t}$ the degree of polymerization of the polymer radicals N^{PR} deduced by the radical moments μ_0, μ_1 as seen in Fig. 1. In the semicontinuous processes SC-3 and SC-1, N^{PR} was more higher than $N^{PR,t}$. This is explained by the hypothesis that the short chains are more important in the termination step as Russell has demonstrated by a balance of radicals [41]. We consider that in the semicontinuous processes, the real distribution of $N^{PR,t}$ was between the distribution of N^{PR} at the end of the addition of the monomers, N^{PR}_{max}, and the distribution which considers n = 2 given by de Gennes, N^{PR}_{min}.

The exponents found by this method were congruent with the fact that for a higher value of W_p corresponds a higher value of the exponent n_i. The sequence of exponents allowed explaining that a lower addition rate of the monomers leads to a lesser diffusion of the polymer radicals, as observed in Table 5. On this way, in the semicontinuous process SC-1 with lowest addition rate of monomers (more effect of diffusion of polymer radicals in the particle), the exponent n_2, associated to the increment of concentration of the polymer, is the highest (1.85) for the same feed composition. Besides, in the process semicontinuous SC-3 with the higher addition rate of monomers, the exponent falls down to 1.70 (less effect of diffusion of polymer radicals in the particle), and in the batch process B-1 n_2 decreases to 1.59 (least effect of diffusion of polymer radicals in the particle). On the other hand, in the batch process B-3 with a higher proportion of BuA, the diffusion exponent n_2 increases to 1.7. Because the simulated different degrees of polymerization in the last two processes (Vg., N^P = 242 for B-1 and N^P = 169 for B-3 at X_O = 50 wt%) and different composition of the terpolymer (Vg., St/MMA/BuA = 35/51/14 mol% for B-1 and St/MMA/BuA = 29/39/32 mol% for B-3 at X_O = 50 wt%), the dependence of the exponent of B-3 to N^P had a different trend. The final result was that the diffusion of the monomers, terpolymer and terpolymer radicals was higher in batch process B-3 (not shown) as it was expected by the low value of the PBuA's Tg, see below. On the other hand, it is worth to say that the value of the exponent n_0, with a polymer concentration c < c*, was selected as 1.4 in the batch process, value found for toluene or benzene in PSt at W_p = 0.5 [42]. The fitting to the experimental data was adequate with this value.

We have also performed the fitting with the addition of the critical value N**, as Russell has proposed [41,43] and with or without the addition of the critical concentration c**. On this way; $D^{PR,t} \propto (N^{PR,t})^{-n0}$ for $N^{PR,t}$ <N** and c<c* (Condition 0, see Equation (9)); $D^{PR,t} \propto (N^{PR,t})^{-n1}\ c^{-n3}$ for $N^{PR,t}$ <N** and c<c** (Condition 1); $D^{PR,t} \propto (N^{PR,t})^{-n2}\ c^{-n4}\ (c^{**})^{-(n3-n4)}$ for $N^{PR,t}$ <N** and c>c** (Condition 2), $D^{PR,t} \propto (N^{PR,t})^{-n2}\ (N^{**})^{-(n1-n2)}\ c^{-n3}$ N>N** and c<c** (Condition 3); and $D^{PR,t} \propto (N^{PR,t})^{-n2}\ (N^{**})^{-(n1-n2)}\ c^{-n4}\ (c^{**})^{-(n3-n4)}$ for c>c** and N>N** (Condition 4). (When we use the methodology of Russell without the normalized concentration c**, it is written c** = 1 in the later equations). We have found that the distribution of N^{PR} of the batch processes with Equation (9i)-(9v) was very similar to the distribution of N^{PR} found by the Russell's equations using c**. The Russell's equations without c** could not be evaluated in the batch processes, because the conditions 0, 1, 2 were present in almost all the reaction. On the other hand, the semicontinuous process helped to determine that the Equation (9i)-(9v) applied better to all the processes because the Russell equations with/without c** gave higher value of N^{PR} at the end of the addition of the monomers (N^{PR}max) and higher values of N^{PR} at intermediate conversion. Besides, the Russell expressions with c** did not give the sequence that a lower addition rate of monomers implies a higher

exponent. For this reason, we did not use the Russell expressions.

Another method to evaluate the distribution of the number of polymer radicals was that proposed by Griffiths [19,44] in which the exponent of the polymer radicals is found by $n_i = 0.664 + 2.02\ W_p$. However, the values of the exponents in the cases of batch processes were near to the value of n = 2, and when these values were used in the calculation of $N^{PR,t}$ (see Tables 4,5 and Fig. 1) the distribution was quite different to N^{PR}. For this reason, we did not use this approximation.

We have also considered the reptation model in which $n_1 = n_2 = 2$ [17]. We have found that k_t^{diff} calculated by Equation (8b) is much lower than the value given by the evaluation of Equation (8) with the values of $k_{p,Tot}$ and $k_{p,Tot0}$ found in the batch and semicontinuous processes. This kind of discrepancy was also found by Faldi et al. for the diffusion coefficients of the polymer radicals D^{PR} [45]. We consider that the exponents of the polymer radicals associated to the termination must be lower than 2 in order to have the same k_t^{diff}. The lower values are indicative that the polymeric solution is not so concentrated. On the other hand, we have found that in accordance to the sequence of Table 4, the value of the diffusion of the polymer radicals associated to termination $D^{PR,t}$ is independent of the selection of the exponents n_0, n_1 and n_2. This is not the case for the values of the diffusion of the polymer radicals (obtained by the method of moments of the MWD) and dead polymers, D^{PR} and D^{P}, respectively. For the report of the values of $D^{PR,t}$ and D^{P}, we have used the values of the exponents n_0, n_1 and n_2 of $N^{PR,t}_{max}$.

It is possible to find a relation between the total propagation coefficient $k_{p,Tot}$ and the total termination coefficient $k_{t,Tot}$. As seen later in Fig. 11 for the batch process B-1, $k^M \approx k_p^{diff}$, $k_{t,Tot} \approx k_t^{diff}$; and considering that $D^{rd} \approx 0$, $N^{PR} \approx N^{PR,t}$ (Fig. 1a) with $D^{PR} \approx D^{PR,t}$, $\sigma_{LJ}{}^R \approx \sigma_{LJ}{}^M$ and not effect of concentration "c" in the diffusion coefficient D^{PR} (Equation (9i)):

$$D^{PR} = \frac{1000\ k_t^{diff}}{8\ \pi\ N_A\ \left(\frac{\sigma_{LJ}^R}{2} + \frac{\sigma_{LJ}^R}{2}\right)} \tag{11}$$

$$\frac{k_p^M}{k_t^{diff}} = \frac{k_p^{diff}}{k_{t,Tot}} = \frac{\left(\frac{1}{k_{p,Tot}} - \frac{1}{k_{p,Tot0}}\right)}{k_{t,Tot}}$$

$$= \left(\frac{D^M}{D^{PR}}\right) \frac{1000\ n_T}{N_A\ [M_T]_p\ v_p} = \left(\frac{D^M}{D^{PR}}\right) \frac{\left(\frac{\#R}{n}\right)}{N_A} = \left(N^{PR}\right)^{n_2} \frac{\left(\frac{\#R}{n}\right)}{N_A} \tag{11b}$$

$$\frac{1}{k_{p,Tot}} = k_{t,Tot} \left(N^{PR}\right)^{n_2} \frac{\left(\frac{\#R}{n}\right)}{N_A} + \frac{1}{k_{p,Tot0}} \tag{11c}$$

Based on this last equation, we can explain the k_p-gel ($k_{p,Tot}$) effect through variables associated to propagation and termination phenomena.

IV. Branching

The evaluation of the instantaneous branch density BD_i and the instantaneous branching fraction BF_i [9], and the corresponding averages of branching density BD [3] and branching fraction BF were done through the following equations.

$$BD_i = \frac{R_{p,cbb}\ \frac{N_p}{N_A}}{R_p} \tag{12a}$$

$$SBD = \sum_1^{niter} BD_i \tag{12b}$$

$$BD = \frac{SBD}{niter} \tag{12c}$$

$$BF_i = \frac{R_{p,cbb}\ \frac{N_p}{N_A}}{\left(R_{pc} + R_{p,cbb}\ \frac{N_p}{N_A}\right)} \tag{12d}$$

$$SBD = \sum_1^{niter} BF_i \tag{13a}$$

$$BF = \frac{SBF}{niter} \tag{13b}$$

Where n_{iter} is the iteration number of the program. SBD and SBF are the accumulated branching density at n_{iter} iterations and the accumulated branching fraction at n_{iter} iterations, respectively.

V. Methodology

Most of the values of the variables found for the k_p-k_t average set of models [12] were used as a reference for the set of models which includes the backbiting of BuA. On this way, the values of the diameter of droplet D_d and correction factor F_c were the

same in order to compare the molecular weight results. Three Methods for evaluating the importance of the viscosity in the increment of $k_{p,BuA}$ at the critical condition 2 (X_{Vfc2}, W_{pc2}) were tested: Method 1 (Lower viscosity in the particles). Critical point of X_{Vfc2} = 0.84 (W_{pc2} = 0.7945) in interval III of polymerization (zero monomer droplets); Method 2 (Middle viscosity in the particle). Critical point at X_{Vfc2} = 0.84 (W_{pc2} = 0.7945) and Vf_{c2} = 0.05. This critical point is present at a higher conversion than that at the beginning of interval III, and Method 3 (Higher viscosity), without these critical points, therefore there is not increment of $k_{p,BuA}$. Thus, Method 2 is a bridge between Method 1 (earlier increment of BuA k_p) and Method 3 (not increment of BuA k_p value). On this way, we have found that a lower viscosity in the particles produced an earlier increment of BuA k_p value (for whichever batch, Method 1) and that a higher viscosity in the particles did not produce an increment of BuA k_p value (SC-1, SC-3 and BS-1, Method 3). Methods 1 and 2 were almost equivalent in the batch processes because the critical condition of Method 2 was obtained in interval III of polymerization as Method 1 (near X_O = 80 wt%).

The values for almost all the parameters for this model of the terpolymerization of St/MMA/BuA were found in the literature. We consider that the selection of these parameters was adequate because the selection was based on similar conditions to the experimental ones. When there were several different values for a parameter one of them close to the average of them was taken for our simulations. On this way, they were selected not with the intention of obtaining the best fitting of the kinetic outputs, but by using a chemical and physical criterion of similar conditions to those of the experimental runs [12].

In order to fit the conversion, we have realized that there are four remaining unknown variables: The saturation concentration of monomers in the particle $[M_i]_{p,sat}$, the ratio of the water mass transfer side resistance to overall mass transfer for desorbed radical "j" δ_j, the three k_p-gel models and the three methods for evaluating the effect of viscosity on the k_p-gel effect. With this in mind, we have used the values of $[M_i]_{p,sat}$ found in the previous work: $[M_{St}]_{p,sat}$ = 5.6, $[M_{MMA}]_{p,sat}$ = 4.4, $[M_{BuA}]_{p,sat}$ = 4.5 (mol/dm^3) for intervals I and II with the hypothesis that a higher concentration of St in the particle decreases the solubility of MMA in the particle. We have used the Maxwell rule for calculate the instantaneous monomer concentration in the particle $[M_i]_p$ in intervals I and II [12]:

$$[M_i]_p = \sum f_{ip} [M_i]_{p,sat} \quad (14)$$

Where f_{ip} is the fraction mol of monomer i in the particle in relation to all monomers. We have found that for B-1, the monomer MMA was more solubilized in the particle than the other monomers, that is, $[MMA]_p$ was higher [12]. On this way, the saturation lower concentration of MMA, $[M_{MMA}]_{p,sat}$= 4.5 mol/dm^3, did not avoid of having a higher solubilization of MMA in the particle than the other monomers, but the maximal solubilization decreased but the presence of the other monomers. In the case of interval III, we have used the saturation values reported in the literature: $[M_{St}]_{p,sat}$=5.6, $[M_{MMA}]_{p,sat}$=6.9, $[M_{BuA}]_{p,sat}$ =5.2 (mol/dm^3) and the prediction was accurate, as for example observed in the semicontinuous processes [12]. On the other hand, we have varied the other three parameters: δ_j in the range [0.02, 0.16], the k_p-gel models (Ray, Wp, Hamielec) and the tree methods for taking into account the viscosity on the k_p-gel effect. The range of δ_j between [0.02, 0.16] was used by Ginsburger [46], and also by Nomura and Fujita [24] for St, MMA or BuA [12]. For simplicity, we have given the same value of δ_j for all the monomer radicals, so $\delta = \delta_j$ as Nomura and Fujita have found for St and MMA [24]. The values of the constants of the k_p-gel effect for all the processes were found by adjusting the conversion of batch B-1, taken as a reference, as explained above and in the previous work [12]. From these k_p-gel models and the three methods which take into account the effect of the viscosity, the most adequate model was selected by considering the lowest error in the fitting to the experimental data. After that, we have verified the that the $[M_i]_{p,sat}$ the constants of the $k_{p,gel}$ effect for the Hamielec's model and the critical free volume V_{fcc} were optimal through the optimization of the values by the algorithm evolutive reported by Kukkonen [47,48] with the aid of a previously found optimum by trial and error. In fact, the optimal $k_{p,gel}$ effect constants for the Hamielec's model have a physical meaning as explained above. It is important to mention that the sensitivity of the models to the above mentioned parameters was very low ant then a change of the mean square error MSE of 0.1 wt% for X_O [12] can be considered important. In the selection of the best models for the semicontinuous processes, we also considered an MSE of the accumulated conversion X_{ac} < 0.5 wt% and the best fitting to the conversion at the end of the addition of the monomers, as occurred with semicontinuous SC-3. Two examples of the manner for selecting the best k_p-gel models are given in Supporting Information Section S-3. On the other hand, the condition of k_p-gel effect in the radical desorption rate R_f was critical in batch B-3 in order to adjust the molecular weights. This condition was used for the other processes in which the k_p-gel effect in R_f was not critical for the evaluation of the molecular weights, as explained in Supporting Information Section S-1.1. All the processes were simulated with k_p-gel effect in the kinetic rate of polymer radical transfer to monomer, condition which was critical for the seeded BS-1. Besides, as a chemical congruence the k_p-gel effect was present in

the propagation rate of the tertiary radicals and transfer to chain transfer agent for all the radicals.

In the literature there are reported works in which the outputs conversion, molecular weight, diameter of particle [46] are considered simultaneously in the parameter estimation algorithm in order to find their optimum values that give the best fitting of the experimental data with the simulation results. In the present work we have chosen a different approach, a sequential one, in which the conversion is fitted first [12] because a valid value of molecular weight needs a correct value of conversion and there is more accuracy in the determination of conversion output than in the other two outputs.

VI. Results

All emulsion terpolymerization processes were simulated taking into account: 1. The decrement of the value of k_p by the k_p-gel effect, 2. The possibility of increment of the k_p value of BuA by the higher proportion of BuA in the terpolymer, as above has been explained. All the better k_p-gel models gave acceptable approximations to the experimental conversion curves, however, always was one that gave a slightly better fitting and then it was chosen as the best k_p-gel model as shown in Fig. 2. The best fitting to the experimental data by the simulation curves obtained with the Hamielec's, Ray's and W_p models were the following (here we are reporting all the cases which satisfied the MSE uncertainty): B-1 (Method 1, best: W_p, second best: Ray, δ = 0.02), B-2 (Method 1, Hamielec, δ = 0.02), B-3 (Method 1, best: Ray, second best: W_p, δ = 0.02), B-4 (Method 1, Hamielec, δ = 0.02), SC-1 (Method 3, best: Ray, second best: W_p , δ = best: 0.04, second best: 0.05), SC-2 (best: Method 2, second best: Method 1, W_p, δ = 0.02), SC-3 (Method 1, best: Hamielec, best: δ= 0.04; second best: Ray, second best: δ = 0.02), SC-4 (Method 3, Hamielec, δ = 0.02), BS-1 (Method 3, W_p, δ = 0.16). We must emphasize that the selection of the method (1, 2 or 3) was dependent on the value of the polymeric solution viscosity inside the particles at the critical point when the proportion of BuA is higher than $X_{Vfc,BuA}$: for processes with a low viscosity then Method 1 should be employed, for high viscosity then Method 3, for a middle viscosity then Method 2. All the batch processes were simulated by Method 1 because their low viscosity at the critical point. Besides, the most similar semicontinuous process to the batch B-1, to say, SC-3, was also simulated by Method 1. The semicontinuous SC-3 had the higher addition rate of monomers and then a lower viscosity in the particles than the other semicontinuous. On this way, it was expected that the polymer particles formed in SC-3 were more similar to the batch process B-1. On the opposite the semicontinuous processes with lower addition rate of monomers, SC-1 and SC-4, had more constraints to the diffusion. This was consequence of the higher proportion of the polymer. The higher proportion of polymer produced a higher viscosity in the particles and then Method 3 (the higher viscosity in the particle does not allow the increment of $k_{p,BuA}$) was more suitable for fitting the conversion. Then, these processes did not have a critical point for an increment of the BuA propagation coefficient. In the same trend, the seeded semicontinuous process BS-1 was simulated by Method 3 due to have the highest proportion of the polymer and then a higher viscosity.

As observed in the previous work [12]; A). The k_p-gel effect in the batch processes is stronger in the W_p and Ray's models and lesser in the Hamielec's model (See Fig. S2, Supporting Information). On this way, the simulation of the semicontinuous process BS-1 by the W_p k_p-gel model indicates the k_p-gel effect is stronger in this process, B). The increment of the addition of monomers decreases the effect of the k_p-gel effect (SC-1 with the lowest addition rate simulated by Ray's and W_p models and SC-3 with the highest addition rate simulated by Hamielec's model), C). A higher rate of polymerization R_p (due to a higher temperature in B-4) produces that the k_p-gel effect is lower in this batch process and then the process is simulated by the Hamielec's k_p-gel model. The same increment of R_p was found by the higher amount of emulsificant in batch B-2 and then the Hamielec's k_p-gel model best fitted this process. On this way, we can say that an increment in the rate of polymerization R_p with respect to B-1 make the batch more prone to be simulated by Hamielec's k_p-gel model.

On the other hand, at exception of BS-1 with δ = 0.16, all the batch and semicontinuous processes have a δ near to 0.02, indicating that the radical desorption was not appreciable. All the batches have the minimum desorption with a value of δ = 0.02 and the highest desorption of the semicontinuous was in SC-1 and SC-3 with δ = 0.04. The value of δ for the semicontinuous process SC-2 and the batch process B-1 was 0.02, SC-3 as intermediate process between SC-2 and the batch process B-1 should also have a value of δ = 0.02, but it has a value of 0.04. This higher value of δ in SC-3 probably indicates that the higher addition rate of monomers produced a lower proportionality between the polymerization and desorption rates R_p/R_f because the desorption of the monomeric radicals was higher.

On the other hand, it was observed that in all the processes the coefficient of desorption $K_{f,BuA}$ was the highest one, Vg., $K_{f,St}$ = 0.0384 1/s, $K_{f,MMA}$ = 0.544 1/s , $K_{f,BuA}$ = 0.792 1/s in B-3; $K_{f,St}$ = 0.164 1/s, $K_{f,MMA}$ = 2.24 1/s , $K_{f,BuA}$ = 3.37 1/s in SC-4 (see equations in Table S1, Supporting Information as a reference). Then, the value of δ = 0.02 in SC-4, where the amount of BuA was higher in the feed, indicates that the resistance to

desorption of the BuA monomeric radicals in SC-4 was similar to the batch processes. It was also found that the radical desorption was the highest ($\delta = 0.16$) in the seeded semicontinuous process with higher diameter of particle, BS-1, indicating that the resistance to water diffusion outside the particles fell down dramatically in relation to the batch processes.

In Fig. 2 are given the fittings of the set of models which includes the backbiting for the BuA-ended radicals and for comparison are shown the fittings by the average k_p-k_t set of models of the previous work [12]. As observed, the batches B-1 and B-3 were best simulated by models which include the backbiting of BuA than the models which used the average values of k_p-k_t.

The batch process B-4 had a higher polymerization rate caused by a higher temperature of reaction than B-1. The best fitting was achieved by the average Hamielec k_p-k_t model than by the Hamielec's model which includes the backbiting of BuA. Indeed, the last model predicts a visible point of change of curvature of the rate of polymerization. We consider that, as a consequence of the high experimental polymerization rate R_p, the point of change of curvature is not appreciable in the data of B-4. Another possible explanation to this fact is that the dependence of the critical values XV_{fc} and/or V_{fc} on the molecular weight of the terpolymers could soften this change of curvature.

The fitting of the conversion curve for the semicontinuous processes was similar in the selected best models for both the k_p-k_t average and the BuA backbiting set of models, as seen in Fig. 3. The maximum difference was in the semicontinuous SC-1 and it was necessary to adjust the value of δ to 0.04 instead of 0.02 in the backbiting models for obtaining a best fit. The k_p-k_t average gel model for fitting SC-1 was the Benyahia's model which used $\delta = 0.16$ with $MSE_{XO} = 1.25$ wt% and $MSE_{Xac} = 5.06$ wt%. A higher value of δ could improve the accuracy of the fitting, but it is outside our valid range of δ [0.02, 0.16]. It was found that the fitting of the Benyahias' k_p-k_t average gel model with a fixed value of $\delta = 0.02$ which used Method 3 was poorer than the Ray's k_p backbiting gel model with $\delta = 0.04$ which used Method 3 with $MSE_{XO} = 1.09$ wt% and $MSE_{Xac} = 3.35$ wt% in the last model. This indicates that fitting of the k_p-k_t average Benyahia's kp-gel model is less probable. On this way, the backbiting procedure gives more insights on the value of δ in emulsion terpolymerization.

In the semicontinuous processes it was found a similar trend in the selection of the k_p-gel model as in the batch processes: a higher polymerization rate R_p makes more suitable the process to be simulated by a free volume Hamielec's V_f k_p-gel model. On this way, the process SC-3, with the highest R_p, was simulated by the Hamielec's V_f k_p-gel model. On the other hand, the process SC-1, with the lowest polymerization rate R_p in semicontinuous, was simulated by Ray's and W_p k_p-gel models.

We have found that the semicontinuous process SC-4 with a higher proportion of BuA than SC-1, had a lower k_p-gel effect and then it was simulated by the Hamielec's V_f k_p-gel model. We conjecture that in this semicontinuous process the higher free volume in the particle (caused by the higher proportion of BuA in the terpolymer and in the monomers) led to a lower k_p-gel effect. On the other hand, the process semicontinuous BS-1 was better simulated by W_p with Method 3, which indicates a higher influence of the viscosity on the increment of the k_p-gel effect. We hypothesize that the higher proportion of polymer in the particle caused this behavior.

We consider that the internal structure of the particle near its surface is different in the batch and semicontinuous processes. Under this hypothesis, the viscosity of the particles and consequently the importance of diffusion of the polymer radicals in the batch processes are lower than in the semicontinuous processes, as it is detailed below. Okubo et al. [49] also found a lower viscosity in a seeded PSt emulsion polymerization with a previously absorbed monomer of MMA (batch process) than in a semicontinuous process in which MMA was added. They also encountered that the surface morphology of the particles was similar at the end of the reaction for both methods. In the emulsion terpolymerization of St/MMA/BuA, the higher viscosity in the particles of the semicontinuous processes was corroborated by the experimental lower conversion after the end of the addition of the monomers. This fact was also encountered in the work of Urretabizkaia et al. [50]. The lower conversion at the end of addition of the monomers was more visible in the semicontinuous SC-1 and in the seeded process BS-1 as seen in Fig. 3. The higher viscosity at the end of the reaction also indicates that the internal structure of the particles in the batch processes is different to that in the semicontinuous processes. The difference of internal structure is at least in the number and size of the domains of the sequences riches of monomers of St and MMA in the terpolymer St/MMA/BuA. Okubo et al. [49] have pointed out this difference of internal structure for the case of PMMA or PSt domains in the mentioned emulsion homopolymerization of MMA in seeds of PSt.

In the same context, Sundberg et al. have demonstrated that acrylic polymers with a lower T_g allows a higher diffusion of the polymer radicals. On this way, it has been found a difference of three orders of magnitude in the diffusion coefficients in the case of styrene polymeric radicals in a seed of PMMA with a T_g of 387 K in comparison with a seed of polymethylacrylate PMA with a T_g of 289 K [18]. Consequently, it is expected that the friction ξ_{seg} in a terpolymer with a high proportion of BuA ($T_{g,PBuA} = 229$ K, [22] See Table S-3, Supporting Information) is much

lower than in the terpolymers with a higher proportion of St or MMA near the surface. For this reason, the diffusion of j-ended radicals is higher in BuA richer domains in the particle. On this way, it was expected a more uniform distribution of St and MMA in the particle in the semicontinuous processes SC-1, with no appreciable islands of BuA. SC-1 had the lowest addition rate of monomers, and consequently, the reaction took place near the surface which was enclosed by subsequent reaction steps. Due to the uniform distribution of MMA and St in SC-1, the viscosity was higher than in batch B-1, in which the distribution of MMA and St was more at random. This randomness was produced by the polymerization in the interior of the particles as a consequence of a higher concentration of monomers and higher diffusion of j-ended radicals inside the particle in B-1 than in SC-1. The higher viscosity was more perceptible after the end of addition of the monomers in SC-1. Consequently, the more uniform distribution of domains of St and MMA in the interior of the particle in this process decreased strongly the polymerization rate at the end of the addition of the monomers as also observed in BS-1 (Fig. 3). Indeed, this change of kinetic behavior at the end of the addition of monomers points out that the consumption of the monomers, after the end of their monomers addition, was from outside to inside the particle. It can be argued the for validating this hypothesis, the diameter of the batch and semicontinuous processes must be similar, but the problem is that the diameter of particles in semicontinuous are commonly lower as seen in Fig. 1 of the previous work for batch B-1 and SC-1 [12]. Nevertheless, we have found that a lower experimental conversion at the end of the reaction was found also in the seeded semicontinuous BS-1 with a higher particle diameter than the batch process B-1 as seen also in Fig. 1 of the previous work. This means that at the end of the addition of the monomers in the semicontinuous processes (with whichever particle diameter), at least the particle surface is different to that of the batch processes. This is reinforced when we analyze that the semicontinuous processes SC-2 with a higher addition rate of the monomers than SC-1 presented a higher experimental polymerization rate in relation to the simulation after the end of the addition of the monomers as seen in Fig. 3. For this reason, we have concluded that SC-2 had particles more similar in structure to the particles of the batch process B-1.

In relation to the outputs of conversion, composition of monomers in the terpolymer, molecular weight and DSC thermograms, they are very similar for both the k_p-k_t average set models and BuA backbiting set models. The conversion curves have already been analyzed, the similarity in the composition is analyzed in Supporting Information Section S-4. On the other hand, the desorption rate of monomeric radicals R_f in the backbiting set of models is more important than in the k_p-k_t average set of models. This concept and the analysis of the molecular weight are given in Supporting Information Section S-5.

In relation to the DSC thermograms, in Table 9 are reported the experimental and simulated range of variation of T_g, $\Delta T_{g,DSC}$, of the batch and semicontinuous processes (See Supporting Information Section S-6. for the procedure and respective equations to simulate the DSC Thermograms). The value of the experimental ΔT_g is given by the intersection of the upper and lower extrapolations of the baseline at the onset of the inflexion [51]. In the case of the simulation, in order to define with more precision the onset for the beginning of T_g, we adjusted the initial baseline to be horizontal. Besides, in Table 9 is given the range of variation of the simulated instantaneous glass transition temperature ΔT_{gi}. Indeed, the lower value of ΔT_{gi} corresponds to the onset of the change of curvature of the simulated DSC Thermogram. It was also found that the simulation of the DSC thermograms was similar for the k_p-k_t average and backbiting including models.

The simulated $\Delta T_{g,DSC}$ for the batch processes has similar values of T_g and a wider range of ΔT_g that the experimental one as observed for B-1 in Fig. 4. This corroborates the results of the simulation. On the contrary, the simulated $T_{g,DSC}$ for the semicontinuous processes with a composition similar to B-1 (SC1, SC-2, SC-3) have higher values of T_g and a narrow range of $\Delta T_{g,DSC}$ that the experimental one. Besides, the final values of T_g were similar for the experimental and simulated semicontinuous processes. The discrepancy between the experimental and simulation results can be due to the fact that homogeneous nucleation was present in SC-1, SC-2 and SC-3 and then lower values of Tg were obtained. On the other hand, it is interesting to note that the simulation of ΔT_g of the semicontinuous SC-4 with a feed composition rich in BuA was correctly simulated by the $\Delta T_{g,DSC}$ program. This indicates that in the semicontinuous process SC-4 the homogenous nucleation was not important and that the range of micelar nucleation was given by $\Delta T_{g,DSC}$. In addition, $\Delta T_{g,DSC}$ for the semicontinuous process SC-2 (See above) was better simulated than that for the processes SC-1 and SC-3. For example, for SC-1: Experimental ΔT_g: 29-61 °C; Simulated ΔT_{gi} by backbiting model: 58-61 °C. SC-2: Experimental ΔT_g: 27-69 °C; Simulated ΔT_{gi} by backbiting model: 45-61 °C. In principle, SC-2 had an intermediate monomers addition rate between SC-1 and SC-3. These results indicate a higher homogeneous nucleation at lower and higher monomers addition rates, but not at intermediate monomers addition rate.

VII. Discussion

a) Number of j-ended radicals

The rate of generation of tertiary radicals R_{ncbb}(Pijk) was more important at the end of the reaction

for the batch B-3 and for the semicontinuous SC-4, as seen in Fig. 5. In consequence, the amount of tertiary radicals in the particle was appreciable at the end of the reaction, as seen in Fig. 6.

At all time, the number of tertiary radicals was mainly diminished by the propagation reaction $R_{p,ncbb}$. On the same way, the rate of propagation of the tertiary radicals $R_{p,ncbb}$ was higher in the process semicontinuous SC-4 than in the batch process B-3 at the beginning of the reaction (See the dashed line in Fig. 5 used as a reference). Then, there was more branching in SC-4 than in B-3 since the beginning of the reaction, as seen below in Fig. 12. So, the batch process B-3 did not present tertiary radicals until X_O = 65 wt% as seen in Fig. 6 and in consequence B-3 had no branching. On the other hand, the increment of BuA-ended tertiary radicals n_{BuA} in SC-4 is caused by having these radicals a degree of polymerization greater than 3 because the backbiting needs a reaction of a BuA-secondary radicals with the antepenultimate BuA monomeric unit of the chain. Since the model considers only the monomeric radical desorption (degree of polymerization of 1) and also due to the low reactivity of the BuA-ended tertiary radicals, it is produced an accumulation of these radicals in the particle.

It noteworthy to clear up that the abrupt changes in the number of radicals in Fig. 5 is due to the transition of interval II to interval III of emulsion polymerization ($X_O \approx$ 40 wt % in B-3), the presence of almost only tertiary radicals in the particle ($X_O \approx$ 80 wt % in B-3), the end of addition of monomers in semicontinuous ($X_O \approx$ 80 wt % in SC-4) and the beginning of the increment for kp, BuA due to the gel effect. The abrupt change of the number of radicals can also be due to the increment of the k_p,BuA due to the k_p gel effect, as it happens in SC-3 ($X_O \approx$ 16 %). These abrupt changes in the number of radicals or $k_{p,BuA}$ produced abrupt changes or shoulders in the values of conversion, diffusion, total kp and instantaneous branching of the terpolymer, as seen in Figs. 2-11.

We have compared the number of j-ended radicals simulated to the number of j-ended radicals of the BuA-backbiting model with the k_p-k_t average model for the batch and the semicontinuous processes. We have found the kinetic variation of the radicals in both models is attenuated when we evaluate the ratio of the product of $k_{p,Tot}$ n_T between the BuA backbiting model and the k_p-k_t average model, R_{KpnT}.

$$R_{KpnT} = \frac{(k_{p,Tot}\ n_T)BuA\ backbiting\ \ including\ \ \mathrm{model}}{(k_{p,Tot}\ n_T)Kp-Kt\ \ average\ \ \mathrm{model}} \quad (15a)$$

Where

$$R_p = \left(\sum_{i,j}^{c} (k_{p,ji}\ n_j\ [M]_{i,p})\ N_p \right) = k_{p,Tot}\ n_T\ [M_T]_p\ N_p \qquad i = a, b, c\ ;\ j = a, b, c, cbb\ . \quad (15b)$$

In Supporting Information Section S-7 is given the example for batch B-3.

b) Gel effect

The increment of BuA k_p was analyzed through the behavior of the free volume V_f, the fraction of free volume of BuA in the terpolymer X_{Vfc} and the fraction of polymer W_p for SC-2 in Fig. 7 (The batch B-1 is analyzed in Supporting Information Section S-3.1).

In the case of the semicontinuous process SC-2, the limit of X_{Vfc2} = 0.84 was exceeded since the beginning of the reaction (X_O = 11 wt%) as seen in Fig. 7. If we included the limit of X_{Vfc2} = 0.84 for the increment of the k_p of BuA as occurred for the Ray and Hamielec k_p free volume gel models with Method 1, the conversion would be higher. On the opposite, the limit W_p = 0.7945 in the semicontinuous process SC-2 was gotten at almost the end of the addition of the monomers and then W_p model with Method 1 fitted better the conversion experimental curve than Ray and Hamielec k_p free volume gel models with Method 1. On the other hand, Methods 1 and 2 gave similar results because the critical value W_p = 0.7945 was the value that was relevant and gotten at the end of the reaction, but Method 2 was slightly better. For this reason, Method 2 was the one selected.

In order to find a microscopic explanation for the fact that R_p indicated what k_p-gel model was used to simulate the conversion curve, we have encountered that the batch B-4 had more radicals per mol of monomer #R/n (Equation (5c)) than the batch B-1, as seen in Fig. 8. We have considered that the time required by a monomer to approach one radical was lesser in B-4 with a higher amount of radicals than in B-1. Also the j-ended polymer radicals had to make shorter movements for reacting with the monomers. Thus, a higher number of radicals per mol of monomer #R/n caused a minor movement by diffusion of the radicals (segmental or translational) in order to react with a monomer. We have expressed the rate of polymerization R_p in function of #R/n in order to clarify the weight of #R/n in the selection of the k_p-gel model as seen in Equation (16a)-(16b).

$$R_p = k_{p,Tot}\ n_T\ [M_T]_p\ \frac{N_p}{N_A^2} = k_{p,Tot}\ n_T\ [M_T]_p\ \frac{V_p}{v_p\ N_A^2} \quad (16a)$$

$$R_p = = k_{p,Tot} \frac{n_T\ 1000}{[M_T]_p\ v_p} \frac{[M_T]_p^2\ V_p}{1000\ N_A^2} = k_{p,Tot} \frac{\#R}{n} \frac{[M_T]_p^2\ V_p}{1000\ N_A^2} \quad (16b)$$

Where V_p is the total volume of the particles (cm^3_p/cm^3_w), v_p is the volume of one particle (cm^3_p /part). On this way, a higher value of R_p is obtained by both increments of $k_{p,Tot}$ and #R/n. We can say that there is a synergistic effect of the increment of $k_{p,Tot}$ and #R/n (through R_p) to decrease the k_p-gel effect. This leads to select the Hamielec's free volume model (Ham) for fitting the conversion curve, as happened for B-2, B-4 and SC-3, all with the same feed composition and with the higher values of #R/n as seen in Fig. 8. On the other hand, the processes B-1 and SC-2 were simulated by the W_p k_p-gel best model (W_p) and the process SC-1 by the Ray's best free volume model (Ray) and then have lowers values of #R/n as seen in Fig. 8. The same behavior was found for processes B-3 and SC-4 which have both the same feed composition: SC-4 was simulated by the Hamielec's k_p-gel effect model by having a higher value of #R/n than B-3 (Ray's k_p-gel effect model) as also seen in Fig. 8. On the other hand, it is also observed in Fig. 8 that the process semicontinuous SC-3 has an abrupt change of slope in the variation of #R/n vs conversion curve. This abrupt change was consequence of the higher polymerization rate R_p at X_O = 18 wt% because the critical point X_{Vfc2} for the increment of k_p of BuA was achieved. Then, the constant of the k_p-gel effect changed from 0.350 to 0.108 in the Hamielec's Vf k_p-gel effect model (See Table 3).

c) Diffusion coefficients and its relation to the k_p-gel constants

Having validated the results of the model, we have calculated the diffusion coefficients in the emulsion terpolymerization of St/MMA/BuA. We have found that the k_p-k_t average set of models had more uncertainty in the values of k_p^{diff} in accordance to Equation (4). This was consequence of the lower variation of the total propagation coefficient $k_{p,Tot}$ in this set of models in relation to the total propagation coefficient without gel effect $k_{p,Tot0}$. For this reason, there were zones in which the values of k_p^{diff} were negative, which does not have a chemical meaning. On the opposite side, the diffusion coefficients obtained in the BuA backbiting set of models have always positive values, by this reason we have only used the values of this set of models. This is the reason why the models using backbiting are useful for the evaluation of diffusion coefficients in the terpolymerization of S/MMA/BuA.

In Fig. 9 are shown the diffusion coefficient for the monomer D^M, the total diffusion coefficient for the contribution of monomers and polymer radicals D^{diff}, the diffusion coefficient of the polymer radical associated to the termination and propagation $D^{PR,t}$, the diffusion coefficient of the polymer radical D^{PR} , the diffusion coefficient of the dead polymer D^P and the diffusion coefficient by reaction diffusion D^{rd}. In this figure it is observed that the diffusion of monomer D^M is several orders of magnitude higher than $D^{PR,t}$ and D^{PR}. The value of D^M corresponds to the diffusion of the monomers which falls down exponentially near the polymer as seen in the Fig. 8 of von Meerwall et al. for PSt [28]. In Fig. 9 is shown that the diffusion of monomers D^M at the beginning of the reaction was higher in the process B-1 than in the processes SC-1 and SC-3 in the sequence: B-1 > SC-3 > SC-1 (Vg. at X_O =50 wt%: D^M = 14.5 X 10^{-6} cm^2/s for B-1 at W_p = 0.52 > D^M = 5.3 X 10^{-6} cm^2/s for SC-3 at W_p = 0.80 > D^M = 3.80 X 10^{-6} cm^2/s for SC-1 at W_p = 0.80). This sequence is related to the increment in the viscosity from B-1 to SC-1 and then to the lower rate of polymerization in SC-1. It is worth to mention that the value of D^M of these processes with BuA as third component is near to the experimental values of D^M = 10 X 10^{-6} cm^2/s for MMA in PMMA at W_p = 0.50, and D^M = 1 X 10^{-6} cm^2/s for St in PSt at W_p = 0.50 [13-14,18]. As it was observed for B-1 and SC-1, the terpolymer composition of BuA was near to 15 mol% at X_O = 50 wt% (Supporting Information Section S-4) and this increased the diffusion of the monomers, as explained above. Indeed, the DSC thermograms indicate a higher T_g of the terpolymer at the beginning of the reaction and a subsequent decrement with the conversion (Supporting Information Fig. S1). On the other hand, the way to evaluate the diffusion coefficient of the polymer radicals and polymers was explained above. The similitude to the experimental values of the polymer diffusion coefficients D^P can be verified with the values of D^P= 7.32 X 10^{-9} cm^2/s, Mw = 80,000 g/mol, St/MMA/BuA = 35/51/14 mol% and W_p = 0.53 at X_O = 50 wt% for B-1 in relation to PMMA $D^P \approx$ 1 X 10^{-8} cm^2/s with Mw = 90,000 g/mol, MMA = 100 mol% and W_p = 0.50 with the values of Faldi and Mills [13,45].

We consider then that the diffusion of the polymer radicals D^{PR} controls the details of the k_p-gel effect, in this case the selection between the V_f or W_p model. In order to verify this hypothesis, we have evaluated the effect of the diffusion coefficient D^{PR} in the selection of the k_p-gel model. We have weighted its influence by the product of n_T times D^{PR} (cm^2/s/particle), because a higher number of radicals increases the possibility of reaction with the monomers and then the k_p-gel effect is decreased. On this way, when we have analyzed the batch processes B-1, B-2 and B-4. The sequence of values of n_T D^{PR} is B-1 < B-2 < B-4 (Vg. at X_O =50 %: n_T D^{PR} = 16 X 10^{-11} cm^2/s/part for B-1 < n_T

D^{PR} = 79 X 10^{-11} cm^2/s/part for B-2 < n_T D^{PR} = 193 X 10^{-11} cm^2/s/part for B-4). This sequence is also shown in Fig. 10 and this progression is correlated to the change of using the Ray's k_p-gel model in B-1 to the Hamielec's k_p-gel model in B-4: A lesser global diffusion of the polymer radicals indicated by the product of n_T D^{PR} implies that the friction is more important in the diffusivity of the polymer radicals. On this way, the selection of the k_p-gel model in SC-1 (Ray's V_f k_p-gel model) and SC-3 (Hamielec's V_f k_p-gel model) was also correlated to the values of n_T D^{PR} (Vg. at X_O =50 %: n_T D^{PR} = 0.16 X 10^{-11} cm^2/s/part for SC-1 < n_T D^{PR} = 0.66 X 10^{-11} cm^2/s for SC-3). As observed, in Fig. 10, the selection of the k_p-gel model by this methodology is more limited than the selection based on the number of radicals per mol of monomer #R/n applied in Fig. 8 because we need to differentiate the batch and the semicontinuous processes. This is consequence of the lower values of n_T and D^{PR} in the semicontinuous processes.

In the batch B-1 is also observed that the diffusion of the polymer radical D^{PR} was lower than the diffusion of the (dead) polymer D^P (Vg. D^{PR} = 153 X 10^{-11} cm^2/s, D^P = 732 X 10^{-11} cm^2/s at X_O = 50 wt %) because the degree of polymerization was lower in the dead polymer (N^{PR} = 652, N^P = 242 for B-1) and the exponent in Equation (9) for obtaining D^{PR} and D^P is higher than 1. This was not the case for the semicontinuous processes in which the degrees of polymerization of the polymer radicals and dead polymers were similar (SC-1: N^{PR} = 312, N^P = 321). On the other hand, as a consequence of the low amount of j-ended radicals in the particle (in general, n_T < 0.5), the reaction diffusion D^{rd} was negligible in emulsion terpolymerization of St/MMA/BuA, as seen in Fig. 9.

When we compare the diffusion of the polymer radicals associated to termination $D^{PR,t}$ with the diffusion of the polymer radicals D^{PR} obtained by the method of moments of the molecular weight in the batch processes, it is observed a similar order of magnitude. This indicates that in the batch processes the termination is produced by the long radical polymer chains. On the other side, in the semicontinuos processes the diffusion of the polymer radicals associated to termination $D^{PR,t}$ is higher than the diffusion of the total polymer radicals D^{PR}. This is due to the lower degree of polymerization $N^{PR,t}$ of the short radicals associated to termination than the degree of polymerization of the total radicals N^{PR} which was obtained by the method of moments as discussed above. This corroborates the hypothesis that the short radicals have more influence in the termination rate [41,45]. On the other hand, the diffusion of the polymer radicals obtained by the method of moments D^{PR} for the batch B-1 (with a higher proportion of styrene, an aromatic monomer) was lower than those of the batch B-3 (with a higher proportion of aliphatic acrylic monomers) (Vg. at X_O = 50 wt %; D^{PR} = 153 X 10^{-11} cm^2/s in B-1; D^{PR} = 653 X 10^{-11} cm^2/s in B-3) as is also affirmed by Griffiths et al. [19] for aliphatic radicals. However, the diffusion coefficients of the polymer radicals associated to the termination reaction $D^{PR,t}$ are similar to ($D^{PR,t}$ = 438 X 10^{-11} cm^2/s in B-1; $D^{PR,t}$ = 416 X 10^{-11} cm^2/s in B-3 at X_O = 50 wt %).

In Fig. 11 are shown the total propagation rate coefficient without gel effect $k_{p,Tot0}$, the total propagation rate coefficient with gel effect $k_{p,Tot}$, the propagation rate coefficient for the monomer k_p^M, the propagation rate coefficient of the total diffusion contribution of monomers and polymer radicals k_p^{diff}, and the propagation rate coefficient for the reaction diffusion k_p^{rd} for the batch process B-1, and the semicontinuous SC-3 and SC-1. The k_p-gel effect was higher in the process SC-1 and for this reason $k_{p,Tot}$ was almost one order of magnitude lesser than $k_{p,Tot0}$ (Fig. 11) As a consequence, the ratio $k_p^{diff}/k_{p,Tot0}$ for SC-1 was lower than the corresponding ones of batch B-1 and semicontinuous SC-3 (see Equation (4)). In other words, the diffusion of monomers was more important in SC-1 than in B-1 or in SC-3.

In Fig. 11 is also observed that the k_t-gel effect was stronger than the k_p-gel effect. In particular, the ratio of $k_t^{diff}/k_{t,Tot0}$ at the beginning of batch B-1 was higher than those of the semicontinuous processes SC-1 and SC-3 (Fig. 11), indicating a lower influence of the polymer radical diffusion on the batch B-1 termination rate.

d) Branching in the terpolymerization of St/MMA/BuA

We have calculated the averages of branching density BD and branching fraction BF. As seen in Fig. 12, the branching was not present in the batch process B-3, with a higher proportion of BuA, since the beginning of the reaction until X_O < 65 wt%. On the opposite side, the processes BS-1 and SC-4, in which the monomers were added in semicontinuous, presented branching in the terpolymer since the beginning of the addition of the monomers. Nevertheless, these processes at the end of the reaction had a lower proportion of branching than B-3 (BD = 18 X 10^{-4} in B-3 > BD = 12 X 10^{-4} in BS-1 > BD = 10 X 10^{-4} in SC-4 at X_O = 96 wt%). Then, the kinetic behavior of $R_{p,cbb}/R_p$ (Equation (12a)-(12c)) in the reaction determines the accumulated branching at the end of the reaction. The seeded process BS-1 had a lower proportion of BuA and a lower amount of the chain transfer agent n-DDM than SC-4. The first condition caused that the branching fell down and the second that the branching went up (see Introduction section). The final result was that the branching density BD in BS-1 was higher than the branching of the semicontinuous SC-4. Besides, the values of BD are consistently one order lower than the experimental value of BD for a homopolymer of BuA without transfer agent (BD = 131

X 10^{-4} at 60°C) and of the same order when is used a chain transfer agent (BD experimental = 28 X 10^{-4} with CBr_4 at 60°C) [3]. On the other hand, the branch fraction BF is not a factor which determines the degree of branching BD. On this way, the seeded process BS-1 had the highest BF at X_O = 96 wt% (Vg. at X_O = 96 wt%: BF = 30 X 10^{-4} in B-3, BF = 46 X 10^{-4} in BS-1 and BF = 19 X 10^{-4} in SC-4), but the branching of BS-1 was not as important as in B-3. As observed in Fig. 12, a higher addition rate of monomers B-3 > SC-4 produces a higher branching.

In principle, the rate of propagation of the tertiary BuA-ended radicals $R_{p,cbb}$ depends on the number of these radicals in the particle $n_{c,bb}$ (Table 1 and Figs. 5 and 6). We have not considered the length dependency of the propagation coefficient nor a lesser backbiting by a lesser degree of polymerization (2nd and 3rd hypothesis, respectively, see above), but have obtained a degree of branching similar to the experimental results. Then, it could be possible that only the abstraction of the hydrogen of the transfer agent n-DDM by the tertiary electrophylic radical was the ground for the decrement of the branching (1st hypothesis, see above).

We have also compared the branching in the processes B-1, SC-3 and SC-1 (with a sequence to lower addition rate and consequently lesser amount of monomers in the particle from left to right in Fig. 13). It was found a maximum of the branching density BD and fraction branching FB at X_O = 96 wt% in the semicontinuous process SC-3 with the intermediate addition rate of the monomers (BD = 14 X 10^{-4}) and a minimum degree of branching in B-1 (BD = 5 X 10^{-4}). On the other hand, the middle degree of branching was found in SC-1 (BD = 10 X 10^{-4}) but at a conversion higher than 96 % the higher branching was in the order B-1 > SC-3 > SC-1 (sequence of less rate of addition of monomers), see Fig. 13. We consider that not only the depletion of the monomers in the particle is an important factor for branching, but also the ratio $R_{p,cbb}/R_p$, at what conversion the branching begins and until what conversion are allowed to react with the monomers.

VIII. Conclusion

From the k_p-k_t average model for the emulsion terpolymerization of St/MMA/BuA previously developed, the inclusion of the reaction of BuA backbiting with the associated k_p-gel effect in the model allows to know in more exact detail the kinetic phenomena of the emulsion terpolymerization of this system. Indeed, the k_p-k_t average model is used as a guide in order to improve the results of the model which includes the BuA backbiting reaction with the associated k_p-gel effect. On this way, it is realized that the rate of desorption of monomeric radicals has influence on the molecular weight and branching of the terpolymer of St/MMA/BuA. In a synergistic way, the results of both set of models support the hypothesis that the internal chemical structure of the particles grown in semicontinuos processes are different that the internal chemical structure of the particles produced in batch. This indicates that the distribution of sequences of monomers in the terpolymer throughout the particle in both kinds of processes was different. On the other hand, we have found that the gel effect depends on the ratio of the radicals to monomers and when this ratio goes up, the free volume model of Hamielec for the k_p-gel effect is more suitable for predicting the kinetic of the terpolymerization. When we have associated the gel effect to the diffusion of the monomers and polymer radicals, we have found that the diffusion of the total polymer radicals in the particle determines what k_p-gel model is adequate for simulating the gel effect. In this sense we can say that the k_p-gel model is a discrete one which takes into account these variables (#R/n or n_T *D^{PR}) for the selection of the most convenient k_p-gel model. This selection was also dependent of the viscosity in the particle, and then we have used three methods in orders to give importance to the influence of the viscosity in the selection of the best method. Besides, the BuA backbiting including model allowed the evaluation of the average diffusion coefficients of the monomers, polymers and polymers radicals. On the other hand, based on the definition of branching density BD, ratio of rate of reaction of tertiary radicals to overall rate of polymerization for all the monomers, we have encountered that the evolution in time of the rate of addition of monomers modifies the percentage of branching.

a) Supporting Information

Supporting Information is available from the Wiley Online Library or from the author.

Notation

A_{jk} Constant "*j*" (*j* = 1 before; *j* = 2 after the critical point for BuA), for the k_p-gel effect of the different "*k*" models of the propagation rate coefficient k_p.

b Bond length (cm).

BD_i, *BD* Instantaneous branching density or average branching density.

BF_i, *BF* Instantaneous branching fraction or average branching fraction.

*c** Concentration for the overlap of the polymers in which they interpenetrate (g/cm^3).

*c*** Critical concentration of polymer for the onset of entanglements (g/cm^3).

$C_{m,ij}$ Monomer transfer constant for "*i*"-ended polymeric radical to monomer "*j*".

$C_{m,iT}$ Chain transfer constant of *i*-ended radical to chain transfer agent *T*.

D_d, D_p Diameter of the droplet or particle (experimental and simulated) (cm, nm).

dn_{cbb}/dt Derive of the generation of BuA-ended tertiary electrophylic radicals (rad/par/s).

D,D^M, D^{PR}, $D^{PR,t}$, D^P Diffusion coefficient, of the monomer near the polymer, of polymer radical or of polymer radical associated to the termination or of the dead polymer (cm^2/s).

D^{rd}, $D^{com,PR}$ $D^{com,PR,t}$, D^P Diffusion coefficient induced by the reaction or the movement of the center of mass of the polymer radical or associated to the termination or the dead polymer (cm^2/s).

F_c Correction factor for the diffusion of the n-DDM from the droplets to the particles.

$f_{j,bb}$ Steric factor of the penultimate monomers "j" in the backbiting reaction of the BuA ended secondary radicals.

k_B Boltzman constant (g $cm/s^2/K$).

K_c Coefficient to calculate the beginning of critical concentration for the beginning of the entanglements (cm^3 (monomeric units)^n/g)

k_{cbb} Backbiting rate coefficient of the backbiting reaction of the BuA ended secondary radicals ($dm^3_w/mol_{rad}/s$).

$K_{f,j}$ K_f Average desorption coefficient from the particle for monomeric radical "j" or for all the monomeric radicals(1/s).

k_p^{chem} Propagation coefficient dependent only on the reactivity of the monomers and j-ended radicals without considering the diffusion of the monomer and the polymer radical ($dm^3_w/mol_{mon}/s$).

k_p^{diff} Propagation coefficient dependent on the reaction diffusion of the monomer and the polymer radical ($dm^3_w/mol_{mon}/s$).

$k_p^M = k_p^{rd,M}$ Propagation coefficient dependent on the reaction diffusion of the monomer ($dm^3_w/mol_{mon}/s$).

$k_{dr}^{rd} = k_p^{rd,PR}$ Propagation coefficient dependent on the reaction diffusion of the polymer radical ($dm^3_w/mol_{mon}/s$).

$k_{p,Tot}$, $k_{p,Tot0}$ Overall propagation coefficient in the particle considering or not considering the gel effect ($dm^3_w/mol_{mon}/s$) .

k_t^{chem} Termination coefficient dependent only on the reactivity of j-ended radicals without considering the diffusion of the polymer radical ($dm^3_w/mol_{mon}/s$).

k_t^{diff} Termination coefficient dependent on the reaction diffusion of the polymer radical ($dm^3_w/mol_{mon}/s$).

$k_{t,Tot}$, $k_{t,Tot0}$ Overall termination coefficient in the particle considering or not considering the gel effect ($dm^3_w/mol_{mon}/s$).

k_{tp} Overall termination coefficient in the particle considering the gel effect ($dm^3_w/mol_{rad}/s$) .

$k_{v,ijw}$ v = termination "t" ($k_{t,ii}$ according to the german or USA convention $k'_{t,ii}$) rate coefficient of i-ended radical to j-ended radical or polymerization "p" rate coefficient of radical "i" to monomer "j" considering the gel effect at w = time "t" or without gel effect "0" ($dm^3_p/mol_{rad}/s$).

L_{pers} , $L_{pers,i}$ Length of persistence of homopolymer "i" (cm).

$[M_j]_p$, $[M_T]_p$ Instantaneous monomer "j" or total monomer concentration in the particle "p" (mol/dm^3_p).

MSE Mean square error.

n_1, n_2 Exponents associated to the dependence of the diffusion coefficient to the degree of polymerization.

n_3, n_4 Exponents associated to the dependence of the diffusion coefficient to the concentration of polymer.

n,n_j, n_T,n_{ncbb} Average number of j-ended radicals without considering the tertiary electrophylic radicals or radical "j" in the particle or total average of radicals or ended tertiary radicals in the particle (rad/part).

N, N^{**}, N^{PR} , $N^{,PR,t}$, $N^{,PR,t}{}_{max}$, $N^{,PR,t}{}_{min}$,N^P Degree of polymerization in a the chain associated to the freely rotating segments or critical number of freely rotating segments which consider entanglements or degree of polymerization in a polymer radical in base to the moments of the molecular weight distribution or polymer radicals associated to the termination or maxima or minimum distribution of polymer radicals associated to termination in semicontinuous or degree of polymerization of a dead polymer.

N_A Avogadro's constant.

N_p Number of particles per unit volume of water ($\#/cm^3_w$).

$P_{ijk}(i,j,k)$ Probability of occurrence of the triad ijk with the j-ended radical "k".

$<r_0^2>^{1/2}$ Root mean square end to end distance of the homopolymer (cm).

$\#R/n = \#M/n$ Number of polymer radicals which react with the same number of monomers per mol of monomers (rad/mol).

R_f Desorption rate of all j-ended monomeric radicals (rad/part/s).

R_g Gyration radius (cm).

R_{KpnT} Ratio of the product of the $k_{p,tot}$ times n_T of the BuA backbiting including model between the same product for the k_p-k_t average model.

R_m, Radical transfer rate to monomers of all j-ended radicals (rad/part/s).

R_{ncbb} Backbiting rate of the BuA-ended secondary radicals (rad/part/s).

R_T Chain transfer rate for all j-ended radicals to the chain transfer agent (rad/part/s).

R_p Total propagation rate of all j-ended radicals on mole basis ($mol/cm^3_w/s$).

R_p Propagation rate j-ended radicals (rad/part/s).

R_t Termination of the j-ended radicals (rad/part/s).

SBD, SBF Accumulated branching density or branching fraction at n iterations.

V_f, V_{fcj}, $V_{f,i0}$ Fraction of free volume in particle at time "t" or critical free volume before the critical point j =1 or

after the critical point $j = 2$; or total free volume of the pure element *I*.

T, T_g Temperature, glass transition temperature or fusion temperature (K, °C).

$T_{g,i}$, T_{gDSC}, Instantaneous , accumulated and obtained by simulated by DSC glass transition temperature (°C).

$V_f^{i,*}$, $V_f^{Seg,*}$ Critical free volume for the beginning of the monomer or segment of the terpolymer to jump.

v_p Volume of one particle (cm^3_p).

V_p Total volume of the particles (cm^3_p/cm^3_w).

W_p, W_{pcj} Mass fraction of the terpolymer in the particle or critical mass fraction before the critical point $j = 1$ or after the critical point $j = 2$.

x Exponent associated to the micelar nucleation.

X_{ac} Accumulated mass conversion a time "*t*".

X_O Monomers overall conversion (experimental o calculated).

X_{Vf}, X_{Vfc} Proportion of *BuA* in the free volume of the terpolymer or critical value for the same parameter.

Greek Symbols

δ_j Ratio of the water mass transfer side resistance to overall mass transfer for desorbed radical "*j*".

Δt Time step for the iteration of the program (s).

$\phi_{0,seg}$, $\phi_{0,i}$ Jump frequency of the polymer segments or monomer (1/s).

$\mu_0, \mu_1, \nu_1, \nu_2$ zero and first moments, of the living j-ended radicals; first and second moment of the dead polymers in the molecular weight distribution.

σ_{LJ}^{M}, σ_{LJ}^{R} Diameter of Lennard Jones of the monomer or of the average of the j-ended radicals in the terpolymer (cm).

σ_{SH}, $\sigma_{SH,i}$ Hindrance factor or steric hindrance of monomer in terpolymer.

ΣR_r Sum of all the reactions of the BuA tertiary electrophylic radicals (rad/part/s).

τ Angle between bonds (°).

ξ_{seg} Friction coefficient of the segment of the polymer, in this case the monomer in the terpolymer (g/s).

References Références Referencias

1. A.K. Khan, B.C. Ray, J. Maiti, and S. K. Dolui, *Pigm. and Res. Technol.*, **38**, 159 (2009).
2. L.J. Borthakur, T. Jana, and S.K. Dolui, *J. Coat. Technol. Res.*, **7**, 765 (2010).
3. Agirre, J.I. Santos, A. Etxeberria, V. Sauerland, and J. R. Leiza, *Polym. Chem.*, **4**, 2062 (2013).
4. D.H. Napper and R.G. Gilbert, *Polymerization in Emulsions*, in *Comprehensive Polymer Science*, G. Allen and J. C. Bevington, Eds., Pergamon Press, Oxford, England, Vol. 3, 171-218 (1989),.
5. W. Wang and R. A. Hutchinson, *AIChE J.*, **57**, 227 (2011).
6. D. Cuccato, E. Mavroudakis, M. Dossi, and D. Moscatelli, *Macromol. Theory Simul.*, **22**, 127 (2013).
7. B. Giese, *Ang. Chem., Int. Edit. Eng.*, **22**, 753 (1983).
8. G. Arzamendi, C. Plessis, J.R. Leiza, and J. M. Asua, *Macromol. Theory Simul.*, **12**, 315 (2003).
9. N. Ballard, J.C. de la Cal, and J.M. Asua, *Macromolecules*, **48**, 987 (2015).
10. B.S. Casey, B.R. Morrison, I.A. Maxwell, R.G. Gilbert, and D. H. Napper, *J. Polym. Sci., Part A: Polym. Chem. Ed.*, **32**, 605 (1994).
11. W.D. Harkins, *J. Am. Chem. Soc.*, **69**, 1428 (1947).
12. J.A. Díaz-Ponce, H. Vázquez-Torres, and C. Martínez-Vera, *Chem. Eng. Sci.*, **138**, 41 (2015).
13. F.M. Mills, R.G. Gilbert, and D. H. Napper, *Macromolecules*, **23**, 4247 (1990).
14. B.S. Casey, I.A. Maxwell, B.R. Morrison, and R.G. Gilbert, *Macromol. Chem., Macromol. Symp.*, **31**, 1 (1990).
15. Y. Yurekli, S.A. Altinkaya, J.M. Zielinski, *J. Polym. Sci., Part B: Polym. Phys. Ed.*, **45**, 1996 (2007).
16. P.G. De Gennes, *Macromolecules*, **9**, 587 (1976a).
17. P.G. De Gennes, *J. Chem. Phys.*, **55**, 572 (1971).
18. J. Stubbs, O. Karlsson, J.E. Jönsson, E. Sundberg, Y. Durant, and D. Sundberg, *Coll. Surf. A*, **153**, 255 (1999).
19. M.C. Griffiths, J. Strauch, M. J. Monteiro, and R.G. Gilbert, *Macromolecules*, **31**, 7835 (1998).
20. T.J. Tulig, and M. Tirrell, *Macromolecules*, **14**, 1501 (1981).
21. P.G. De Gennes, *Macromolecules*, **9**, 594 (1976b).
22. J. A. Díaz-Ponce, *M. Sc. Thesis*, UNAM, Mexico City, September (1990).
23. J. O. Pastor-Vega, *Bac. Thesis*, UNAM (Mexico City) (1990).
24. M. Nomura, and K. Fujita, *Makromol. Chem., Supp.*, **10/11**, 25 (1985).
25. D.C. Sundberg, J.Y. Hsieh, S.K., Soh, and R.F. Baldus, in *Emulsion Polymers and Emulsion Polymerization*, D.R., Basset and A.E. Hamielec, Eds., Academic Press, ACS, Symposium Series 165; American Chemical Society, Washington DC, USA, 327-343 (1981).
26. Okninski, A., *Catastrophe Theory*, in *Chemical Kinetics* Vol. 33, R. G. Compton, Ed., Elsevier, Amsterdam (1992).
27. G.A. O'Neil, and J.M. Torkelson, *Trends Polym. Sci.*, **5**, 349 (1997).
28. E.D. Von Meerwall, E.J. Amis, and J.D. Ferry, *Macromolecules*, **18**, 260 (1985).
29. B. Benyahia, M.A. Latifí, C. Fonteix, F. Pla, and S. Nacef, *Chem. Eng. Sci.*, **65**, 850 (2010).
30. HG. Elias, *Macromolecules, Vol 3: Physical Structures and Properties*, Wiley-VSC, Weinheim, Germany (2008).

31. J.D. Ferry, *Viscoelastic properties of polymers*, 3rd ed., John Wiley and Sons, New York USA (1980).
32. J. Klein, *Macromolecules*, **11**, 852 (1978).
33. J.L. Rivail, in *Chemical reactivity in liquids*, M. Moreau and P. Turq, Eds., Plenum Press, New York, 336-344 (1987).
34. D.R. D'hooge, M.F. Marin, and G. B. Reyniers, *Macromolec. React. Eng.*, **7**, 362 (2013).
35. G.T. Russell, D.H. Napper, and R.G. Gilbert, *Macromolecules*, **21**, 2133 (1988).
36. C.S. Chern, and G.W. Poehlein, *J. Polym. Sci., Part A: Polym. Chem. Ed.*, **25**, 617 (1987).
37. S.K. Soh, and D.C. Sundberg, *J. Polym. Sci., Part A: Polym. Chem. Ed.*, **20**, 1315 (1982).
38. G.T. Russell, R.G. Gilbert, and D.H. Napper, *Macromolecules*, **26**, 3538 (1993).
39. W. Brown, and P. Zhou, *Macromolecules*, **22**, 4031 (1989).
40. P.T. Callaghan, and D.N. Pinder, *Macromolecules*, **13**, 1085 (1980).
41. G.T. Russell, *Macromol. Theory Simul.*, **4**, 407 (1995).
42. M.C. Piton, R.G. Gilbert, B.E. Chapman, and P.W. Kuchel, *Macromolecules*, **26**, 4472 (1993).
43. D.S. Achillas, *Macromol. Theory Simul.*, **16**, 319 (2007).
44. D. Victoria-Valenzuela, J. Herrera-Ordonez, and G. Luna-Barcenas, *Macromol. Theory Simul.*, **25**, 28 (2016).
45. A. Faldi, M. Tirrell, and T.P. Lodge, *Macromolecules*, **27**, 4176 (1994).
46. E. Ginsburger, F. Pla, C. Fonteix, S. Hoppe, S. Massebeuf, P. Hobbes, and P. Swaels, *Chem. Eng. Sci.*, **58**, 4493 (2003).
47. S. Kukkonen and J. Lampinen, in *Multi-objective Optimization in Computational Intelligence: Theory and Practice*, L.T. Bui and S. Alam, Eds., Information Science Reference, New York (2008).
48. Z. Michalewicz, *Genetic algorithms + Data structures = Evolution programs*, 2nd Edn., Springer-Verlag, Berlín (1994).
49. M. Okubo, A. Yamada, and T. Matsumoto, *J. Polym. Sci., Part A: Polym. Chem. Ed.*, **18**, 3219 (1980).
50. A. Urretabizkaia, and J.M. Asua, *J. Polym. Sci., Part A: Polym. Chem. Ed.*, **32**, 1761 (1994).
51. J. Rabek, *Experimental methods in polymer chemistry*, Wiley, New York USA (1981).

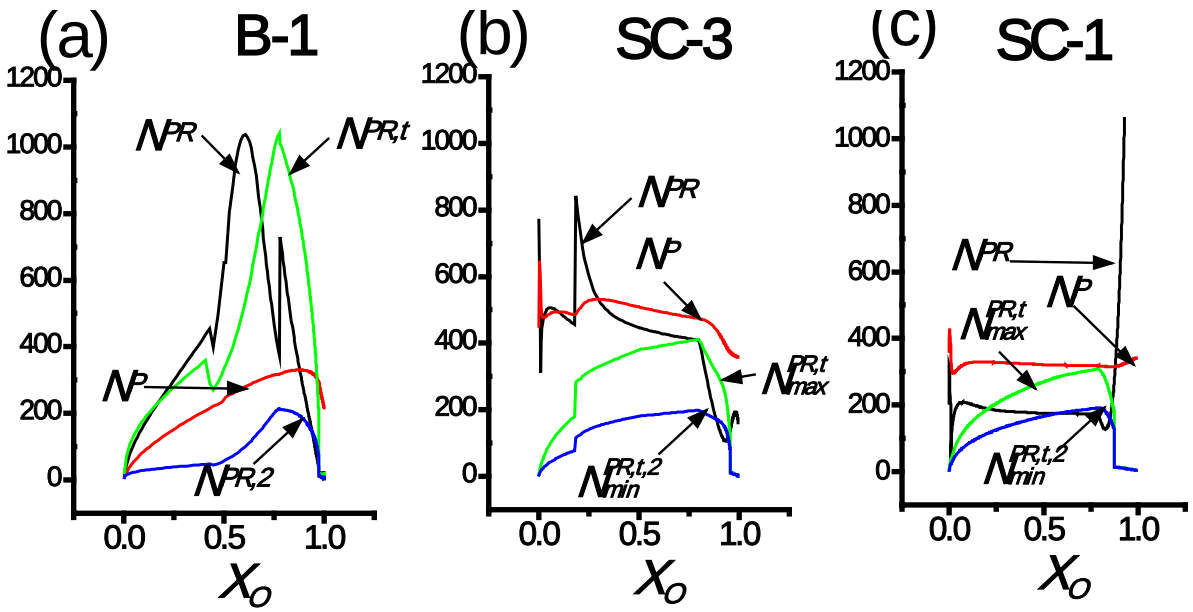

Fig. 1: Fitting of the values of degree of polymerization of the polymer radicals N^{PR} with the maximum degree of polymerization of the polymer radicals associated to the termination $N^{PR,t}{}_{max}$. N^{P} and $N^{PR,2}{}_{min}$ are also shown as reference (see text).

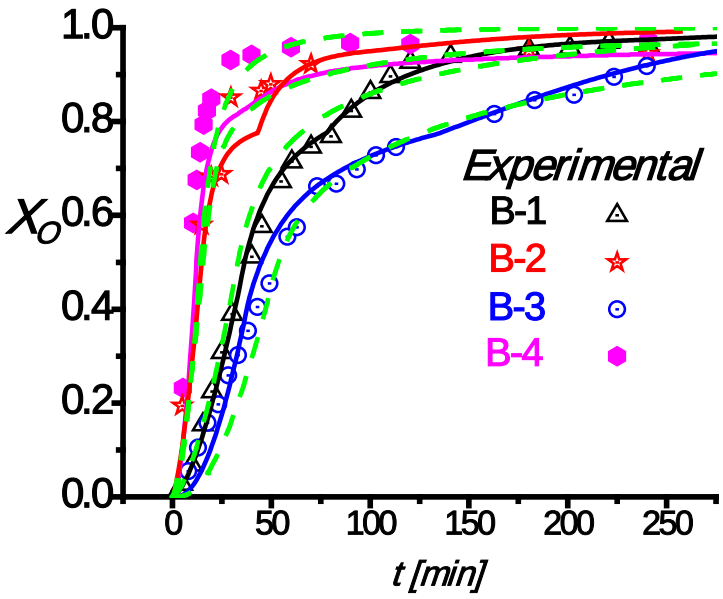

Fig. 2: Comparison of the simulation of the batch processes by the k_p-k_t average [12] (dashed lines) and the backbiting-including BuA set of models (solid lines), see text above.

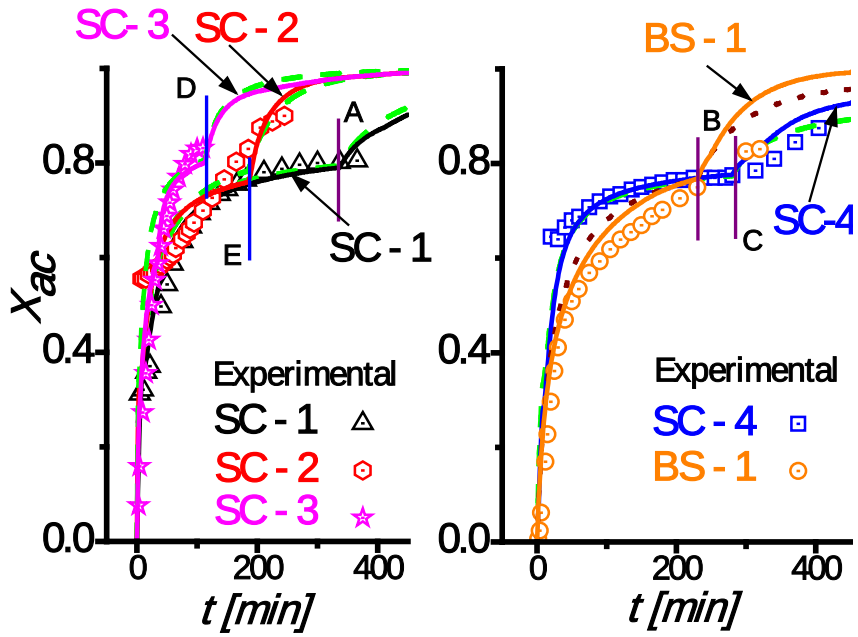

Fig. 3: Accumulated conversion X_{ac} for the semicontinuous processes SC-1 to SC-4, and for the seeded process BS-1 of the k_p-k_t average (dashed lines) and the backbiting-including BuA set of models (solid lines). The intersection of the lines A to E with the conversion curves of SC-1, BS-1, SC-4, SC-3, SC-2, respectively, indicates the conversion in which the addition of monomers has ended.

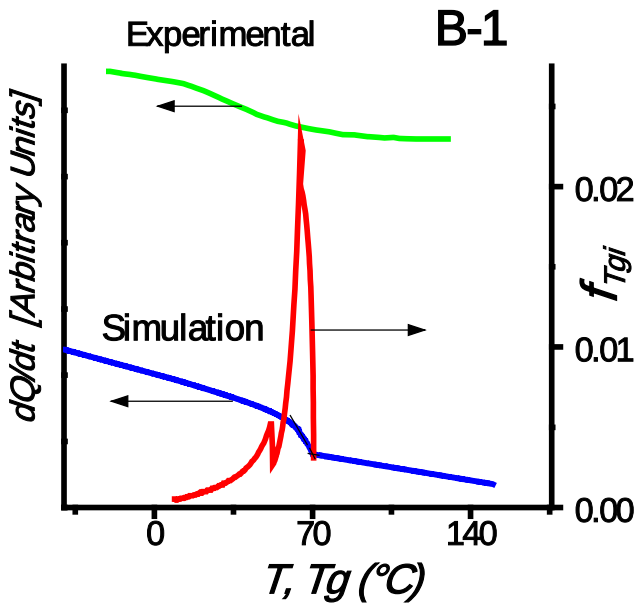

Fig. 4: Experimental and simulated curves by the backbiting model of DSC thermogram for B-1. The histogram of the instantaneous T_{gi} is also shown.

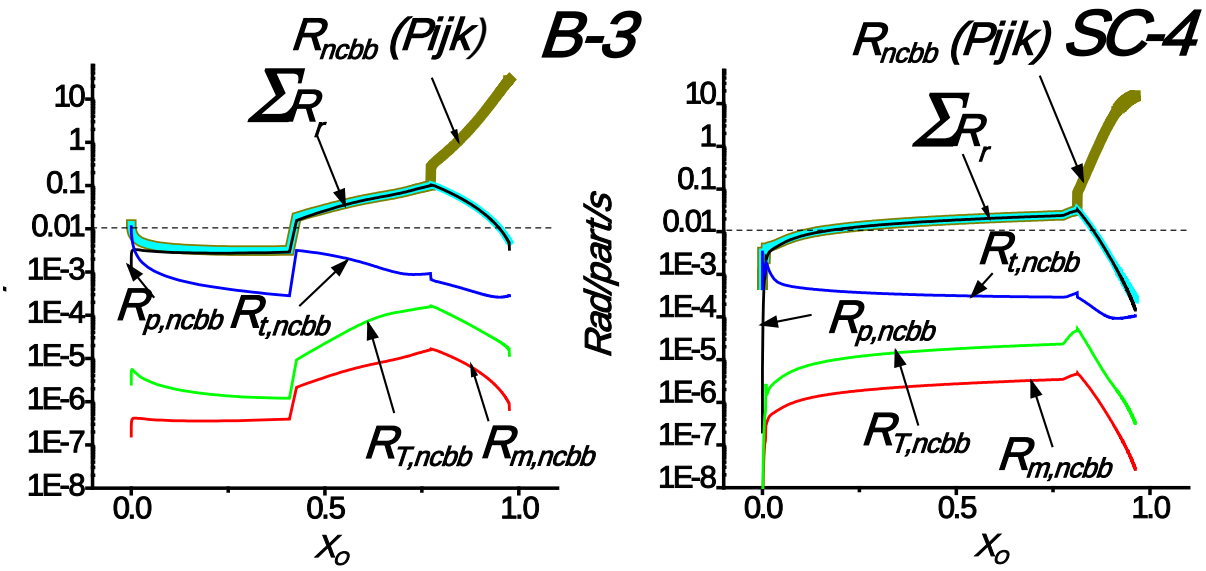

Fig. 5: Rates associated to the backbiting reaction (see text) in the processes batch B-3 and semicontinuous SC-4 with similar feed compositions.

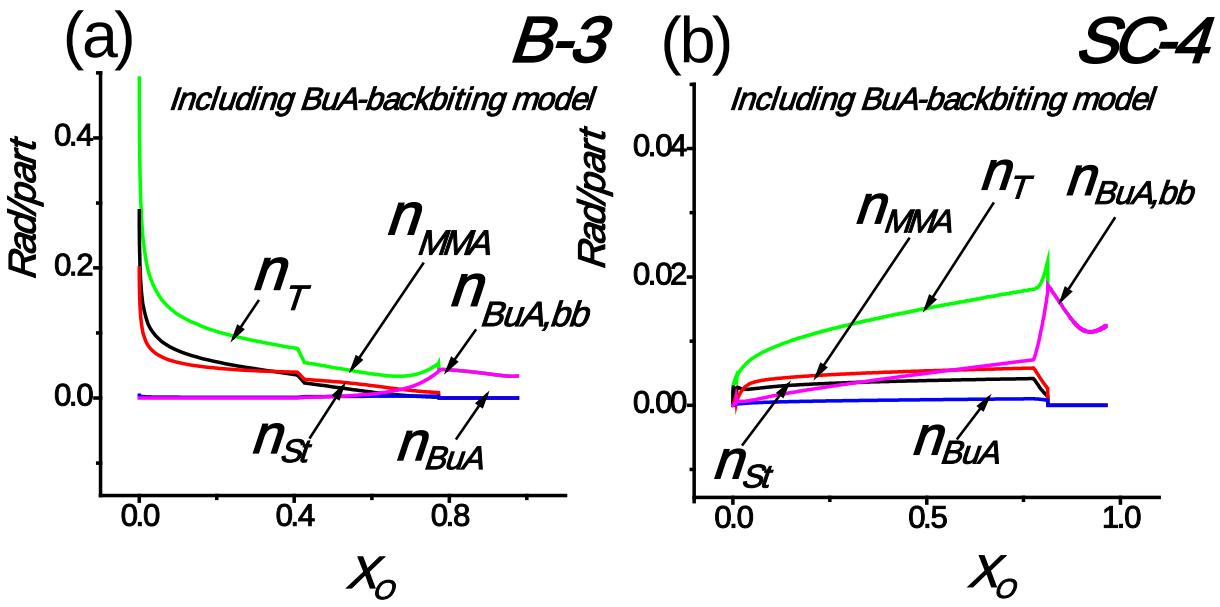

Fig. 6: Number of radicals for the batch B-3 and semicontinuous SC-4, which have the same composition in the including backbiting BuA model.

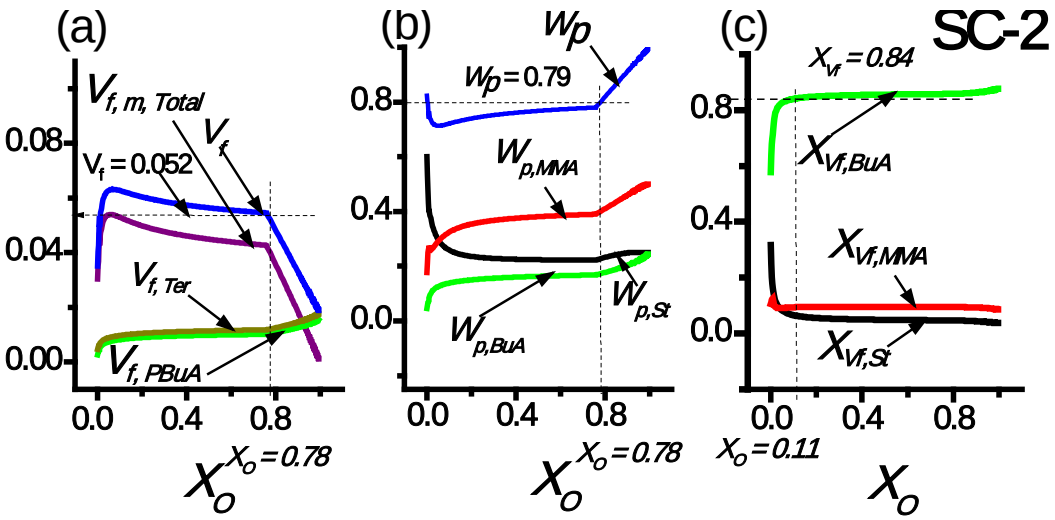

Fig. 7: Behavior of the (a). Free volume V_f, (b). Fraction of polymer W_p and (c). Fraction of BuA in the terpolymer X_{Vf} for the semicontinuous process SC-2.

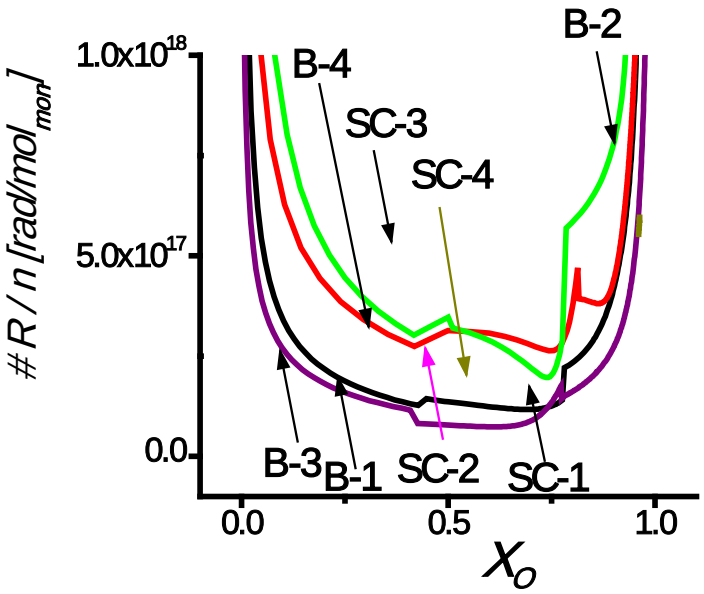

Fig. 8: Radicals per mole of monomer #R/n for the different process batch and semicontinuous of the terpolymerization of St/MMA/BuA.

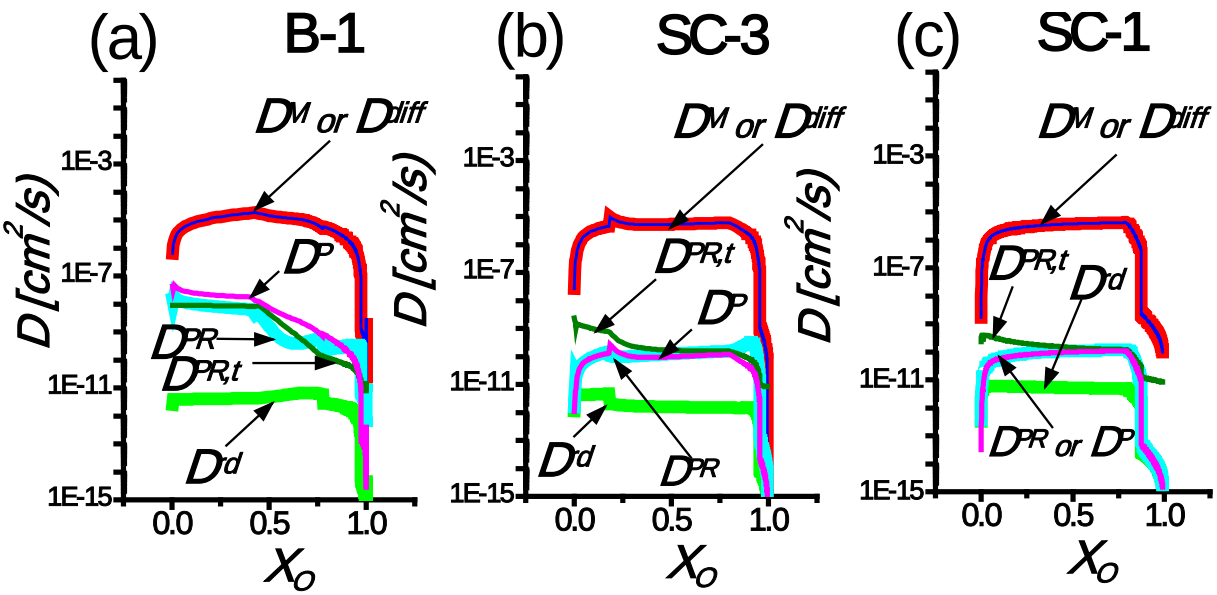

Fig. 9: Diffusion coefficients for the batch process B-1, and the semicontinuous SC-3 and SC-1.

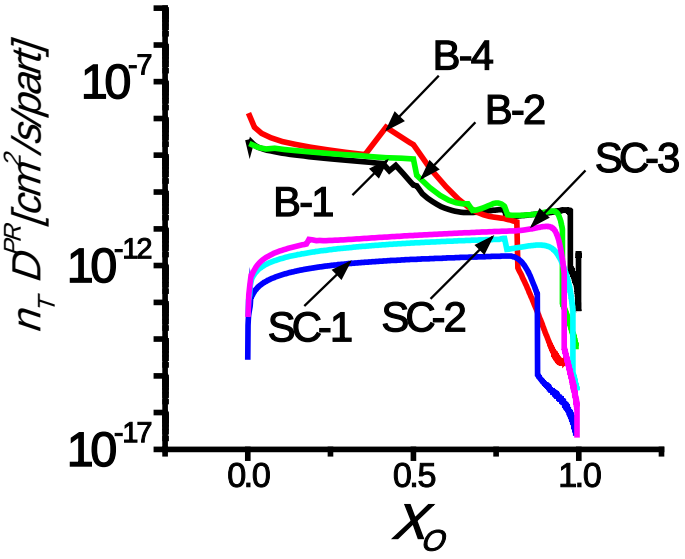

Fig. 10: Global diffusion of the radicals in the particle indicated by the product $n_T D^{PR}$ for the batch processes B-1, B-2 and B-4 and the semicontinuous processes SC-1 to SC-3. All this processes with the same feed composition.

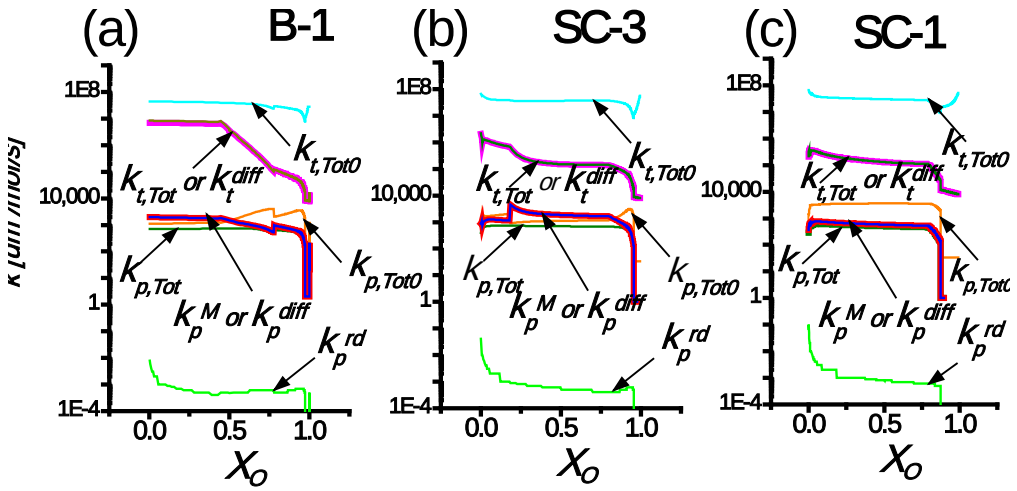

Fig. 11: Propagation and termination rate coefficients for the batch process B-1, and the semicontinuous SC-3 and SC-1.

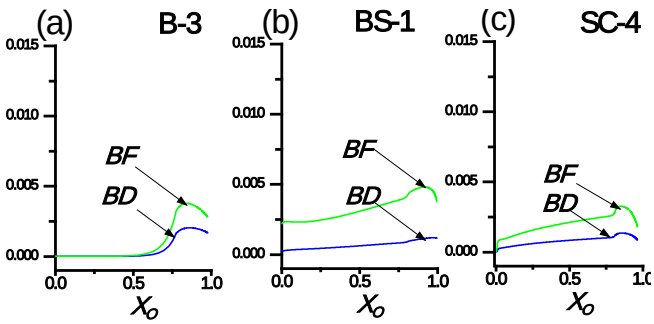

Fig. 12: Average branching density BD and branching fraction BF: a. batch B-3, b. seeded process BS-1, and c. semicontinuous SC-4.

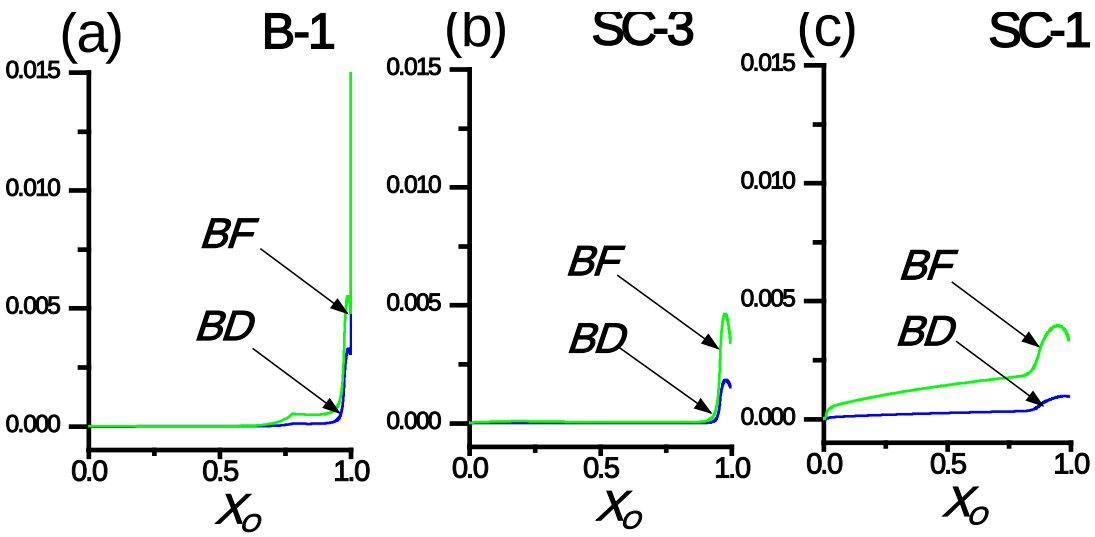

Fig. 13: Average branching density BD and branching fraction BF for: a. batch B-1, b. semicontinuous process SC-3, and c. semicontinuous process SC-1. The processes are ordered in accordance to higher addition rate of monomers from left to right.

Table 1: Kinetic rates of polymer radicals backbiting.

Units	Equations	Comments
n_{cbb} #·rad/part	$\frac{dncbb}{dt} = R_{ncbb}(P_{ijk}) - R_{p,ncbb} - R_{t,ncbb} - R_{m,ncbb} - R_{T,ncbb}$ $= R_{ncbb}(P_{ijk}) - \Sigma R_r$	This work (TW). It was taken into account the penultimate effect in the rate of backbiting R_{ncbb}, in which the factors of styrene and methyl methacrylate as penultimate monomers in the polymer radical are $f_{a,bb}$ = 0.6 and $f_{b,bb}$ = 0.6, respectively. For the monomers of BuA $f_{c,bb}$ = 1 [5]. The j-ended radicals are St = a, MMA = b, secondary radicals of BuA = c and tertiary electrophylic radicals of BuA = cbb. The monomers are: St = a, MMA = b, BuA = c. The crossed terms are the geometric mean of the individual parameters. The transfer constants of the BuA tertiary electrophylic radicals $C_{m,ncbbi}$ and $C_{T,ncbb}$ were taken equal to the secondary radicals of BuA. The gel effect was taken into account in $R_{p,ncbb}$, R_T,ncbb, $R_{t,ncbb}$ and $R_{m,ncbb}$ in a similar way to the kinetic rates of the other radicals.
	$n_{cbb,t} = n_{cbb,t-\Delta t} + \left(\frac{dncbb}{dt}\right)_{t-\Delta t} \Delta t$	
	$R_{ncbb} = K_{cbb}\,(f_{a,bb}\,P_{ijk}(c,a,c) + f_{b,bb}\,P_{ijk}(c,b,c)\,f_{ab} + f_{c,bb}\,P_{ijk}(c,c,c))\,\frac{(n_{t-3\Delta t}\ n_{t-2\Delta t}\ n_{t-\Delta t})}{3}$	
	$P_{ijk}(i,j,k) = \frac{n_{i,t-3\Delta t}}{n_{t-3\Delta t}}\ \frac{n_{j,t-2\Delta t}}{n_{t-2\Delta t}}\ \frac{n_{i,t-\Delta t}}{n_{t-\Delta t}}$ with *i,j,k = a, b, c*	
	$R_{p,ncbb} = \sum_i k_{p,cbbi}\ n_{cbb}\ [M_i]_p$ with *i = a, b, c*	
	$R_{t,ncbb} = k_{t,cbb}\ \frac{n_T^2}{v_p}\ \frac{10^3}{N_A}$	
	$k_{t,cbb} = \frac{1}{n_T^2}(n_{cbb}^2\ k_{t,cbb} + \sum_{j,j\neq cbb} 2n_{cbb}\ n_j\ k_{t;cbb,j})$ with *j = a,b,c*	
	$R_{m,ncbb} = \sum_i k_{p;cbb,i,0}\ C_{m,cbbi}\ n_{cbb}\ [M_i]_p$ with *i = a,b,c*	
	j = a, b, c	
	$R_{T,ncbb} = k_{p;cbb,}\ C_{m,cbb,T}\ n_{cbb}\ [M_T]_p$	

Table 2: Equations used to evaluate the gel effect of the polymerization rate constant k_p of the BuA-ended radicals (dm^3/mol) [12].

1. Before $X_{Vfc2} = 0.84$, j = c, cbb.

$$k_{p,ji} = \frac{k_{p,jj0}}{r_{ji}} \exp[-A_{1kj}(\frac{1}{V_f} - \frac{1}{V_{fc1kj}})] \quad k = 1,2$$

$$k_{p,ji} = \frac{k_{p,jj0}}{r_{ji}} \exp[-A_{1kj}(W_p - W_{pc1kj})] \quad k = 3$$

2. After the critical value $X_{Vfc2} = 0.84$; j = c, cbb

$$k_{p,ji} = \frac{k_{p,jj0}}{r_{ji}} \exp[-A_{2kj}(\frac{1}{V_f} - \frac{1}{V_{fc1kj}})] \quad k = 1,2$$

$$k_{p,ji} = \frac{k_{p,jji0}}{r_{ij}} \exp[-A_{2kj}(W_p - W_{pc1kj})] \quad k = 3$$

Batch B-3.

$$k_{p,ji} = \frac{k_{p,jj0}}{r_{ji}} \exp[-A_{1kj}(\frac{1}{V_{fc2kj}} - \frac{1}{V_{fc1kj}}) - A_{2kj}(\frac{1}{V_f} - \frac{1}{V_{fc2kj}})] \quad k = 1,2$$

$$k_{p,ji} = \frac{k_{p,jj0}}{r_{ji}} \exp[-A_{1kj}(W_{pc2kj} - W_{pc1kj}) - A_{2kj}(W_p - W_{2pckj})] \quad k = 3$$

a. We consider that the gel constants and critical values of V_f and W_p are equal for the secondary and tertiary radical of BuA.
b. The monomers are indicated by "i" and the kind of k_p-gel model by "k".

Table 3: Kinetic constants for k_p-gel effect Equations used in the simulation model.

	Hamielec		Ray		Wp		
	A_{h1}	V_{fch}	A_{h2}	V_{fch}	A_{h3}	W_{pch}	h =1 Before, h = 2 After
St	0.015	0.07	10.50	0.07	1.62	0.67	k_p- k_t average model [12]
MMA	0.015	0.07	10.50	0.07	1.62	0.67	k_p- k_t average model [12]
BuA	0.05	0.10	24.24	0.10	3.75	0.48	k_p- k_t average model [12]
	0.350	0.14	40.00	0.14	5.74	0.19	Before $X_{Vfc2} = 0.84$ ($W_{pc2} = 0.7945$), TW.
	0.11	0.14	21.91	0.14	3.65	0.19	After X_{Vfc2}=0.84 (W_{pc2} =0.7945), almost all processes, TW.
	0.11	0.05	21.91	0.05	3.65	0.80	After $X_{Vfc2} = 0.84$ ($W_{pc2} = 0.7945$); Only B-3, TW.

Table 4: Sequence for the evaluation of the diffusion coefficients in the polymerization reaction[a] (From left to right).

1

$$\frac{1}{k_p^{diff}} = \frac{1}{k_{p,Tot}} - \frac{1}{k_{p,Tot0}}$$

$$k_{p,Tot} = \frac{\sum_{i,j}^{c} k_{p,ji}\ n_j\ [M_i]_p}{n_T\ [M_T]_p}$$

$$k_{p,Tot0} = \frac{\sum_{i,j}^{c} k_{p,ji0}\ n_j\ [M_i]_p}{n_T\ [M_T]_p}$$

$$k_p^{diff} = k_p^{rd} + k_p^{M}$$

$$k_p^{rd} = 4\ \pi\ \frac{n_T}{[M_T]_p\ v_p}\ D^{rd}\ \left(\frac{\sigma_{LJ}^M}{2}+\frac{\sigma_{LJ}^R}{2}\right)$$

$$D^{rd} = k_{p,Tot}\ [M_T]_p\ \frac{a_{PR}^2}{6}.$$

$$a_{PR}^2 = \sum_{j=a}^{c} X_j \left(\left[\frac{< r_0^2 >_j}{N_i}\right]^{1/2}\right)^2$$

$$\sigma_{LJ}^R = \frac{\sum_{j=a}^{cbb} n_j\ o_j^R}{n_T}$$

$$\sigma^M = \frac{\sum_{i=a}^{c} [M_i]_p\ o_i^M}{[M_T]_p}$$

$$k_p^M = k_p^{diff} - k_p^{rd}$$

$$k_p^M = 4\ \pi\ \frac{n_T}{[M_T]_p\ v_p}\ D^M\ \left(\frac{\sigma_{LJ}^M}{2}+\frac{\sigma_{LJ}^R}{2}\right)$$

2

$$D^M = \frac{k_p^M\ [M_T]_p\ v_p}{4\ \pi\ n_T\ \left(\frac{\sigma_{LJ}^M}{2}+\frac{\sigma_{LJ}^R}{2}\right)}$$

On the other hand,

$$\frac{1}{k_t^{diff}} = \frac{1}{k_{t,Tot}} - \frac{1}{k_{t,Tot0}}$$

$k_{t,Tot}$ and $k_{t,\ Tot0}$ are given in Table S-2 (Supporting Information).

$$N^P = \frac{\nu_1}{\nu_0}$$

$$N^{PR} = \frac{\mu_1}{\mu_0}$$

$$c^* = \frac{3\ N^P\ PM_{aver}}{4\ \pi\ N_A\ R_g^3}$$

$$PM_{aver} = \sum_{j=a}^{c} X_j PM_j$$

$$R_g = \left(\frac{a_{PR}^2\ N^P}{6}\right)^{1/2}$$

3

Vg. For condition 2 in B-1

$n_i = n_3 = 0.75$, $n_j = n_2 = 1.59$

$$N^{PR,t} = \left(\frac{D^M}{\left[\frac{1000\ k_t^{diff}}{8\ \pi\ N_A\ \left(\frac{\sigma_{LJ}^R}{2}+\frac{\sigma_{LJ}^R}{2}\right)} - D^{rd}\right] c^{n_i}}\right)^{(1/n_j)}$$

Iteration in the values of n_0, n_1 and n_2 until finding a distribution of $N^{PR,t}$ similar a N^{PR}.

Evaluation of the values of $D^{PR,t}$ in Equation (9bi)-(9biii).

Substitution of $N^{PR,t}$ by N^{PR} and N^P in order to evaluate D^{PR} and D^P(without D^{rd}), respectively. As reference is calculated $D^{PR,t,2}$ with $n_1 = 2$ and $n_2 = 2$.

$$D^{com,P,2} = D^{P,2} = \frac{D^M}{\left(N^P\right)^2}$$

a. The subindex "i" for the monomers, subindex "j" for the j-ended radicals.

Table 5: Exponents of the degree of polymerization[a] of the radicals associated to the termination $N^{PR,t}$ in order to fit the degree of polymerization of the radicals N^{PR}.

	B-1	B-2	B-3	B-4	SC-1	SC-2	SC-3	SC-4
n_0	1.40	1.40	1.40	1.40	-	-	-	-
n_1	1.40	1.50	1.47	1.60	-	-	-	-
n_2	1.59	1.62	1.72	1.41	1.85	1.78	1.78	1.89
Conditions[b]	0,1,2,4 Almost 2	0,1,2	0,1,2	0,1,2 Almost 2	2,4 Almost 2	2,4 Almost 4	4	1,2,4 Almost 2
Range W_p[c]	0.48-0.96	0.48-0.97	0.45-0.92	0.47-0.96	0.79-0.82	0.80-0.91	0.62-0.82	0.74-0.89

a. $n_3 = 0.75$, $n_4 = 1.75$ (See Text).
b. See Equation (9).
c. In the semicontinuous processes, the increment of W_p at almost zero of conversion is not considered.

Table 6: Experimental and simulated range of the transition of T_g, ΔT_g, for the batch and semicontinuous processes.

	B-1	B-2	B-3[b]	SC-1	SC-2	SC-3	SC-4
ΔT_g (°C) Experimental.	19-70	25-55	20-44	29-61	27-69	27-63	12-23
k_p-k_t average model							
$\Delta T_{g,DSC}$(°C)	9-70	32-70	12-42	67-70	46-64	59-64	9-32
ΔT_g'[a] (°C)	9-70	32-70	-24-42	67-68	45-62	59-62	9-29
Backbiting model							
$\Delta T_{\alpha,DSC}$(°C)	9-70	17-70	16-42	60-69	45-60	59-65	21-32
$\Delta T_{\alpha i}$ (°C)	9,-70	17-70	-24-42	58-61	45-61	59-63	4-23

a. For the semicontinuous processes the higher value of the range of T_{gi} was obtained by the intersection of the tangent to the curve of T_{gi} versus X_O at the beginning of the reaction and the tangent when the conversion goes from 10 to 30 wt%.
b. It was difficult to define the onset of the experimental T_g of B-3.

Global Journals Inc. (US) Guidelines Handbook 2017

www.GlobalJournals.org

FELLOWS

FELLOW OF ASSOCIATION OF RESEARCH SOCIETY IN ENGINEERING (FARSE)

Global Journals Incorporate (USA) is accredited by Open Association of Research Society (OARS), U.S.A and in turn, awards "FARSE" title to individuals. The 'FARSE' title is accorded to a selected professional after the approval of the Editor-in-Chief /Editorial Board Members/Dean.

- The "FARSE" is a dignified title which is accorded to a person's name viz. Dr. John E. Hall, Ph.D., FARSE or William Walldroff, M.S., FARSE.

FARSE accrediting is an honor. It authenticates your research activities. After recognition as FARSE, you can add 'FARSE' title with your name as you use this recognition as additional suffix to your status. This will definitely enhance and add more value and repute to your name. You may use it on your professional Counseling Materials such as CV, Resume, and Visiting Card etc.

The following benefits can be availed by you only for next three years from the date of certification:

FARSE designated members are entitled to avail a 40% discount while publishing their research papers (of a single author) with Global Journals Incorporation (USA), if the same is accepted by Editorial Board/Peer Reviewers. If you are a main author or co-author in case of multiple authors, you will be entitled to avail discount of 10%.

Once FARSE title is accorded, the Fellow is authorized to organize a symposium/seminar/conference on behalf of Global Journal Incorporation (USA).The Fellow can also participate in conference/seminar/symposium organized by another institution as representative of Global Journal. In both the cases, it is mandatory for him to discuss with us and obtain our consent.

You may join as member of the Editorial Board of Global Journals Incorporation (USA) after successful completion of three years as Fellow and as Peer Reviewer. In addition, it is also desirable that you should organize seminar/symposium/conference at least once.

We shall provide you intimation regarding launching of e-version of journal of your stream time to time.This may be utilized in your library for the enrichment of knowledge of your students as well as it can also be helpful for the concerned faculty members.

The FARSE can go through standards of OARS. You can also play vital role if you have any suggestions so that proper amendment can take place to improve the same for the benefit of entire research community.

As FARSE, you will be given a renowned, secure and free professional email address with 100 GB of space e.g. johnhall@globaljournals.org. This will include Webmail, Spam Assassin, Email Forwarders,Auto-Responders, Email Delivery Route tracing, etc.

The FARSE will be eligible for a free application of standardization of their researches. Standardization of research will be subject to acceptability within stipulated norms as the next step after publishing in a journal. We shall depute a team of specialized research professionals who will render their services for elevating your researches to next higher level, which is worldwide open standardization.

The FARSE member can apply for grading and certification of standards of their educational and Institutional Degrees to Open Association of Research, Society U.S.A. Once you are designated as FARSE, you may send us a scanned copy of all of your credentials. OARS will verify, grade and certify them. This will be based on your academic records, quality of research papers published by you, and some more criteria. After certification of all your credentials by OARS, they will be published on your Fellow Profile link on website https://associationofresearch.org which will be helpful to upgrade the dignity.

The FARSE members can avail the benefits of free research podcasting in Global Research Radio with their research documents. After publishing the work, (including published elsewhere worldwide with proper authorization) you can upload your research paper with your recorded voice or you can utilize chargeable services of our professional RJs to record your paper in their voice on request.

The FARSE member also entitled to get the benefits of free research podcasting of their research documents through video clips. We can also streamline your conference videos and display your slides/ online slides and online research video clips at reasonable charges, on request.

The FARSE is eligible to earn from sales proceeds of his/her researches/reference/review Books or literature, while publishing with Global Journals. The FARSE can decide whether he/she would like to publish his/her research in a closed manner. In this case, whenever readers purchase that individual research paper for reading, maximum 60% of its profit earned as royalty by Global Journals, will be credited to his/her bank account. The entire entitled amount will be credited to his/her bank account exceeding limit of minimum fixed balance. There is no minimum time limit for collection. The FARSE member can decide its price and we can help in making the right decision.

The FARSE member is eligible to join as a paid peer reviewer at Global Journals Incorporation (USA) and can get remuneration of 15% of author fees, taken from the author of a respective paper. After reviewing 5 or more papers you can request to transfer the amount to your bank account.

MEMBER OF ASSOCIATION OF RESEARCH SOCIETY IN ENGINEERING (MARSE)

The 'MARSE ' title is accorded to a selected professional after the approval of the Editor-in-Chief / Editorial Board Members/Dean.

The "MARSE" is a dignified ornament which is accorded to a person's name viz. Dr. John E. Hall, Ph.D., MARSE or William Walldroff, M.S., MARSE.

MARSE accrediting is an honor. It authenticates your research activities. After becoming MARSE, you can add 'MARSE' title with your name as you use this recognition as additional suffix to your status. This will definitely enhance and add more value and repute to your name. You may use it on your professional Counseling Materials such as CV, Resume, Visiting Card and Name Plate etc.

The following benefitscan be availed by you only for next three years from the date of certification.

MARSE designated members are entitled to avail a 25% discount while publishing their research papers (of a single author) in Global Journals Inc., if the same is accepted by our Editorial Board and Peer Reviewers. If you are a main author or co-author of a group of authors, you will get discount of 10%.

As MARSE, you will be given a renowned, secure and free professional email address with 30 GB of space e.g. johnhall@globaljournals.org. This will include Webmail, Spam Assassin, Email Forwarders,Auto-Responders, Email Delivery Route tracing, etc.

We shall provide you intimation regarding launching of e-version of journal of your stream time to time.This may be utilized in your library for the enrichment of knowledge of your students as well as it can also be helpful for the concerned faculty members.

The MARSE member can apply for approval, grading and certification of standards of their educational and Institutional Degrees to Open Association of Research, Society U.S.A.

Once you are designated as MARSE, you may send us a scanned copy of all of your credentials. OARS will verify, grade and certify them. This will be based on your academic records, quality of research papers published by you, and some more criteria.

It is mandatory to read all terms and conditions carefully.

AUXILIARY MEMBERSHIPS

Institutional Fellow of Open Association of Research Society (USA)-OARS (USA)

Global Journals Incorporation (USA) is accredited by Open Association of Research Society, U.S.A (OARS) and in turn, affiliates research institutions as "Institutional Fellow of Open Association of Research Society" (IFOARS).

The "FARSC" is a dignified title which is accorded to a person's name viz. Dr. John E. Hall, Ph.D., FARSC or William Walldroff, M.S., FARSC.

The IFOARS institution is entitled to form a Board comprised of one Chairperson and three to five board members preferably from different streams. The Board will be recognized as "Institutional Board of Open Association of Research Society"-(IBOARS).

The Institute will be entitled to following benefits:

The IBOARS can initially review research papers of their institute and recommend them to publish with respective journal of Global Journals. It can also review the papers of other institutions after obtaining our consent. The second review will be done by peer reviewer of Global Journals Incorporation (USA) The Board is at liberty to appoint a peer reviewer with the approval of chairperson after consulting us.

The author fees of such paper may be waived off up to 40%.

The Global Journals Incorporation (USA) at its discretion can also refer double blind peer reviewed paper at their end to the board for the verification and to get recommendation for final stage of acceptance of publication.

The IBOARS can organize symposium/seminar/conference in their country on behalf of Global Journals Incorporation (USA)-OARS (USA). The terms and conditions can be discussed separately.

The Board can also play vital role by exploring and giving valuable suggestions regarding the Standards of "Open Association of Research Society, U.S.A (OARS)" so that proper amendment can take place for the benefit of entire research community. We shall provide details of particular standard only on receipt of request from the Board.

The board members can also join us as Individual Fellow with 40% discount on total fees applicable to Individual Fellow. They will be entitled to avail all the benefits as declared. Please visit Individual Fellow-sub menu of GlobalJournals.org to have more relevant details.

We shall provide you intimation regarding launching of e-version of journal of your stream time to time. This may be utilized in your library for the enrichment of knowledge of your students as well as it can also be helpful for the concerned faculty members.

After nomination of your institution as "Institutional Fellow" and constantly functioning successfully for one year, we can consider giving recognition to your institute to function as Regional/Zonal office on our behalf.
The board can also take up the additional allied activities for betterment after our consultation.

The following entitlements are applicable to individual Fellows:

Open Association of Research Society, U.S.A (OARS) By-laws states that an individual Fellow may use the designations as applicable, or the corresponding initials. The Credentials of individual Fellow and Associate designations signify that the individual has gained knowledge of the fundamental concepts. One is magnanimous and proficient in an expertise course covering the professional code of conduct, and follows recognized standards of practice.

Open Association of Research Society (US)/ Global Journals Incorporation (USA), as described in Corporate Statements, are educational, research publishing and professional membership organizations. Achieving our individual Fellow or Associate status is based mainly on meeting stated educational research requirements.

Disbursement of 40% Royalty earned through Global Journals : Researcher = 50%, Peer Reviewer = 37.50%, Institution = 12.50% E.g. Out of 40%, the 20% benefit should be passed on to researcher, 15 % benefit towards remuneration should be given to a reviewer and remaining 5% is to be retained by the institution.

We shall provide print version of 12 issues of any three journals [as per your requirement] out of our 38 journals worth $ 2376 USD.

Other:

The individual Fellow and Associate designations accredited by Open Association of Research Society (US) credentials signify guarantees following achievements:

- The professional accredited with Fellow honor, is entitled to various benefits viz. name, fame, honor, regular flow of income, secured bright future, social status etc.

- In addition to above, if one is single author, then entitled to 40% discount on publishing research paper and can get 10%discount if one is co-author or main author among group of authors.
- The Fellow can organize symposium/seminar/conference on behalf of Global Journals Incorporation (USA) and he/she can also attend the same organized by other institutes on behalf of Global Journals.
- The Fellow can become member of Editorial Board Member after completing 3yrs.
- The Fellow can earn 60% of sales proceeds from the sale of reference/review books/literature/publishing of research paper.
- Fellow can also join as paid peer reviewer and earn 15% remuneration of author charges and can also get an opportunity to join as member of the Editorial Board of Global Journals Incorporation (USA)
- • This individual has learned the basic methods of applying those concepts and techniques to common challenging situations. This individual has further demonstrated an in–depth understanding of the application of suitable techniques to a particular area of research practice.

Note :

"

- In future, if the board feels the necessity to change any board member, the same can be done with the consent of the chairperson along with anyone board member without our approval.
- In case, the chairperson needs to be replaced then consent of 2/3rd board members are required and they are also required to jointly pass the resolution copy of which should be sent to us. In such case, it will be compulsory to obtain our approval before replacement.
- In case of "Difference of Opinion [if any]" among the Board members, our decision will be final and binding to everyone.

"

Process of submission of Research Paper

The Area or field of specialization may or may not be of any category as mentioned in 'Scope of Journal' menu of the GlobalJournals.org website. There are 37 Research Journal categorized with Six parental Journals GJCST, GJMR, GJRE, GJMBR, GJSFR, GJHSS. For Authors should prefer the mentioned categories. There are three widely used systems UDC, DDC and LCC. The details are available as 'Knowledge Abstract' at Home page. The major advantage of this coding is that, the research work will be exposed to and shared with all over the world as we are being abstracted and indexed worldwide.

The paper should be in proper format. The format can be downloaded from first page of 'Author Guideline' Menu. The Author is expected to follow the general rules as mentioned in this menu. The paper should be written in MS-Word Format (*.DOC,*.DOCX).

The Author can submit the paper either online or offline. The authors should prefer online submission.Online Submission: There are three ways to submit your paper:

(A) (I) First, register yourself using top right corner of Home page then Login. If you are already registered, then login using your username and password.

(II) Choose corresponding Journal.

(III) Click 'Submit Manuscript'. Fill required information and Upload the paper.

(B) If you are using Internet Explorer, then Direct Submission through Homepage is also available.

(C) If these two are not conveninet , and then email the paper directly to dean@globaljournals.org.

Offline Submission: Author can send the typed form of paper by Post. However, online submission should be preferred.

Preferred Author Guidelines

MANUSCRIPT STYLE INSTRUCTION (Must be strictly followed)

Page Size: 8.27" X 11'"

- Left Margin: 0.65
- Right Margin: 0.65
- Top Margin: 0.75
- Bottom Margin: 0.75
- Font type of all text should be Swis 721 Lt BT.
- Paper Title should be of Font Size 24 with one Column section.
- Author Name in Font Size of 11 with one column as of Title.
- Abstract Font size of 9 Bold, "Abstract" word in Italic Bold.
- Main Text: Font size 10 with justified two columns section
- Two Column with Equal Column with of 3.38 and Gaping of .2
- First Character must be three lines Drop capped.
- Paragraph before Spacing of 1 pt and After of 0 pt.
- Line Spacing of 1 pt
- Large Images must be in One Column
- Numbering of First Main Headings (Heading 1) must be in Roman Letters, Capital Letter, and Font Size of 10.
- Numbering of Second Main Headings (Heading 2) must be in Alphabets, Italic, and Font Size of 10.

You can use your own standard format also.
Author Guidelines:

1. General,

2. Ethical Guidelines,

3. Submission of Manuscripts,

4. Manuscript's Category,

5. Structure and Format of Manuscript,

6. After Acceptance.

1. GENERAL

Before submitting your research paper, one is advised to go through the details as mentioned in following heads. It will be beneficial, while peer reviewer justify your paper for publication.

Scope

The Global Journals Inc. (US) welcome the submission of original paper, review paper, survey article relevant to the all the streams of Philosophy and knowledge. The Global Journals Inc. (US) is parental platform for Global Journal of Computer Science and Technology, Researches in Engineering, Medical Research, Science Frontier Research, Human Social Science, Management, and Business organization. The choice of specific field can be done otherwise as following in Abstracting and Indexing Page on this Website. As the all Global

Journals Inc. (US) are being abstracted and indexed (in process) by most of the reputed organizations. Topics of only narrow interest will not be accepted unless they have wider potential or consequences.

2. ETHICAL GUIDELINES

Authors should follow the ethical guidelines as mentioned below for publication of research paper and research activities.

Papers are accepted on strict understanding that the material in whole or in part has not been, nor is being, considered for publication elsewhere. If the paper once accepted by Global Journals Inc. (US) and Editorial Board, will become the copyright of the Global Journals Inc. (US).

Authorship: The authors and coauthors should have active contribution to conception design, analysis and interpretation of findings. They should critically review the contents and drafting of the paper. All should approve the final version of the paper before submission

The Global Journals Inc. (US) follows the definition of authorship set up by the Global Academy of Research and Development. According to the Global Academy of R&D authorship, criteria must be based on:

1) Substantial contributions to conception and acquisition of data, analysis and interpretation of the findings.

2) Drafting the paper and revising it critically regarding important academic content.

3) Final approval of the version of the paper to be published.

All authors should have been credited according to their appropriate contribution in research activity and preparing paper. Contributors who do not match the criteria as authors may be mentioned under Acknowledgement.

Acknowledgements: Contributors to the research other than authors credited should be mentioned under acknowledgement. The specifications of the source of funding for the research if appropriate can be included. Suppliers of resources may be mentioned along with address.

Appeal of Decision: The Editorial Board's decision on publication of the paper is final and cannot be appealed elsewhere.

Permissions: It is the author's responsibility to have prior permission if all or parts of earlier published illustrations are used in this paper.

Please mention proper reference and appropriate acknowledgements wherever expected.

If all or parts of previously published illustrations are used, permission must be taken from the copyright holder concerned. It is the author's responsibility to take these in writing.

Approval for reproduction/modification of any information (including figures and tables) published elsewhere must be obtained by the authors/copyright holders before submission of the manuscript. Contributors (Authors) are responsible for any copyright fee involved.

3. SUBMISSION OF MANUSCRIPTS

Manuscripts should be uploaded via this online submission page. The online submission is most efficient method for submission of papers, as it enables rapid distribution of manuscripts and consequently speeds up the review procedure. It also enables authors to know the status of their own manuscripts by emailing us. Complete instructions for submitting a paper is available below.

Manuscript submission is a systematic procedure and little preparation is required beyond having all parts of your manuscript in a given format and a computer with an Internet connection and a Web browser. Full help and instructions are provided on-screen. As an author, you will be prompted for login and manuscript details as Field of Paper and then to upload your manuscript file(s) according to the instructions.

To avoid postal delays, all transaction is preferred by e-mail. A finished manuscript submission is confirmed by e-mail immediately and your paper enters the editorial process with no postal delays. When a conclusion is made about the publication of your paper by our Editorial Board, revisions can be submitted online with the same procedure, with an occasion to view and respond to all comments.

Complete support for both authors and co-author is provided.

4. MANUSCRIPT'S CATEGORY

Based on potential and nature, the manuscript can be categorized under the following heads:

Original research paper: Such papers are reports of high-level significant original research work.

Review papers: These are concise, significant but helpful and decisive topics for young researchers.

Research articles: These are handled with small investigation and applications

Research letters: The letters are small and concise comments on previously published matters.

5.STRUCTURE AND FORMAT OF MANUSCRIPT

The recommended size of original research paper is less than seven thousand words, review papers fewer than seven thousands words also.Preparation of research paper or how to write research paper, are major hurdle, while writing manuscript. The research articles and research letters should be fewer than three thousand words, the structure original research paper; sometime review paper should be as follows:

Papers: These are reports of significant research (typically less than 7000 words equivalent, including tables, figures, references), and comprise:

(a)Title should be relevant and commensurate with the theme of the paper.

(b) A brief Summary, "Abstract" (less than 150 words) containing the major results and conclusions.

(c) Up to ten keywords, that precisely identifies the paper's subject, purpose, and focus.

(d) An Introduction, giving necessary background excluding subheadings; objectives must be clearly declared.

(e) Resources and techniques with sufficient complete experimental details (wherever possible by reference) to permit repetition; sources of information must be given and numerical methods must be specified by reference, unless non-standard.

(f) Results should be presented concisely, by well-designed tables and/or figures; the same data may not be used in both; suitable statistical data should be given. All data must be obtained with attention to numerical detail in the planning stage. As reproduced design has been recognized to be important to experiments for a considerable time, the Editor has decided that any paper that appears not to have adequate numerical treatments of the data will be returned un-refereed;

(g) Discussion should cover the implications and consequences, not just recapitulating the results; conclusions should be summarizing.

(h) Brief Acknowledgements.

(i) References in the proper form.

Authors should very cautiously consider the preparation of papers to ensure that they communicate efficiently. Papers are much more likely to be accepted, if they are cautiously designed and laid out, contain few or no errors, are summarizing, and be conventional to the approach and instructions. They will in addition, be published with much less delays than those that require much technical and editorial correction.

The Editorial Board reserves the right to make literary corrections and to make suggestions to improve briefness.

It is vital, that authors take care in submitting a manuscript that is written in simple language and adheres to published guidelines.

Format

Language: The language of publication is UK English. Authors, for whom English is a second language, must have their manuscript efficiently edited by an English-speaking person before submission to make sure that, the English is of high excellence. It is preferable, that manuscripts should be professionally edited.

Standard Usage, Abbreviations, and Units: Spelling and hyphenation should be conventional to The Concise Oxford English Dictionary. Statistics and measurements should at all times be given in figures, e.g. 16 min, except for when the number begins a sentence. When the number does not refer to a unit of measurement it should be spelt in full unless, it is 160 or greater.

Abbreviations supposed to be used carefully. The abbreviated name or expression is supposed to be cited in full at first usage, followed by the conventional abbreviation in parentheses.

Metric SI units are supposed to generally be used excluding where they conflict with current practice or are confusing. For illustration, 1.4 l rather than 1.4 × 10-3 m3, or 4 mm somewhat than 4 × 10-3 m. Chemical formula and solutions must identify the form used, e.g. anhydrous or hydrated, and the concentration must be in clearly defined units. Common species names should be followed by underlines at the first mention. For following use the generic name should be constricted to a single letter, if it is clear.

Structure

All manuscripts submitted to Global Journals Inc. (US), ought to include:

Title: The title page must carry an instructive title that reflects the content, a running title (less than 45 characters together with spaces), names of the authors and co-authors, and the place(s) wherever the work was carried out. The full postal address in addition with the e-mail address of related author must be given. Up to eleven keywords or very brief phrases have to be given to help data retrieval, mining and indexing.

Abstract, used in Original Papers and Reviews:

Optimizing Abstract for Search Engines

Many researchers searching for information online will use search engines such as Google, Yahoo or similar. By optimizing your paper for search engines, you will amplify the chance of someone finding it. This in turn will make it more likely to be viewed and/or cited in a further work. Global Journals Inc. (US) have compiled these guidelines to facilitate you to maximize the web-friendliness of the most public part of your paper.

Key Words

A major linchpin in research work for the writing research paper is the keyword search, which one will employ to find both library and Internet resources.

One must be persistent and creative in using keywords. An effective keyword search requires a strategy and planning a list of possible keywords and phrases to try.

Search engines for most searches, use Boolean searching, which is somewhat different from Internet searches. The Boolean search uses "operators," words (and, or, not, and near) that enable you to expand or narrow your affords. Tips for research paper while preparing research paper are very helpful guideline of research paper.

Choice of key words is first tool of tips to write research paper. Research paper writing is an art.A few tips for deciding as strategically as possible about keyword search:

- One should start brainstorming lists of possible keywords before even begin searching. Think about the most important concepts related to research work. Ask, "What words would a source have to include to be truly valuable in research paper?" Then consider synonyms for the important words.
- It may take the discovery of only one relevant paper to let steer in the right keyword direction because in most databases, the keywords under which a research paper is abstracted are listed with the paper.
- One should avoid outdated words.

Keywords are the key that opens a door to research work sources. Keyword searching is an art in which researcher's skills are bound to improve with experience and time.

Numerical Methods: Numerical methods used should be clear and, where appropriate, supported by references.

Acknowledgements: Please make these as concise as possible.

References

References follow the Harvard scheme of referencing. References in the text should cite the authors' names followed by the time of their publication, unless there are three or more authors when simply the first author's name is quoted followed by et al. unpublished work has to only be cited where necessary, and only in the text. Copies of references in press in other journals have to be supplied with submitted typescripts. It is necessary that all citations and references be carefully checked before submission, as mistakes or omissions will cause delays.

References to information on the World Wide Web can be given, but only if the information is available without charge to readers on an official site. Wikipedia and Similar websites are not allowed where anyone can change the information. Authors will be asked to make available electronic copies of the cited information for inclusion on the Global Journals Inc. (US) homepage at the judgment of the Editorial Board.

The Editorial Board and Global Journals Inc. (US) recommend that, citation of online-published papers and other material should be done via a DOI (digital object identifier). If an author cites anything, which does not have a DOI, they run the risk of the cited material not being noticeable.

The Editorial Board and Global Journals Inc. (US) recommend the use of a tool such as Reference Manager for reference management and formatting.

Tables, Figures and Figure Legends

Tables: Tables should be few in number, cautiously designed, uncrowned, and include only essential data. Each must have an Arabic number, e.g. Table 4, a self-explanatory caption and be on a separate sheet. Vertical lines should not be used.

Figures: Figures are supposed to be submitted as separate files. Always take in a citation in the text for each figure using Arabic numbers, e.g. Fig. 4. Artwork must be submitted online in electronic form by e-mailing them.

Preparation of Electronic Figures for Publication

Even though low quality images are sufficient for review purposes, print publication requires high quality images to prevent the final product being blurred or fuzzy. Submit (or e-mail) EPS (line art) or TIFF (halftone/photographs) files only. MS PowerPoint and Word Graphics are unsuitable for printed pictures. Do not use pixel-oriented software. Scans (TIFF only) should have a resolution of at least 350 dpi (halftone) or 700 to 1100 dpi (line drawings) in relation to the imitation size. Please give the data for figures in black and white or submit a Color Work Agreement Form. EPS files must be saved with fonts embedded (and with a TIFF preview, if possible).

For scanned images, the scanning resolution (at final image size) ought to be as follows to ensure good reproduction: line art: >650 dpi; halftones (including gel photographs) : >350 dpi; figures containing both halftone and line images: >650 dpi.

Figure Legends: Self-explanatory legends of all figures should be incorporated separately under the heading 'Legends to Figures'. In the full-text online edition of the journal, figure legends may possibly be truncated in abbreviated links to the full screen version. Therefore, the first 100 characters of any legend should notify the reader, about the key aspects of the figure.

6. AFTER ACCEPTANCE

Upon approval of a paper for publication, the manuscript will be forwarded to the dean, who is responsible for the publication of the Global Journals Inc. (US).

6.1 Proof Corrections

The corresponding author will receive an e-mail alert containing a link to a website or will be attached. A working e-mail address must therefore be provided for the related author.

Acrobat Reader will be required in order to read this file. This software can be downloaded

(Free of charge) from the following website:

www.adobe.com/products/acrobat/readstep2.html. This will facilitate the file to be opened, read on screen, and printed out in order for any corrections to be added. Further instructions will be sent with the proof.

Proofs must be returned to the dean at dean@globaljournals.org within three days of receipt.

As changes to proofs are costly, we inquire that you only correct typesetting errors. All illustrations are retained by the publisher. Please note that the authors are responsible for all statements made in their work, including changes made by the copy editor.

6.2 Early View of Global Journals Inc. (US) (Publication Prior to Print)

The Global Journals Inc. (US) are enclosed by our publishing's Early View service. Early View articles are complete full-text articles sent in advance of their publication. Early View articles are absolute and final. They have been completely reviewed, revised and edited for publication, and the authors' final corrections have been incorporated. Because they are in final form, no changes can be made after sending them. The nature of Early View articles means that they do not yet have volume, issue or page numbers, so Early View articles cannot be cited in the conventional way.

6.3 Author Services

Online production tracking is available for your article through Author Services. Author Services enables authors to track their article - once it has been accepted - through the production process to publication online and in print. Authors can check the status of their articles online and choose to receive automated e-mails at key stages of production. The authors will receive an e-mail with a unique link that enables them to register and have their article automatically added to the system. Please ensure that a complete e-mail address is provided when submitting the manuscript.

6.4 Author Material Archive Policy

Please note that if not specifically requested, publisher will dispose off hardcopy & electronic information submitted, after the two months of publication. If you require the return of any information submitted, please inform the Editorial Board or dean as soon as possible.

6.5 Offprint and Extra Copies

A PDF offprint of the online-published article will be provided free of charge to the related author, and may be distributed according to the Publisher's terms and conditions. Additional paper offprint may be ordered by emailing us at: editor@globaljournals.org .

You must strictly follow above Author Guidelines before submitting your paper or else we will not at all be responsible for any corrections in future in any of the way.

Before start writing a good quality Computer Science Research Paper, let us first understand what is Computer Science Research Paper? So, Computer Science Research Paper is the paper which is written by professionals or scientists who are associated to Computer Science and Information Technology, or doing research study in these areas. If you are novel to this field then you can consult about this field from your supervisor or guide.

TECHNIQUES FOR WRITING A GOOD QUALITY RESEARCH PAPER:

1. Choosing the topic: In most cases, the topic is searched by the interest of author but it can be also suggested by the guides. You can have several topics and then you can judge that in which topic or subject you are finding yourself most comfortable. This can be done by asking several questions to yourself, like Will I be able to carry our search in this area? Will I find all necessary recourses to accomplish the search? Will I be able to find all information in this field area? If the answer of these types of questions will be "Yes" then you can choose that topic. In most of the cases, you may have to conduct the surveys and have to visit several places because this field is related to Computer Science and Information Technology. Also, you may have to do a lot of work to find all rise and falls regarding the various data of that subject. Sometimes, detailed information plays a vital role, instead of short information.

2. Evaluators are human: First thing to remember that evaluators are also human being. They are not only meant for rejecting a paper. They are here to evaluate your paper. So, present your Best.

3. Think Like Evaluators: If you are in a confusion or getting demotivated that your paper will be accepted by evaluators or not, then think and try to evaluate your paper like an Evaluator. Try to understand that what an evaluator wants in your research paper and automatically you will have your answer.

4. Make blueprints of paper: The outline is the plan or framework that will help you to arrange your thoughts. It will make your paper logical. But remember that all points of your outline must be related to the topic you have chosen.

5. Ask your Guides: If you are having any difficulty in your research, then do not hesitate to share your difficulty to your guide (if you have any). They will surely help you out and resolve your doubts. If you can't clarify what exactly you require for your work then ask the supervisor to help you with the alternative. He might also provide you the list of essential readings.

6. Use of computer is recommended: As you are doing research in the field of Computer Science, then this point is quite obvious.

7. Use right software: Always use good quality software packages. If you are not capable to judge good software then you can lose quality of your paper unknowingly. There are various software programs available to help you, which you can get through Internet.

8. Use the Internet for help: An excellent start for your paper can be by using the Google. It is an excellent search engine, where you can have your doubts resolved. You may also read some answers for the frequent question how to write my research paper or find model research paper. From the internet library you can download books. If you have all required books make important reading selecting and analyzing the specified information. Then put together research paper sketch out.

9. Use and get big pictures: Always use encyclopedias, Wikipedia to get pictures so that you can go into the depth.

10. Bookmarks are useful: When you read any book or magazine, you generally use bookmarks, right! It is a good habit, which helps to not to lose your continuity. You should always use bookmarks while searching on Internet also, which will make your search easier.

11. Revise what you wrote: When you write anything, always read it, summarize it and then finalize it.

12. Make all efforts: Make all efforts to mention what you are going to write in your paper. That means always have a good start. Try to mention everything in introduction, that what is the need of a particular research paper. Polish your work by good skill of writing and always give an evaluator, what he wants.

13. Have backups: When you are going to do any important thing like making research paper, you should always have backup copies of it either in your computer or in paper. This will help you to not to lose any of your important.

14. Produce good diagrams of your own: Always try to include good charts or diagrams in your paper to improve quality. Using several and unnecessary diagrams will degrade the quality of your paper by creating "hotchpotch." So always, try to make and include those diagrams, which are made by your own to improve readability and understandability of your paper.

15. Use of direct quotes: When you do research relevant to literature, history or current affairs then use of quotes become essential but if study is relevant to science then use of quotes is not preferable.

16. Use proper verb tense: Use proper verb tenses in your paper. Use past tense, to present those events that happened. Use present tense to indicate events that are going on. Use future tense to indicate future happening events. Use of improper and wrong tenses will confuse the evaluator. Avoid the sentences that are incomplete.

17. Never use online paper: If you are getting any paper on Internet, then never use it as your research paper because it might be possible that evaluator has already seen it or maybe it is outdated version.

18. Pick a good study spot: To do your research studies always try to pick a spot, which is quiet. Every spot is not for studies. Spot that suits you choose it and proceed further.

19. Know what you know: Always try to know, what you know by making objectives. Else, you will be confused and cannot achieve your target.

20. Use good quality grammar: Always use a good quality grammar and use words that will throw positive impact on evaluator. Use of good quality grammar does not mean to use tough words, that for each word the evaluator has to go through dictionary. Do not start sentence with a conjunction. Do not fragment sentences. Eliminate one-word sentences. Ignore passive voice. Do not ever use a big word when a diminutive one would suffice. Verbs have to be in agreement with their subjects. Prepositions are not expressions to finish sentences with. It is incorrect to ever divide an infinitive. Avoid clichés like the disease. Also, always shun irritating alliteration. Use language that is simple and straight forward. put together a neat summary.

21. Arrangement of information: Each section of the main body should start with an opening sentence and there should be a changeover at the end of the section. Give only valid and powerful arguments to your topic. You may also maintain your arguments with records.

22. Never start in last minute: Always start at right time and give enough time to research work. Leaving everything to the last minute will degrade your paper and spoil your work.

23. Multitasking in research is not good: Doing several things at the same time proves bad habit in case of research activity. Research is an area, where everything has a particular time slot. Divide your research work in parts and do particular part in particular time slot.

24. Never copy others' work: Never copy others' work and give it your name because if evaluator has seen it anywhere you will be in trouble.

25. Take proper rest and food: No matter how many hours you spend for your research activity, if you are not taking care of your health then all your efforts will be in vain. For a quality research, study is must, and this can be done by taking proper rest and food.

26. Go for seminars: Attend seminars if the topic is relevant to your research area. Utilize all your resources.

27. Refresh your mind after intervals: Try to give rest to your mind by listening to soft music or by sleeping in intervals. This will also improve your memory.

28. Make colleagues: Always try to make colleagues. No matter how sharper or intelligent you are, if you make colleagues you can have several ideas, which will be helpful for your research.

29. Think technically: Always think technically. If anything happens, then search its reasons, its benefits, and demerits.

30. Think and then print: When you will go to print your paper, notice that tables are not be split, headings are not detached from their descriptions, and page sequence is maintained.

31. Adding unnecessary information: Do not add unnecessary information, like, I have used MS Excel to draw graph. Do not add irrelevant and inappropriate material. These all will create superfluous. Foreign terminology and phrases are not apropos. One should NEVER take a broad view. Analogy in script is like feathers on a snake. Not at all use a large word when a very small one would be sufficient. Use words properly, regardless of how others use them. Remove quotations. Puns are for kids, not grunt readers. Amplification is a billion times of inferior quality than sarcasm.

32. Never oversimplify everything: To add material in your research paper, never go for oversimplification. This will definitely irritate the evaluator. Be more or less specific. Also too, by no means, ever use rhythmic redundancies. Contractions aren't essential and shouldn't be there used. Comparisons are as terrible as clichés. Give up ampersands and abbreviations, and so on. Remove commas, that are, not necessary. Parenthetical words however should be together with this in commas. Understatement is all the time the complete best way to put onward earth-shaking thoughts. Give a detailed literary review.

33. Report concluded results: Use concluded results. From raw data, filter the results and then conclude your studies based on measurements and observations taken. Significant figures and appropriate number of decimal places should be used. Parenthetical remarks are prohibitive. Proofread carefully at final stage. In the end give outline to your arguments. Spot out perspectives of further study of this subject. Justify your conclusion by at the bottom of them with sufficient justifications and examples.

34. After conclusion: Once you have concluded your research, the next most important step is to present your findings. Presentation is extremely important as it is the definite medium though which your research is going to be in print to the rest of the crowd. Care should be taken to categorize your thoughts well and present them in a logical and neat manner. A good quality research paper format is essential because it serves to highlight your research paper and bring to light all necessary aspects in your research.

Informal Guidelines of Research Paper Writing

Key points to remember:

- Submit all work in its final form.
- Write your paper in the form, which is presented in the guidelines using the template.
- Please note the criterion for grading the final paper by peer-reviewers.

Final Points:

A purpose of organizing a research paper is to let people to interpret your effort selectively. The journal requires the following sections, submitted in the order listed, each section to start on a new page.

The introduction will be compiled from reference matter and will reflect the design processes or outline of basis that direct you to make study. As you will carry out the process of study, the method and process section will be constructed as like that. The result segment will show related statistics in nearly sequential order and will direct the reviewers next to the similar intellectual paths throughout the data that you took to carry out your study. The discussion section will provide understanding of the data and projections as to the implication of the results. The use of good quality references all through the paper will give the effort trustworthiness by representing an alertness of prior workings.

Writing a research paper is not an easy job no matter how trouble-free the actual research or concept. Practice, excellent preparation, and controlled record keeping are the only means to make straightforward the progression.

General style:

Specific editorial column necessities for compliance of a manuscript will always take over from directions in these general guidelines.

To make a paper clear

· Adhere to recommended page limits

Mistakes to evade

- Insertion a title at the foot of a page with the subsequent text on the next page
- Separating a table/chart or figure - impound each figure/table to a single page
- Submitting a manuscript with pages out of sequence

In every sections of your document

· Use standard writing style including articles ("a", "the," etc.)

· Keep on paying attention on the research topic of the paper

· Use paragraphs to split each significant point (excluding for the abstract)

· Align the primary line of each section

· Present your points in sound order

· Use present tense to report well accepted

· Use past tense to describe specific results

· Shun familiar wording, don't address the reviewer directly, and don't use slang, slang language, or superlatives

· Shun use of extra pictures - include only those figures essential to presenting results

Title Page:

Choose a revealing title. It should be short. It should not have non-standard acronyms or abbreviations. It should not exceed two printed lines. It should include the name(s) and address (es) of all authors.

Abstract:

The summary should be two hundred words or less. It should briefly and clearly explain the key findings reported in the manuscript--must have precise statistics. It should not have abnormal acronyms or abbreviations. It should be logical in itself. Shun citing references at this point.

An abstract is a brief distinct paragraph summary of finished work or work in development. In a minute or less a reviewer can be taught the foundation behind the study, common approach to the problem, relevant results, and significant conclusions or new questions.

Write your summary when your paper is completed because how can you write the summary of anything which is not yet written? Wealth of terminology is very essential in abstract. Yet, use comprehensive sentences and do not let go readability for briefness. You can maintain it succinct by phrasing sentences so that they provide more than lone rationale. The author can at this moment go straight to shortening the outcome. Sum up the study, with the subsequent elements in any summary. Try to maintain the initial two items to no more than one ruling each.

- Reason of the study - theory, overall issue, purpose
- Fundamental goal
- To the point depiction of the research
- Consequences, including definite statistics - if the consequences are quantitative in nature, account quantitative data; results of any numerical analysis should be reported
- Significant conclusions or questions that track from the research(es)

Approach:

- Single section, and succinct
- As a outline of job done, it is always written in past tense
- A conceptual should situate on its own, and not submit to any other part of the paper such as a form or table
- Center on shortening results - bound background information to a verdict or two, if completely necessary
- What you account in an conceptual must be regular with what you reported in the manuscript
- Exact spelling, clearness of sentences and phrases, and appropriate reporting of quantities (proper units, important statistics) are just as significant in an abstract as they are anywhere else

Introduction:

The **Introduction** should "introduce" the manuscript. The reviewer should be presented with sufficient background information to be capable to comprehend and calculate the purpose of your study without having to submit to other works. The basis for the study should be offered. Give most important references but shun difficult to make a comprehensive appraisal of the topic. In the introduction, describe the problem visibly. If the problem is not acknowledged in a logical, reasonable way, the reviewer will have no attention in your result. Speak in common terms about techniques used to explain the problem, if needed, but do not present any particulars about the protocols here. Following approach can create a valuable beginning:

- Explain the value (significance) of the study
- Shield the model - why did you employ this particular system or method? What is its compensation? You strength remark on its appropriateness from a abstract point of vision as well as point out sensible reasons for using it.
- Present a justification. Status your particular theory (es) or aim(s), and describe the logic that led you to choose them.
- Very for a short time explain the tentative propose and how it skilled the declared objectives.

Approach:

- Use past tense except for when referring to recognized facts. After all, the manuscript will be submitted after the entire job is done.
- Sort out your thoughts; manufacture one key point with every section. If you make the four points listed above, you will need a least of four paragraphs.

- Present surroundings information only as desirable in order hold up a situation. The reviewer does not desire to read the whole thing you know about a topic.
- Shape the theory/purpose specifically - do not take a broad view.
- As always, give awareness to spelling, simplicity and correctness of sentences and phrases.

Procedures (Methods and Materials):

This part is supposed to be the easiest to carve if you have good skills. A sound written Procedures segment allows a capable scientist to replacement your results. Present precise information about your supplies. The suppliers and clarity of reagents can be helpful bits of information. Present methods in sequential order but linked methodologies can be grouped as a segment. Be concise when relating the protocols. Attempt for the least amount of information that would permit another capable scientist to spare your outcome but be cautious that vital information is integrated. The use of subheadings is suggested and ought to be synchronized with the results section. When a technique is used that has been well described in another object, mention the specific item describing a way but draw the basic principle while stating the situation. The purpose is to text all particular resources and broad procedures, so that another person may use some or all of the methods in one more study or referee the scientific value of your work. It is not to be a step by step report of the whole thing you did, nor is a methods section a set of orders.

Materials:

- Explain materials individually only if the study is so complex that it saves liberty this way.
- Embrace particular materials, and any tools or provisions that are not frequently found in laboratories.
- Do not take in frequently found.
- If use of a definite type of tools.
- Materials may be reported in a part section or else they may be recognized along with your measures.

Methods:

- Report the method (not particulars of each process that engaged the same methodology)
- Describe the method entirely
- To be succinct, present methods under headings dedicated to specific dealings or groups of measures
- Simplify - details how procedures were completed not how they were exclusively performed on a particular day.
- If well known procedures were used, account the procedure by name, possibly with reference, and that's all.

Approach:

- It is embarrassed or not possible to use vigorous voice when documenting methods with no using first person, which would focus the reviewer's interest on the researcher rather than the job. As a result when script up the methods most authors use third person passive voice.
- Use standard style in this and in every other part of the paper - avoid familiar lists, and use full sentences.

What to keep away from

- Resources and methods are not a set of information.
- Skip all descriptive information and surroundings - save it for the argument.
- Leave out information that is immaterial to a third party.

Results:

The principle of a results segment is to present and demonstrate your conclusion. Create this part a entirely objective details of the outcome, and save all understanding for the discussion.

The page length of this segment is set by the sum and types of data to be reported. Carry on to be to the point, by means of statistics and tables, if suitable, to present consequences most efficiently.You must obviously differentiate material that would usually be incorporated in a study editorial from any unprocessed data or additional appendix matter that would not be available. In fact, such matter should not be submitted at all except requested by the instructor.

Content

- Sum up your conclusion in text and demonstrate them, if suitable, with figures and tables.
- In manuscript, explain each of your consequences, point the reader to remarks that are most appropriate.
- Present a background, such as by describing the question that was addressed by creation an exacting study.
- Explain results of control experiments and comprise remarks that are not accessible in a prescribed figure or table, if appropriate.
- Examine your data, then prepare the analyzed (transformed) data in the form of a figure (graph), table, or in manuscript form.

What to stay away from

- Do not discuss or infer your outcome, report surroundings information, or try to explain anything.
- Not at all, take in raw data or intermediate calculations in a research manuscript.
- Do not present the similar data more than once.
- Manuscript should complement any figures or tables, not duplicate the identical information.
- Never confuse figures with tables - there is a difference.

Approach

- As forever, use past tense when you submit to your results, and put the whole thing in a reasonable order.
- Put figures and tables, appropriately numbered, in order at the end of the report
- If you desire, you may place your figures and tables properly within the text of your results part.

Figures and tables

- If you put figures and tables at the end of the details, make certain that they are visibly distinguished from any attach appendix materials, such as raw facts
- Despite of position, each figure must be numbered one after the other and complete with subtitle
- In spite of position, each table must be titled, numbered one after the other and complete with heading
- All figure and table must be adequately complete that it could situate on its own, divide from text

Discussion:

The Discussion is expected the trickiest segment to write and describe. A lot of papers submitted for journal are discarded based on problems with the Discussion. There is no head of state for how long a argument should be. Position your understanding of the outcome visibly to lead the reviewer through your conclusions, and then finish the paper with a summing up of the implication of the study. The purpose here is to offer an understanding of your results and hold up for all of your conclusions, using facts from your research and generally accepted information, if suitable. The implication of result should be visibly described. Infer your data in the conversation in suitable depth. This means that when you clarify an observable fact you must explain mechanisms that may account for the observation. If your results vary from your prospect, make clear why that may have happened. If your results agree, then explain the theory that the proof supported. It is never suitable to just state that the data approved with prospect, and let it drop at that.

- Make a decision if each premise is supported, discarded, or if you cannot make a conclusion with assurance. Do not just dismiss a study or part of a study as "uncertain."
- Research papers are not acknowledged if the work is imperfect. Draw what conclusions you can based upon the results that you have, and take care of the study as a finished work
- You may propose future guidelines, such as how the experiment might be personalized to accomplish a new idea.
- Give details all of your remarks as much as possible, focus on mechanisms.
- Make a decision if the tentative design sufficiently addressed the theory, and whether or not it was correctly restricted.
- Try to present substitute explanations if sensible alternatives be present.
- One research will not counter an overall question, so maintain the large picture in mind, where do you go next? The best studies unlock new avenues of study. What questions remain?
- Recommendations for detailed papers will offer supplementary suggestions.

Approach:

- When you refer to information, differentiate data generated by your own studies from available information
- Submit to work done by specific persons (including you) in past tense.
- Submit to generally acknowledged facts and main beliefs in present tense.

Please carefully note down following rules and regulation before submitting your Research Paper to Global Journals Inc. (US):

Segment Draft and Final Research Paper: You have to strictly follow the template of research paper. If it is not done your paper may get rejected.

- The **major constraint** is that you must independently make all content, tables, graphs, and facts that are offered in the paper. You must write each part of the paper wholly on your own. The Peer-reviewers need to identify your own perceptive of the concepts in your own terms. NEVER extract straight from any foundation, and never rephrase someone else's analysis.

- Do not give permission to anyone else to "PROOFREAD" your manuscript.

- Methods to avoid Plagiarism is applied by us on every paper, if found guilty, you will be blacklisted by all of our collaborated research groups, your institution will be informed for this and strict legal actions will be taken immediately.)
- To guard yourself and others from possible illegal use please do not permit anyone right to use to your paper and files.

Criterion for Grading a Research Paper (Compilation) by Global Journals Inc. (US)

Please note that following table is only a Grading of "Paper Compilation" and not on "Performed/Stated Research" whose grading solely depends on Individual Assigned Peer Reviewer and Editorial Board Member. These can be available only on request and after decision of Paper. This report will be the property of Global Journals Inc. (US).

Topics	Grades		
	A-B	**C-D**	**E-F**
Abstract	Clear and concise with appropriate content, Correct format. 200 words or below	Unclear summary and no specific data, Incorrect form Above 200 words	No specific data with ambiguous information Above 250 words
Introduction	Containing all background details with clear goal and appropriate details, flow specification, no grammar and spelling mistake, well organized sentence and paragraph, reference cited	Unclear and confusing data, appropriate format, grammar and spelling errors with unorganized matter	Out of place depth and content, hazy format
Methods and Procedures	Clear and to the point with well arranged paragraph, precision and accuracy of facts and figures, well organized subheads	Difficult to comprehend with embarrassed text, too much explanation but completed	Incorrect and unorganized structure with hazy meaning
Result	Well organized, Clear and specific, Correct units with precision, correct data, well structuring of paragraph, no grammar and spelling mistake	Complete and embarrassed text, difficult to comprehend	Irregular format with wrong facts and figures
Discussion	Well organized, meaningful specification, sound conclusion, logical and concise explanation, highly structured paragraph reference cited	Wordy, unclear conclusion, spurious	Conclusion is not cited, unorganized, difficult to comprehend
References	Complete and correct format, well organized	Beside the point, Incomplete	Wrong format and structuring

Index

Global Journal of Researches in Engineering

Visit us on the Web at www.GlobalJournals.org | www.EngineeringResearch.org
or email us at helpdesk@globaljournals.org

ISSN 9755861